Journal of Applied Biology & Biotechnology Vol. 12(2), pp. 100-149, Mar-Apr, 2024
Available online at http://www.jabonline.in
DOI: 10.7324/JABB.2024.125317

The *de novo* genome assembly of lemon grass to identify the genes in essential oil production

Navajeet Chakravartty, Nageswara Rao Reddy Neelapu*

Department of Biochemistry and Bioinformatics, GITAM School of Science, Gandhi Institute of Technology and Management (Deemed to be University), Visakhapatnam, Andhra Pradesh, India.

ARTICLE INFO

Article history:
Received on: July 28, 2023
Accepted on: December 04, 2023
Available online: February 20, 2024

Keywords:
Chloroplast genome,
Cymbopogon citratus
Genome assembly,
Lemon grass Mitochondrial genome,
Nuclear genome.

ABSTRACT

Lemon grass (*Cymbopogon citratus* L.) is a member of the *Poaceae* family and is famous for its culinary, cultural, cosmetic, and medicinal properties. Therefore, the present study aims to assemble the genome of the lemon grass and provide a valuable resource for mining biochemical pathways. The raw genome data is retrieved from NCBI and cleaned with AdapterRemoval version 2.3.2 for high-quality clean data. The genome size was estimated using Jellyfish 2.2.10 and GenomeScope version 1.0. MaSurCa version 3.3.2. was used to generate genome assembly. BUSCO version 4.1.2. is used to assess the completeness and quality of genome assembly. This analysis resulted in a draft nuclear genome of 364,442,032 bps with 127,303 scaffolds. RepeatModeler version 2.0.1., AUGUSTUS version 3.3.2., and tRNAscan-SE version 2.0.6. are used to identify repeats, genes, and tRNA genes, respectively. This study identified 41.66% repeats, 41,775 genes, and 681 tRNAs. UniProt protein database, OrthoFinder version 2.2.7, InterproScan, Plant metabolic network analysis, and Gene Ontology categorization annotate the genome functionally. GetOrganelle version 1.6.4., is used to generate the mitochondrial and chloroplast genome assembly of 367,579 bps and 139,690 bps. CPGAVAS2 version 1 and AGORA version 1 annotate the genome of chloroplast and mitochondria, respectively. The genes and pathways (photosynthesis, glycolysis, pyruvate, terpenoid backbone synthesis, and tricarboxylic acid cycle) associated with essential oil production are identified and mapped. Thus, this study reports the draft nuclear and organelle genome assembly; and genes and pathways participating in the biosynthesis of essential oil production in *C. citratus* L.

ARTICLE HIGHLIGHTS

1. The nuclear genome size is predicted to be 454,049,232 bps for lemon grass. The *de-novo* assembly generated 127,303 scaffolds, with an assembly size of 364,442,032 bps. The genome assembly of lemon grass was complete by 60.9%.
2. A complete circular chloroplast genome of 139,690 bps was generated and annotated without any gap for lemon grass.
3. A complete circular mitochondrial genome of 367,579 bps was generated and annotated without any gap for lemon grass.
4. The genes and pathways (photosynthesis, glycolysis, pyruvate, terpenoid backbone synthesis, and tricarboxylic acid cycle) associated with essential oil production are identified and mapped.

**Corresponding Author:*
Nageswara Rao Reddy Neelapu,
Department of Biochemistry and Bioinformatics, GITAM School of Science, Gandhi Institute of Technology and Management (Deemed to be University), Visakhapatnam, Andhra Pradesh, India.
E-mail: nneelapu @ gitam.edu

1. INTRODUCTION

The essential oil-producing plants are primarily distributed across the plant kingdom and cover many families, including *Lamiaceae* (mint, basil, lavender), *Rosaceae* (roses), and *Poaceae* (aromatic grasses) [1]. The genus *Cymbopogon* of the *Poaceae* family is well known for its aromatic properties and consists of approximately 180 species distributed worldwide [2], of which 45 species are reported in India [3]. These fragrant grasses consist of a differential blend of several terpenoid constituents and are significant reserves of monoterpene-rich essential oils [4]. The major components reported in the essential oil of lemon grass are monoterpene alcohols, aldehydes, and acetates [5]. The monoterpene alcohols like geraniol (GOL) and citronellol (COL) are previously reported [5]. The aldehydes include geranial (GAL), neral (NAL), and citronellal (CAL) [5]. Acetates include citronellyl acetate and geranyl acetate [5].

Essential oils are significant in food flavors, cosmetics, oral healthcare products, fragrances, insect repellents, and aromatherapy. For instance, citral is a raw material for perfumery, confectionery, Vitamin A, and ionones [6]. Likewise, alcohol COL, a raw material for producing rose oxide, and its aldehyde CAL are used to manufacture flavor and fragrance agents [7]. In addition, essential oils and their

constituents from aromatic grasses possess potent pharmacological activities like cytotoxic, anti-inflammatory, antifungal, and antioxidant [8]. Besides oil production, citronella grass is a flavoring agent for culinary purposes. Thus, there is a need to understand the genomic architecture of this highly significant species with relevance to essential oils.

Currently, 911 genes and 1,769 protein sequences are available at NCBI for the genus *Cymbopogon* [9], whereas 128 genes and 347 protein sequences are available at NCBI for *Cymbopogon citratus* L. [10]. The non-availability of high-quality genome sequence assembly for the species *C. citratus* is a bottleneck in understanding the genomic architecture of the species. The whole-genome sequencing (WGS) is a precise method for analyzing entire genomes [11]. The rapidly reducing sequencing costs and the ability to produce large volumes of data with today's high throughput sequencers have made WGS a powerful tool for genomics research [11,12]. The raw genome

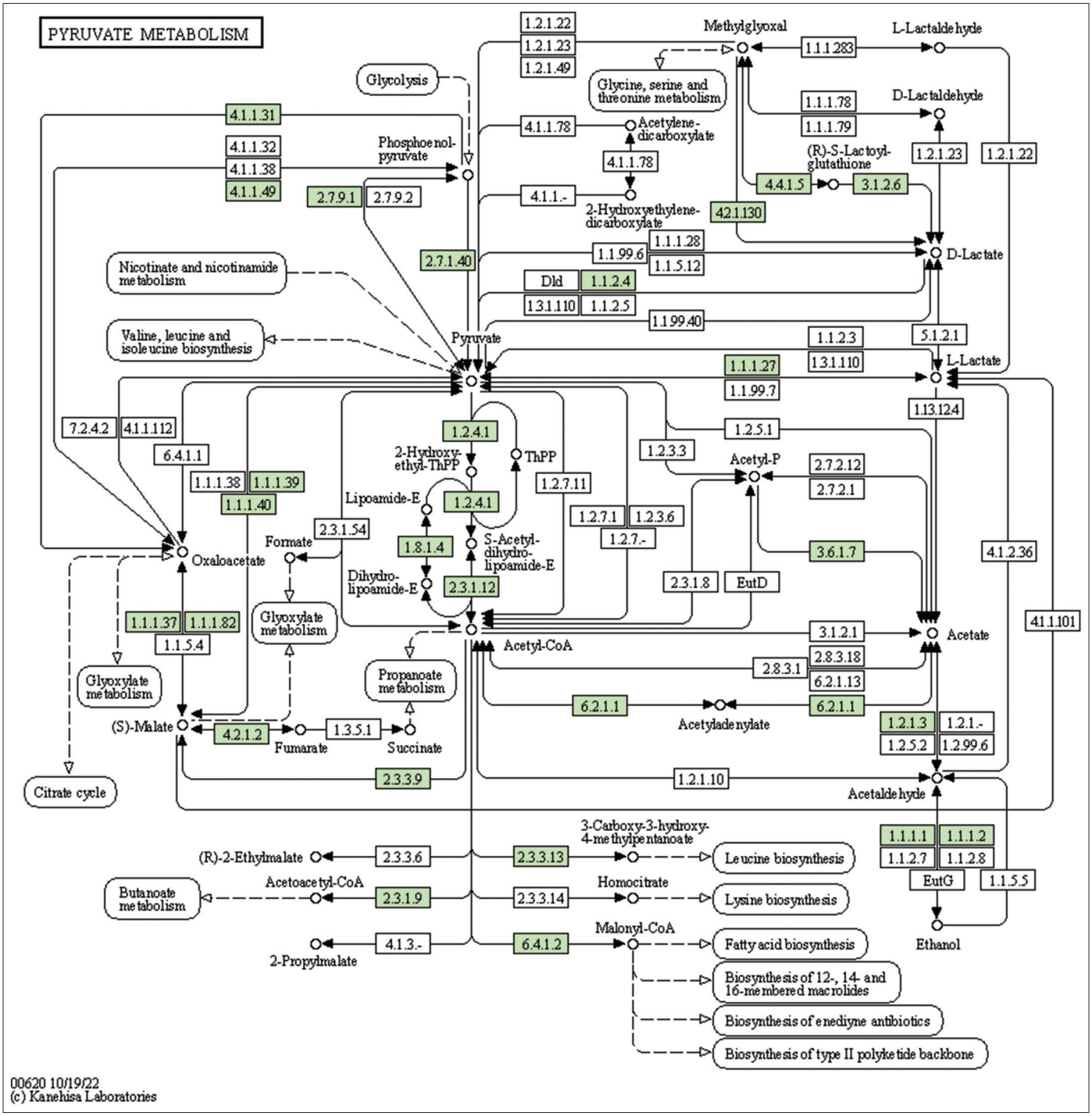

Figure 1: The genes associated with metabolites of the pyruvate metabolism. This figure shows genes associated with metabolites of the pyruvate metabolism, and the genes are highlighted in the pathway. These genes are mapped onto the pathway and was retrieved from KAAS.

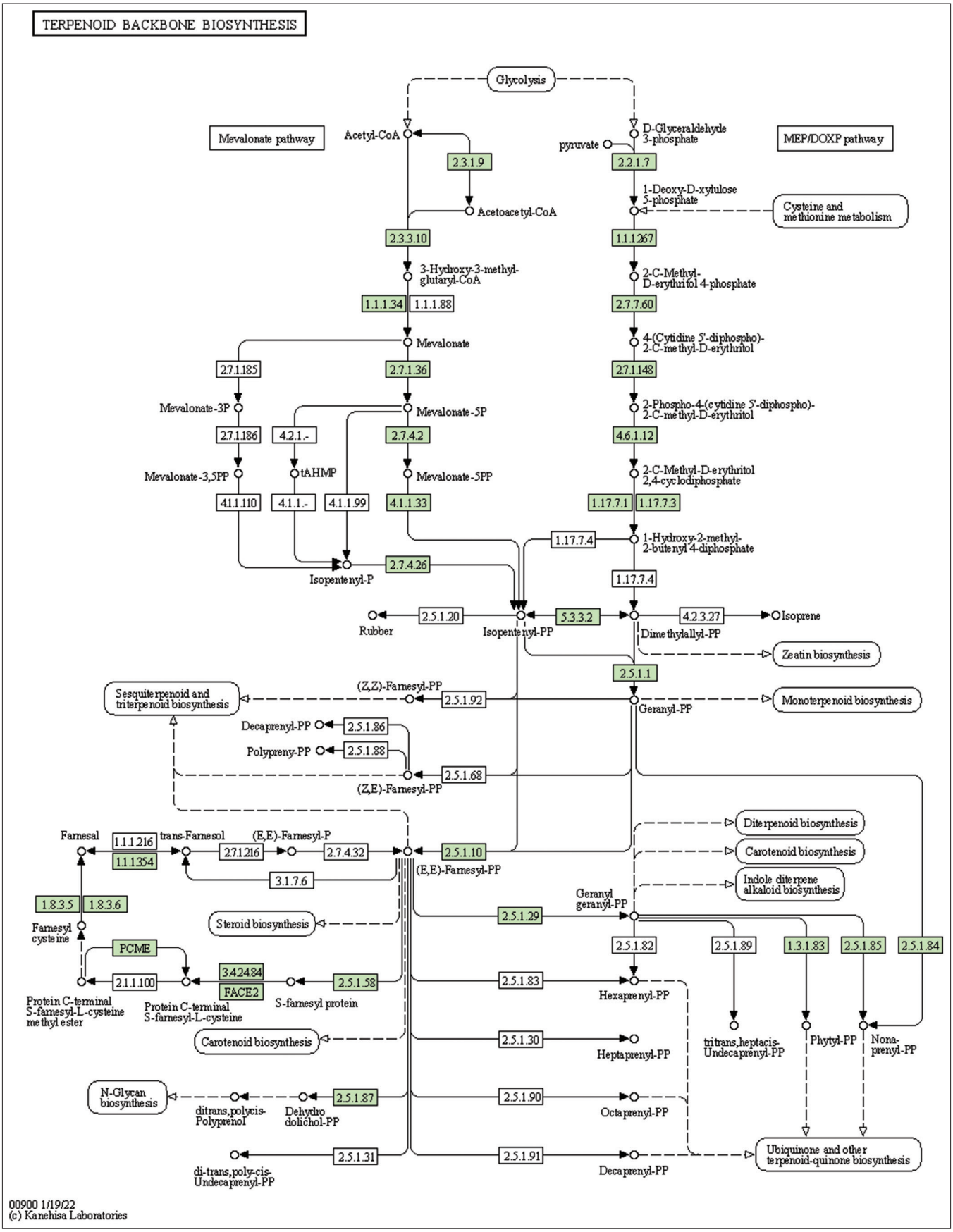

Figure 2: The genes associated with metabolites of the terpenoid backbone synthesis. This figure shows genes associated with metabolites of the terpenoid backbone synthesis, and the genes are highlighted in the pathway. These genes are mapped onto the pathway and was retrieved from KAAS.

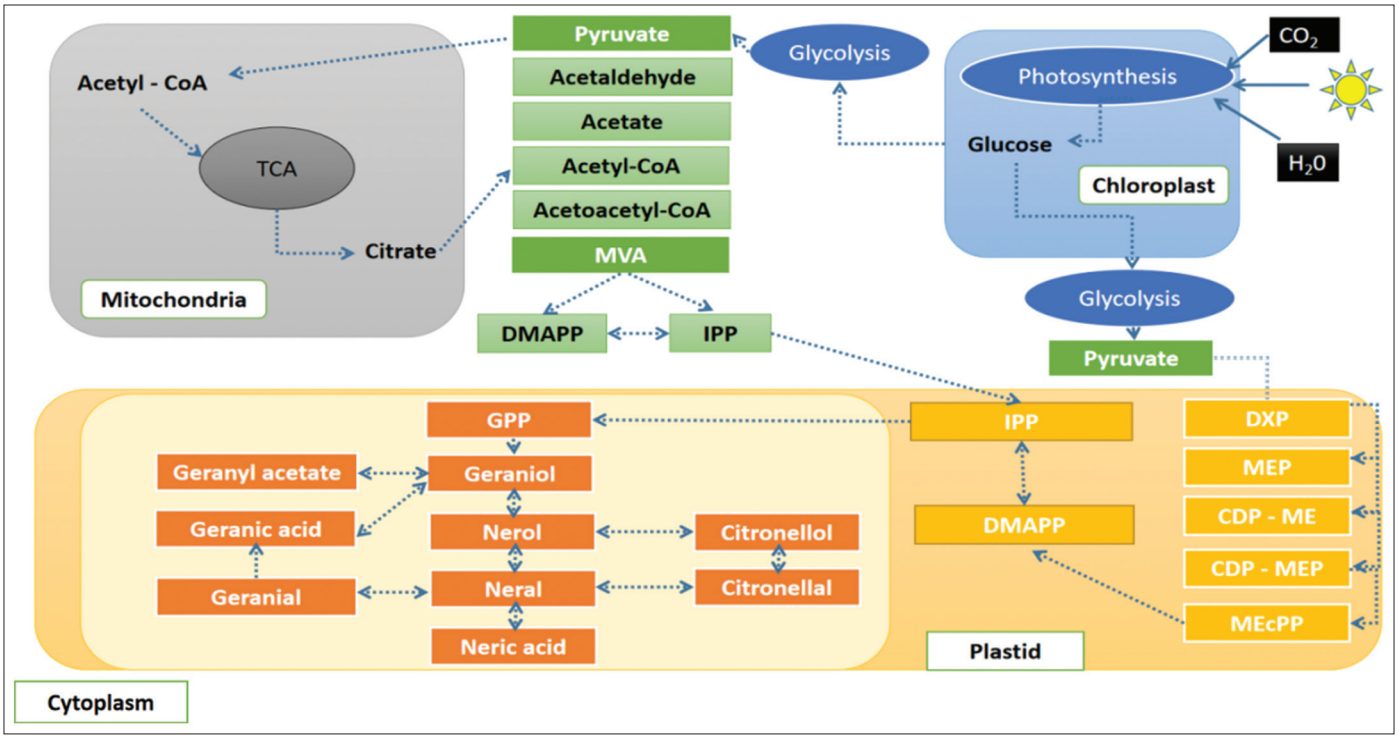

Figure 3: The summary of the pathway for biosynthesis of essential oil in lemon grass. The figure summarizes the pathway for the biosynthesis of lemon grass essential oil, its crosstalk with other metabolic processes, and the role of different organelles.

sequence data of *C. citratus* is available at NCBI (BioProject ID: PRJNA610008) [13]. Thus, the present study aims to report the draft genome assembly of lemon grass with genes, repeats, and functional relevance; genes associated with metabolites and secondary metabolites; genes related to culinary properties in lemon grass; and genes and pathways associated with essential oil production in lemon grass.

2. MATERIALS AND METHODS

The genome of *C. citratus* was assembled and annotated with the modified protocol of Chakravartty and Neelapu [14].

2.1. Assembly and Annotation of the Nuclear Genome in Lemon Grass

2.1.1. Genome sample and assembly

The raw genome sequence data of *C. citratus* was downloaded from NCBI (BioProject ID: PRJNA610008), evaluated, and checked. AdapterRemoval version 2.3.2 was employed to remove contaminated adapter sequences and bases of low-quality (with Q30) from reads to provide high-quality clean data [15]. The *de novo* assembly is generated based on high-quality clean data. Jellyfish 2.2.10 [16] and GenomeScope version 1.0 [17] are employed to estimate the genome size, and MaSurCa version 3.3.2 [18] generated *de novo* assembly. BUSCO version 4.1.2 [19] is used to check the *de novo* assembly and was considered for downstream analysis to check the completeness and quality of the genome assembly. The plant dataset viridiplantae_odb10 is provided as a model for BUSCO version 4.1.2 [19].

2.1.2. Genome annotation and analysis

RepeatModeler version 2.0.1 [20] and RepeatMasker version 4.0.9 [21] are employed to identify repeats and mask the genome. AUGUSTUS version 3.3.2 [22] predicts genes with *Arabidopsis* as the model, and tRNAscan-SE version 2.0.6 [23] recognizes tRNAs. OrthoFinder version 2.2.7 [24] is employed to carry out orthologous analysis. The orthologous analysis was performed for predicted protein sequences of *C. citratus* by considering protein sequences of eight model species, i.e., *Aegilops tauschii*, *Arabidopsis thaliana*, *Dichanthelium oligosanthes*, *Oryza sativa*, *Setaria italica*, *Sorghum bicolor*, *Triticum aestivum*, and *Zea mays*. UniProt protein database [25] is employed to process functional annotation of the predicted genes based on homology. The top hits in the homology search are assigned to the genes in the functional annotation [25]. MISA version 2.1 [26] is utilized to predict simple sequence repeats markers, and primer3 version 2.5.0 [27] is employed to design primers.

2.1.3. Identifying genes and pathways associated with metabolites, secondary metabolites, and culinary properties in lemon grass

Mapman [28] and KEGG [29] predicted genes and pathways associated with the metabolism of essential oils in lemon grass. The orthologous analysis is carried out between *C. citratus*, and four culinary herbs *Ocimum basilicum* L., *Origanum majorana* L., *Origanum vulgare* L, and *Rosmarinus officinalis* L, to predict genes associated with the culinary properties in lemon grass. OrthoFinder version 2.2.7 [24] is employed to carry out orthologous analysis.

2.2. Assembly and Annotation of Organelle Genome in Lemon Grass

GetOrganelle version 1.6.4 [30] generated the mitochondria and chloroplast assembly. CPGAVAS2 version 1 [31] annotated the chloroplast genome, whereas AGORA version 1 [32] annotated the mitochondrial genome considering Y08501.2 as a model.

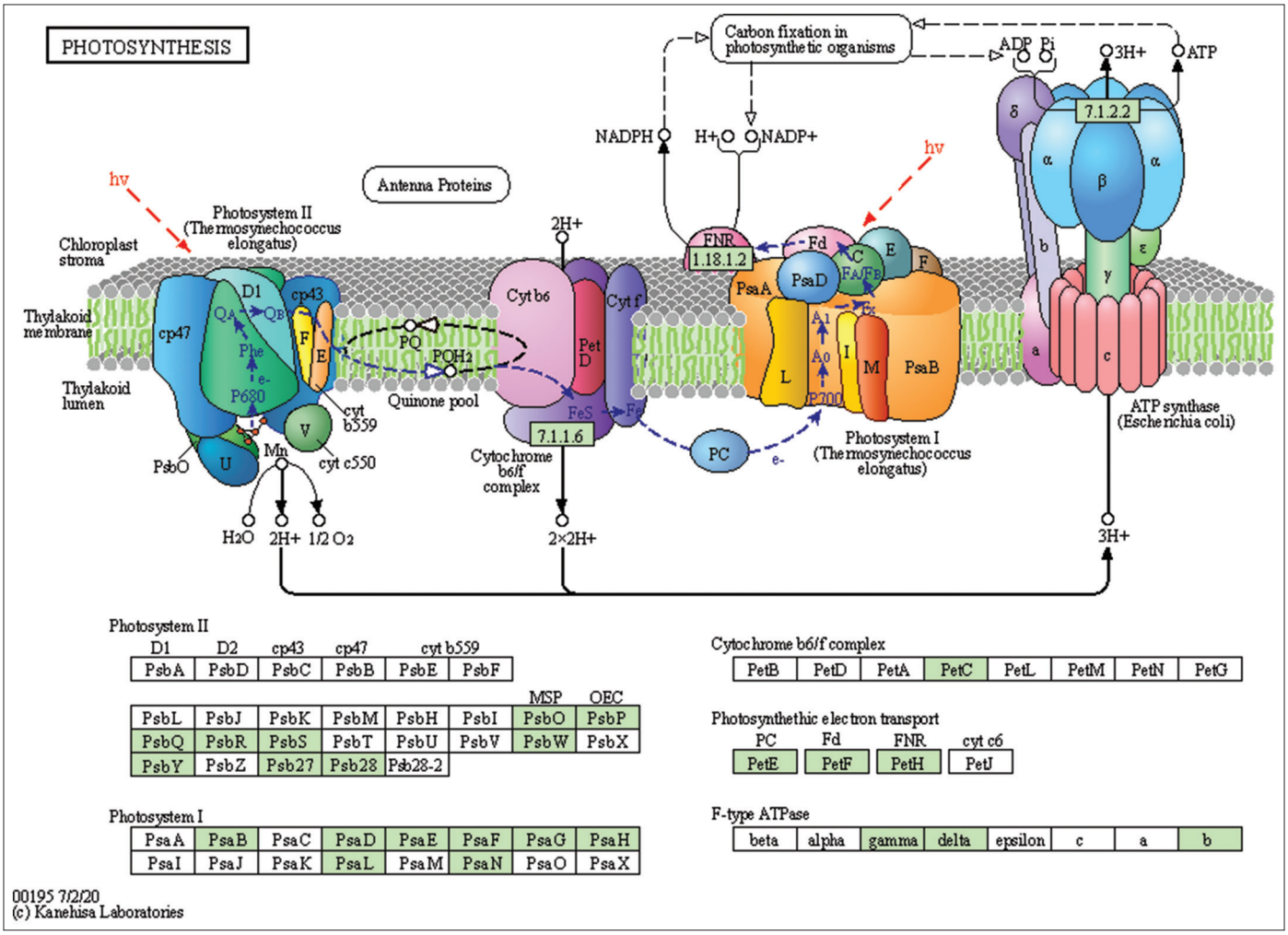

Figure 4: The genes associated with metabolites of the photosynthetic pathway. This figure shows genes associated with metabolites of the photosynthetic pathway, and the genes are highlighted in the pathway. These genes are mapped onto the pathway and was retrieved from KAAS.

3. RESULTS AND DISCUSSION

3.1. Draft Genome (Nuclear and Organelle) Assembly of Lemon Grass

The whole-genome sequence data of 28.96 GBs from NCBI Bio project PRJNA610008 is retrieved. There were 194,645,804 reads, 44.237% of G.C. content, and 94.72% data ≥Q30 with read length 2 × 150bp. The adapter removal and quality trimming resulted in 194,640,684 reads, 44.23% of G.C. content, and 94.8% data ≥Q30. The genome size of 454,049,232 bps is predicted for lemon grass [Supplementary Figure 1]. The *de-novo* assembly generated 127,303 scaffolds, with an assembly size of 364,442,032 bps. The longest scaffold is 67,673 bps, and the shortest scaffold is 301 bps. Table 1 presents the genome estimation summary of lemon grass. The assembled genome's G.C. content and scaffold length distribution are calculated and shown in Supplementary Figures 2 and 3, respectively. The G.C. content of the assembled genome is ~43.86%. The evaluation of the genome using BUSCO version 4.1.2., predicted that the genome assembly of lemon grass was complete by 60.9% [Table 1 and Supplementary Table 1].

The repeat analysis predicted that 41.66% of the genome contains repetitive elements. Table 1 and Supplementary Table 2 provides the repeat classification. The repeat classification revealed 0.02% of SINEs, 3.64% of LINEs, 9.98% of LTR elements, 1.49% of DNA elements, and unclassified repeats of 25.41%. The analysis revealed 50779, 10874, 11942, 1515, 461, 451, and 4784 mono-nucleotide repeats, di-nucleotide repeats, tri-nucleotide repeats, tetra-nucleotide repeats, penta-nucleotide repeats, hexa-nucleotide repeats, and complex type repeats, respectively [Supplementary Table 3]. Out of the simple repeats predicted, the primers were designed successfully for 47,048 mono-nucleotides, 9321 di-nucleotides, 10,901 tri-nucleotides, 1378 tetra-nucleotides, 414 penta-nucleotides, 385 hexa-nucleotides and 4241 complex type repeats [Supplementary Table 3]. The tRNAs identified in the assembly of lemon grass are 681.

The gene prediction based on AUGUSTUS version 3.3.2 revealed 41,775 genes. Nearly 34,239 were annotated based on best hits with the UniProt protein database [Table 1]. InterproScan was used to annotate genes resulting in the annotation of 34,348 genes. The KEGG analysis predicted many significant pathways in lemon grass. The Gene Ontology categorization identified 1745 genes associated with biological processes, 484 genes related to cellular components, and 1373 genes linked with molecular function [Supplementary Figures 4-6]. The Mapman analysis identified 43.09% of genes having a significant role in metabolic pathways [Supplementary Figure 7]. Plant metabolic network analysis identified 8550 genes associated with metabolic pathways. A linear tree presents phylogenetic relationships

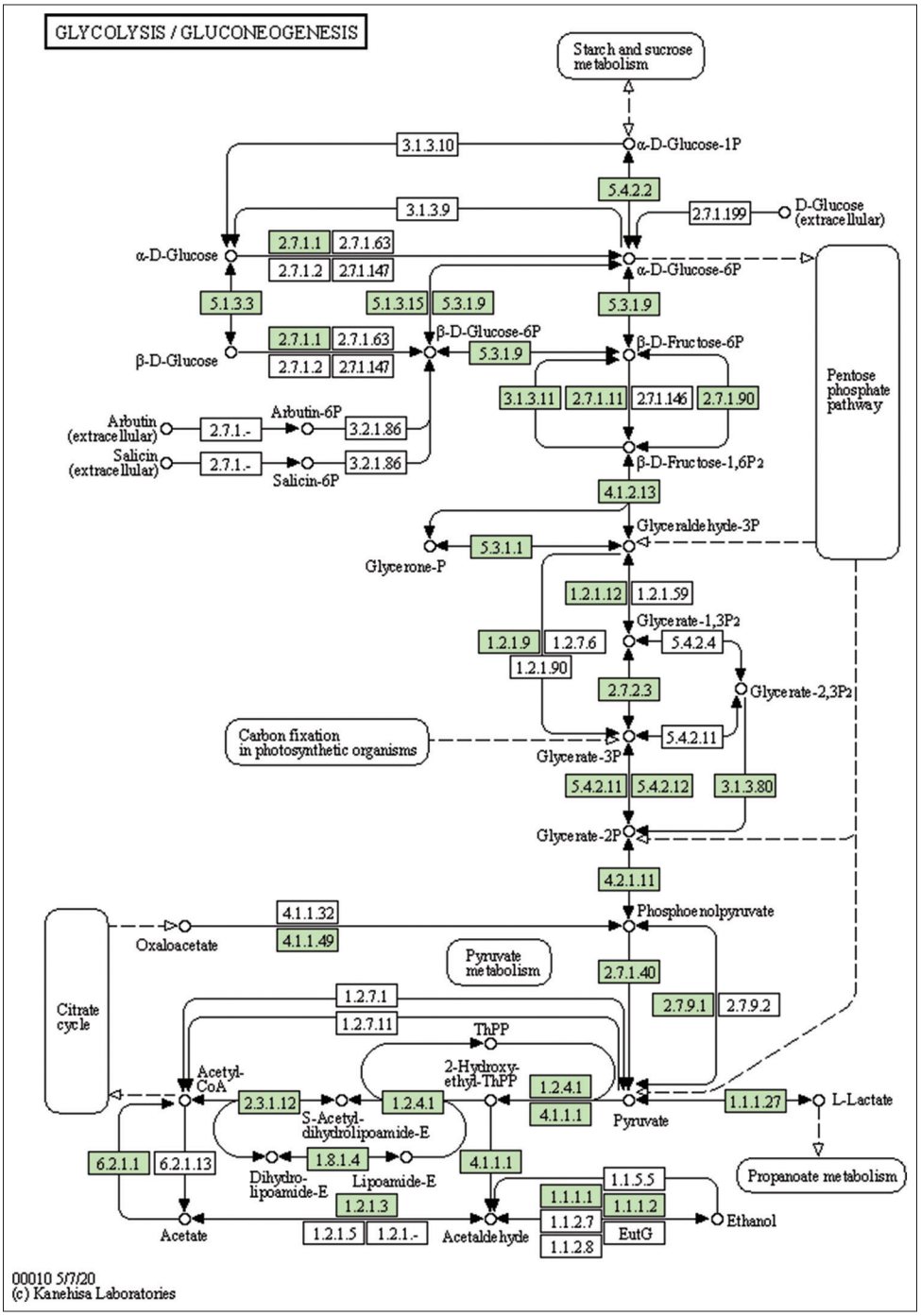

Figure 5: The genes associated with metabolites of the glycolysis pathway. This figure shows genes associated with metabolites of the glycolytic pathway, and the genes are highlighted in the pathway. These genes are mapped onto the pathway and was retrieved from KAAS.

of nine species based on the maximum likelihood method [24,33]. It is viewed in Figtree [34] to understand the phylogenetic relationship between the models and *C. citratus*, as shown in Supplementary Figure 8. The linear tree showed that lemon grass is close to *S. bicolor*, followed by *Z. mays*, *S. italica*, and *D. oligosanthes.* The orthologous study considered 562,517 genes, and nearly 447,596 (79.57%) genes are in orthogroups. The number of orthogroups identified in this study is 26,100, and Supplementary Table 4 presents the orthologous summary.

A complete circular chloroplast genome of 139,690 bps was generated and annotated without any gap [Supplementary Figure 9]. A complete circular mitochondrial genome of 367,579 bps was generated and annotated without any gap [Supplementary Figure 10]. *A. thaliana* ecotype Col-0 mitochondrion, complete genome (Y08501.2) was used as a reference for genome annotation in the mitochondria.

3.2. The Genes Associated with Metabolites and Secondary Metabolites in Lemon Grass

The study identified genes associated with metabolites and secondary metabolites of lemon grass. Metabolites and secondary metabolites are essential for producing essential oils in lemon grass. Table 2

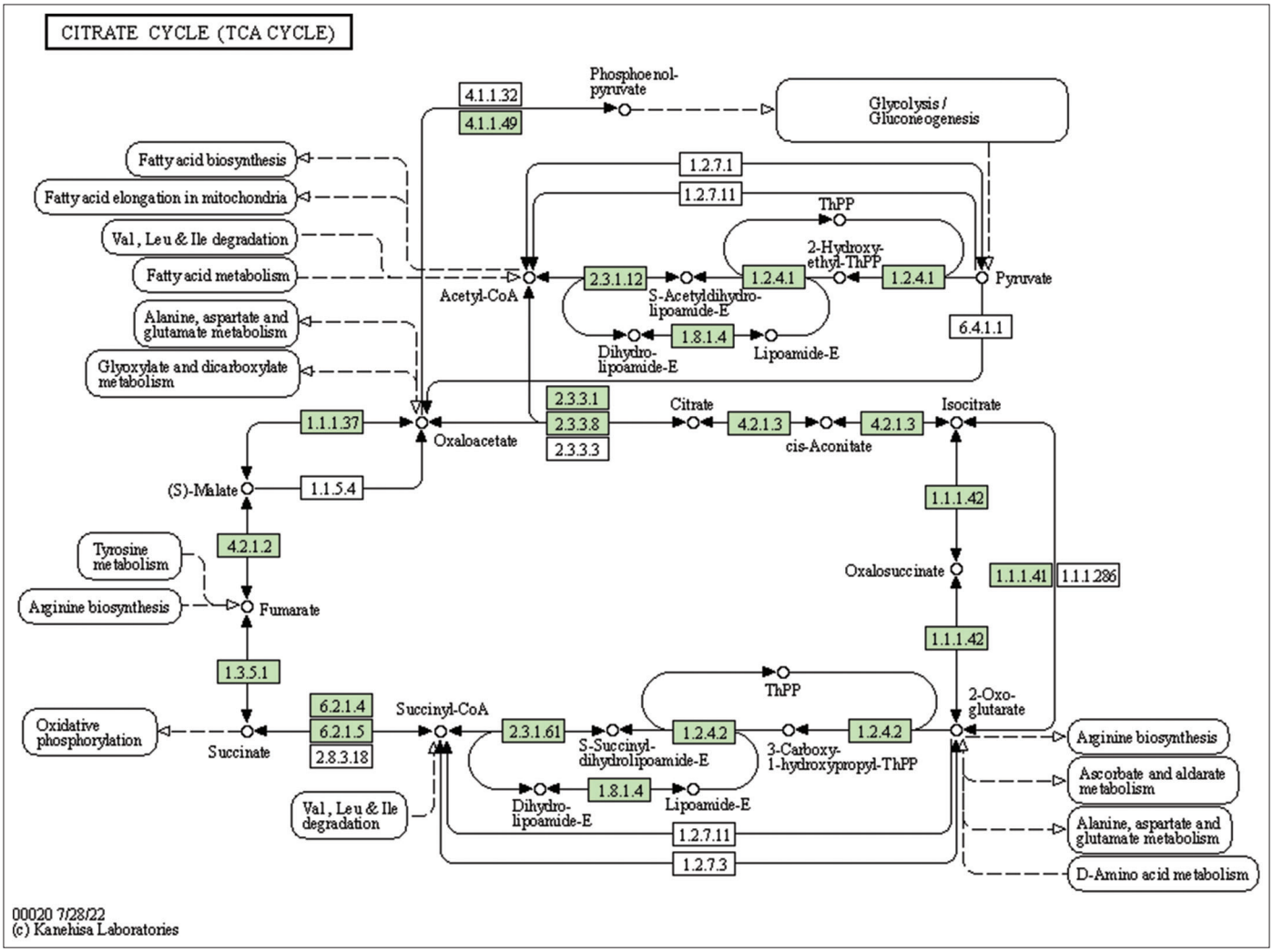

Figure 6: The genes associated with metabolites of the TCA cycle. This figure shows genes associated with metabolites of the TCA cycle; the genes are highlighted in the pathway. These genes are mapped onto the pathway and was retrieved from KAAS.

summarizes lemon grass's KO ID, gene count, and metabolic pathways [Figure 1 and Supplementary Figures 11-33]. The number of genes identified in purine metabolism, cysteine and methionine metabolism, glycerophospholipid metabolism, pyruvate metabolism, starch and sucrose metabolism, and pyrimidine metabolism is 43, 43, 35, 32, 31, and 30, respectively. Similarly, this study identifies fifteen genes in sulfur metabolism, sphingolipid, alpha-Linolenic acid, phenylalanine, tryptophan, and Beta-alanine.

Table 2 summarizes genes associated with secondary metabolites [Figure 2 and Supplementary Figures 34-39]. The number of genes identified in folate biosynthesis, isoquinoline alkaloid biosynthesis, flavonoid biosynthesis, phenylpropanoid biosynthesis, diterpenoid biosynthesis, carotenoid biosynthesis, terpenoid backbone biosynthesis, and ubiquinone and other terpenoid-quinone biosynthesis are 15, 8, 13, 15, 9, 15, 28, and 20 respectively.

3.3. The Genes Associated with Culinary Properties in Lemon Grass

The orthologous analysis between *C. citratus* and four culinary herbs, *O. basilicum* L., *O. majorana* L., *O. vulgare* L., and *R. officinalis* L. identified the genes associated with culinary properties in lemon grass. Nearly 5442, 219, 9943, and 558 protein sequences are available for *O. basilicum* L., *O. majorana* L., *O. vulgare* L., and *R. officinalis* L. at NCBI. The orthologous study identified 7775 orthogroups; out of them, 74.8% of genes were present in the orthogroup. The Venn analysis revealed 19 orthogroups that are common between all the five culinary herbs, and Table 3 presents the orthologous summary. A linear tree shows the phylogenetic relationship of the five species based on the maximum likelihood method [27,33]. It is viewed in Figtree [34] to understand the phylogenetic relationship between the models and *C. citratus*, as shown in Supplementary Figure 40. The analysis also helped to identify genes associated with culinary properties in lemon grass, paving the way to culinary genomics.

3.4. The Genes and Pathways Associated with Essential oil Production in Lemon Grass

The lemon grass essential oil is a mixture of cyclic and acyclic monoterpenes (GAL, NAL, and CAL). Figure 3 shows the biosynthesis of essential oil in lemon grass, the role of different cellular organelles, and crosstalk with other metabolic processes [35]. Like most other plants,

Table 1: The summary of genome assembly, BUSCO score parameters, repeats, gene prediction, and annotation on lemon grass

S. No.	Statistics	Count
Genome Assembly Statistics		
1	Number of scaffolds	127303
2	Total size of scaffolds	364442032
3	Longest scaffold	67673
4	Shortest scaffold	301
5	Number of scaffolds >1K nt	97384
6	Percentage of scaffolds >1K nt	76.5
7	Number of scaffolds >10K nt	4251
8	Percentage of scaffolds >10K nt	3.3
9	Mean scaffold size	2863
10	Median scaffold size	1864
11	N50 scaffold length	4347
12	L50 scaffold count	23781
13	scaffold %A	28
14	scaffold %C	21.91
15	scaffold %G	21.95
16	scaffold %T	28.11
17	scaffold %N	0.03
BUSCO Statistics		
1	Complete BUSCOs (C)	60.90%
2	Complete and single-copy BUSCOs (S)	58.80%
3	Complete and duplicated BUSCOs (D)	2.10%
4	Fragmented BUSCOs (F)	21.40%
5	Missing BUSCOs (M)	17.7%
6	Total BUSCO groups searched	100.00%
Repeat Statistics		
1	SINEs	665
2	LINEs	26231
3	LTR elements	51540
4	DNA elements	12288
5	Unclassified	366513
6	Small RNA	355
7	Satellites	229
8	Simple repeats	63921
9	Low complexity	7157
Gene prediction and annotation		
1	Number of CDS predicted	41,775
2	Number of CDS got annotated with UniProt protein db	34,239
3	Number of CDS got annotated with INTERPRO	34,348
4	Number of CDS got annotated with the plant metabolic network	8,550

Table 2: The genes identified and associated with the metabolism of lemon grass

S. No.	KO ID	Metabolic pathways	Number of genes
1	230	Purine metabolism	43
2	270	Cysteine and methionine metabolism	43
3	564	Glycerophospholipid metabolism	35
4	620	Pyruvate metabolism	32
5	500	Starch and sucrose metabolism	31
6	240	Pyrimidine metabolism	30
7	260	Glycine, serine, and threonine metabolism	29
8	630	Glyoxylate and dicarboxylate metabolism	28
9	561	Glycerolipid metabolism	27
10	250	Alanine, aspartate and glutamate metabolism	27
11	562	Inositol phosphate metabolism	23
12	330	Arginine and proline metabolism	22
13	480	Glutathione metabolism	20
14	53	Ascorbate and aldarate metabolism	19
15	350	Tyrosine metabolism	18
16	51	Fructose and mannose metabolism	17
17	52	Galactose metabolism	16
18	680	Methane metabolism	16
19	920	Sulfur metabolism	15
20	600	Sphingolipid metabolism	15
21	592	alpha-Linolenic acid metabolism	15
22	380	Tryptophan metabolism	15
23	410	beta-Alanine metabolism	15
24	790	Folate biosynthesis	15
25	950	Isoquinoline alkaloid biosynthesis	8
26	941	Flavonoid biosynthesis	13
27	940	Phenylpropanoid biosynthesis	15
28	904	Diterpenoid biosynthesis	9
29	906	Carotenoid biosynthesis	15
30	900	Terpenoid backbone biosynthesis	28
31	130	Ubiquinone and other terpenoid-quinone biosynthesis	20

the lemongrass chloroplast produces glucose through photosynthesis. The present study identified and mapped the genes participating in the photosynthesis pathway of lemon grass [Table 4 and Figure 4]. The glucose undergoes glycolysis in the cytoplasm, yielding pyruvate, a two-carbon compound. The present study identified and mapped the genes participating in the pathway's glycolysis and pyruvate of lemon grass [Table 4, Figures 1 and 5]. Lemongrass uses pyruvate as a substrate for the biosynthesis of isopentenyl diphosphate (IPP) units, either through the cytoplasmic mevalonate (MVA) pathway or plastidic methylerythritol phosphate (MEP) pathway in their young and rapidly growing leaves [35]. MVA Pathway (MVA pathway) is a multi-step (three-step) process that starts with two acetyl-CoA molecules and forms IPP units [36]. MVA-independent Pathway (MEP Pathway) is a multi-step (seven-step) process that begins with glyceraldehyde 3-phosphate and forms IPP [36].

The present study identified and mapped the genes in lemon grass's terpenoid backbone synthesis pathway [Table 4 and Figure 2]. This pathway shows the information on terpenoid backbone synthesis, MVA, and MEP pathways. Alternatively, Mitochondria can import pyruvate and yield citrate through the tricarboxylic acid (TCA) cycle [35]. The present study identified and mapped the genes participating in the pathway TCA cycle of lemon grass [Table 4 and Figure 6]. The citrate can transform into Acetyl-CoA and join the

Table 3: Orthologous analysis between five culinary herbs

S. No.	Summary of Orthogroups and Genes	Counts				
		Cymbopogon citratus	*Ocimum basilicum*	*Origanum majorana*	*Origanum vulgare*	*Rosmarinus officinalis*
1	Number of genes	41775	5442	219	9943	558
2	Number of genes in orthogroups	32567	3348	182	6679	544
3	Number of unassigned genes	9208	2094	37	3264	14
4	Percentage of genes in orthogroups	78	61.5	83.1	67.2	97.5
5	Percentage of unassigned genes	22	38.5	16.9	32.8	2.5
6	Number of orthogroups containing species	5809	1849	94	2306	110
7	Percentage of orthogroups containing species	74.7	23.8	1.2	29.7	1.4
8	Number of species-specific orthogroups	4880	350	0	858	4
9	Number of genes in species-specific orthogroups	28564	1122	0	2873	26
10	Percentage of genes in species-specific orthogroups	68.4	20.6	0	28.9	4.7

Table 4: The genes associated with pathways of essential oil production identified in lemon grass.

S. No.	Gene ID	KO ID	Gene Name	Annotation of the gene
Photosynthesis (map00195)				
1	G867.t1	K02695	psaH	photosystem I subunit VI
2	G2701.t1	K08902	psb27	photosystem II Psb27 protein
3	G3233.t1	K02638	petE	Plastocyanin
4	G3376.t1	K02692	psaD	photosystem I subunit II
5	G3404.t1	K02115	ATPF1, atpG	F-type H+-transporting ATPase subunit gamma
6	G3831.t1	K03542	psbS	photosystem II 22kDa protein
7	G6122.t1	K02699	psaL	photosystem I subunit XI
8	G6505.t1	K02717	psbP	photosystem II oxygen-evolving enhancer protein 2
9	G7149.t1	K08903	psb28	photosystem II 13kDa protein
10	G9610.t1	K02701	psaN	photosystem I subunit PsaN
11	G12274.t1	K02690	psaB	photosystem I P700 chlorophyll a apoprotein A2
12	G14580.t1	K02639	petF	Ferredoxin
13	G16158.t1	K02721	psbW	photosystem II PsbW protein
14	G17949.t1	K08901	psbQ	photosystem II oxygen-evolving enhancer protein 3
15	G19732.t1	K02636	petC	cytochrome b6-f complex iron-sulfur subunit [EC: 7.1.1.6]
16	G20807.t1	K02693	psaE	photosystem I subunit IV
17	G23499.t1	K02641	petH	ferredoxin--NADP+reductase [EC: 1.18.1.2]
18	G25025.t1	K03541	psbR	photosystem II 10kDa protein
19	G26577.t1	K02109	ATPF0, atpF	F-type H+-transporting ATPase subunit b
20	G27268.t1	K02113	ATPF1, atpH	F-type H+-transporting ATPase subunit delta
21	G28907.t1	K02694	psaF	photosystem I subunit III
22	G30260.t1	K02716	psbO	photosystem II oxygen-evolving enhancer protein 1
23	G36823.t1	K08905	psaG	photosystem I subunit V
24	G37457.t1	K02723	psbY	photosystem II PsbY protein
Glycolysis/Gluconeogenesis (map00010)				
25	G762.t1	K03841	FBP, fbp	fructose-1,6-bisphosphatase I [EC: 3.1.3.11]
26	G1358.t1	K00382	DLD, lpd, pdhD	dihydrolipoamide dehydrogenase [EC: 1.8.1.4]
27	G2227.t1	K15633	gpmI	2,3-bisphosphoglycerate-independent phosphoglycerate mutase [EC: 5.4.2.12]
28	G3925.t1	K00134	GAPDH, gapA	glyceraldehyde 3-phosphate dehydrogenase (phosphorylating) [EC: 1.2.1.12]
29	G4309.t1	K01006	ppdK	pyruvate, orthophosphate dikinase [EC: 2.7.9.1]

(*Contd...*)

Table 4: (*Continued*).

S. No.	Gene ID	KO ID	Gene Name	Annotation of the gene
30	G6749.t1	K00128	ALDH	aldehyde dehydrogenase (NAD+) [EC: 1.2.1.3]
31	G7450.t1	K00895	pfp, PFP	diphosphate-dependent phosphofructokinase [EC: 2.7.1.90]
32	G9335.t1	K01810	GPI, pgi	glucose-6-phosphate isomerase [EC: 5.3.1.9]
33	G9705.t1	K01610	E4.1.1.49, pckA	phosphoenolpyruvate carboxykinase (ATP) [EC: 4.1.1.49]
34	G10700.t1	K01785	galM, GALM	aldose 1-epimerase [EC: 5.1.3.3]
35	G11810.t1	K00873	PK, pyk	pyruvate kinase [EC: 2.7.1.40]
36	G12188.t1	K01835	Pgm	phosphoglucomutase [EC: 5.4.2.2]
37	G12423.t1	K01568	PDC, pdc	pyruvate decarboxylase [EC: 4.1.1.1]
38	G12843.t1	K00844	HK	hexokinase [EC: 2.7.1.1]
39	G13296.t1	K01689	ENO, eno	enolase [EC: 4.2.1.11]
40	G14904.t1	K01785	galM, GALM	aldose 1-epimerase [EC: 5.1.3.3]
41	G16892.t1	K00002	AKR1A1, adh	alcohol dehydrogenase (NADP+) [EC: 1.1.1.2]
42	G17507.t1	K00627	DLAT, aceF, pdhC	pyruvate dehydrogenase E2 component (dihydrolipoamide acetyltransferase) [EC: 2.3.1.12]
43	G18230.t1	K00131	gapN	glyceraldehyde-3-phosphate dehydrogenase (NADP+) [EC: 1.2.1.9]
44	G18839.t1	K00927	PGK, pgk	phosphoglycerate kinase [EC: 2.7.2.3]
45	G20474.t1	K01623	ALDO	fructose-bisphosphate aldolase, class I [EC: 4.1.2.13]
46	G22816.t1	K01834	PGAM, gpmA	2,3-bisphosphoglycerate-dependent phosphoglycerate mutase [EC: 5.4.2.11]
47	G24955.t1	K00016	LDH, ldh	L-lactate dehydrogenase [EC: 1.1.1.27]
48	G26444.t1	K01792	E5.1.3.15	glucose-6-phosphate 1-epimerase [EC: 5.1.3.15]
49	G30535.t1	K01895	ACSS1_2, acs	acetyl-CoA synthetase [EC: 6.2.1.1]
50	G34419.t1	K01803	TPI, tpiA	triosephosphate isomerase (TIM) [EC: 5.3.1.1]
51	G34750.t1	K03103	MINPP1	multiple inositol-polyphosphate phosphatase/2,3-bisphosphoglycerate 3-phosphatase [EC: 3.1.3.62 3.1.3.80]
Pyruvate metabolism (map00620)				
52	G1358.t1	K00382	DLD, lpd, pdhD	dihydrolipoamide dehydrogenase [EC: 1.8.1.4]
53	G1431.t1	K01759	GLO1, gloA	lactoylglutathione lyase [EC: 4.4.1.5]
54	G2339.t1	K00627	DLAT, aceF, pdhC	pyruvate dehydrogenase E2 component (dihydrolipoamide acetyltransferase) [EC: 2.3.1.12]
55	G3152.t1	K00626	ACAT, atoB	acetyl-CoA C-acetyltransferase [EC: 2.3.1.9]
56	G4066.t1	K00029	E1.1.1.40, maeB	malate dehydrogenase (oxaloacetate-decarboxylating)(NADP+) [EC: 1.1.1.40]
57	G4673.t1	K01759	GLO1, gloA	lactoylglutathione lyase [EC: 4.4.1.5]
58	G4880.t1	K00873	PK, pyk	pyruvate kinase [EC: 2.7.1.40]
59	G6227.t1	K11262	ACACA	acetyl-CoA carboxylase/biotin carboxylase 1 [EC: 6.4.1.2 6.3.4.14 2.1.3.15]
60	G6396.t1	K01512	acyP	acylphosphatase [EC: 3.6.1.7]
61	G7753.t1	K01069	gloB, gloC, HAGH	hydroxyacylglutathione hydrolase [EC: 3.1.2.6]
62	G8777.t1	K01595	Ppc	phosphoenolpyruvate carboxylase [EC: 4.1.1.31]
63	G9662.t1	K01638	aceB, glcB	malate synthase [EC: 2.3.3.9]
64	G13833.t1	K01895	ACSS1_2, acs	acetyl-CoA synthetase [EC: 6.2.1.1]
65	G17101.t1	K01649	leuA, IMS	2-isopropylmalate synthase [EC: 2.3.3.13]
66	G17414.t1	K00028	E1.1.1.39	malate dehydrogenase (decarboxylating) [EC: 1.1.1.39]
67	G18607.t1	K00382	DLD, lpd, pdhD	dihydrolipoamide dehydrogenase [EC: 1.8.1.4]
68	G18719.t1	K00051	E1.1.1.82	malate dehydrogenase (NADP+) [EC: 1.1.1.82]
69	G24955.t1	K00016	LDH, ldh	L-lactate dehydrogenase [EC: 1.1.1.27]
70	G31224.t1	K00025	MDH1	malate dehydrogenase [EC: 1.1.1.37]
71	G32233.t1	K00102	LDHD, dld	D-lactate dehydrogenase (cytochrome) [EC: 1.1.2.4]
72	G35811.t1	K01595	Ppc	phosphoenolpyruvate carboxylase [EC: 4.1.1.31]
73	G9705.t1	K01610	E4.1.1.49, pckA	phosphoenolpyruvate carboxykinase (ATP) [EC: 4.1.1.49]
Terpenoid backbone biosynthesis (map00900)				
74	G1288.t1	K15889	PCME	prenylcysteine alpha-carboxyl methylesterase [EC: 3.1.1.-]

(*Contd...*)

Table 4: (*Continued*).

S. No.	Gene ID	KO ID	Gene Name	Annotation of the gene
75	G1832.t1	K10960	chlP, bchP	geranylgeranyl diphosphate/geranylgeranyl-bacteriochlorophyllide a reductase [EC: 1.3.1.83 1.3.1.111]
76	G2230.t1	K00787	FDPS	farnesyl diphosphate synthase [EC: 2.5.1.1 2.5.1.10]
77	G2323.t1	K00869	MVK, mvaK1	mevalonate kinase [EC: 2.7.1.36]
78	G3152.t1	K00626	ACAT, atoB	acetyl-CoA C-acetyltransferase [EC: 2.3.1.9]
79	G6541.t1	K06981	ipk	isopentenyl phosphate kinase [EC: 2.7.4.26]
80	G8703.t1	K05954	FNTB	protein farnesyltransferase subunit beta [EC: 2.5.1.58]
81	G8827.t1	K01823	idi, IDI	isopentenyl-diphosphate Delta-isomerase [EC: 5.3.3.2]
82	G9071.t1	K00099	dxr	1-deoxy-D-xylulose-5-phosphate reductoisomerase [EC: 1.1.1.267]
83	G9850.t1	K15891	FLDH	NAD+-dependent farnesol dehydrogenase [EC: 1.1.1.354]
84	G10131.t1	K01641	HMGCS	hydroxymethylglutaryl-CoA synthase [EC: 2.3.3.10]
85	G10476.t1	K01662	dxs	1-deoxy-D-xylulose-5-phosphate synthase [EC: 2.2.1.7]
86	G10495.t1	K11778	DHDDS, RER2, SRT1	ditrans, polycis-polyprenyl diphosphate synthase [EC: 2.5.1.87]
87	G10803.t1	K05356	SPS, sds	all-trans-nonaprenyl-diphosphate synthase [EC: 2.5.1.84 2.5.1.85]
88	G11653.t1	K00991	ispD	2-C-methyl-D-erythritol 4-phosphate cytidylyltransferase [EC: 2.7.7.60]
89	G11679.t1	K00919	ispE	4-diphosphocytidyl-2-C-methyl-D-erythritol kinase [EC: 2.7.1.148]
90	G13764.t1	K00938	E2.7.4.2, mvaK2	phosphomevalonate kinase [EC: 2.7.4.2]
91	G14936.t1	K06013	STE24	STE24 endopeptidase [EC: 3.4.24.84]
92	G15260.t1	K01770	ispF	2-C-methyl-D-erythritol 2,4-cyclodiphosphate synthase [EC: 4.6.1.12]
93	G23454.t1	K13789	GGPS1	geranylgeranyl diphosphate synthase, type III [EC: 2.5.1.1 2.5.1.10 2.5.1.29]
94	G27299.t1	K00021	HMGCR	hydroxymethylglutaryl-CoA reductase (NADPH) [EC: 1.1.1.34]
95	G29757.t1	K08658	RCE1, FACE2	prenyl protein peptidase [EC: 3.4.22.-]
96	G38362.t1	K01597	MVD, mvaD	diphosphomevalonate decarboxylase [EC: 4.1.1.33]
97	G39569.t1	K05906	PCYOX1, FCLY	prenylcysteine oxidase/farnesylcysteine lyase [EC: 1.8.3.5 1.8.3.6]
Citrate cycle (TCA cycle) (map00020)				
98	G115.t1	K01647	CS, gltA	citrate synthase [EC: 2.3.3.1]
99	G777.t1	K01899	LSC1	succinyl-CoA synthetase alpha subunit [EC: 6.2.1.4 6.2.1.5]
100	G1358.t1	K00382	DLD, lpd, pdhD	dihydrolipoamide dehydrogenase [EC: 1.8.1.4]
101	G1497.t1	K00234	SDHA, SDH1	succinate dehydrogenase (ubiquinone) flavoprotein subunit [EC: 1.3.5.1]
102	G2517.t1	K01647	CS, gltA	citrate synthase [EC: 2.3.3.1]
103	G7103.t1	K00164	OGDH, sucA	2-oxoglutarate dehydrogenase E1 component [EC: 1.2.4.2]
104	G9705.t1	K01610	E4.1.1.49, pckA	phosphoenolpyruvate carboxykinase (ATP) [EC: 4.1.1.49]
105	G11248.t1	K01648	ACLY	ATP citrate (pro-S)-lyase [EC: 2.3.3.8]
106	G13750.t1	K00658	DLST, sucB	2-oxoglutarate dehydrogenase E2 component (dihydrolipoamide succinyltransferase) [EC: 2.3.1.61]
107	G15077.t1	K01681	ACO, acnA	aconitate hydratase [EC: 4.2.1.3]
108	G17507.t1	K00627	DLAT, aceF, pdhC	pyruvate dehydrogenase E2 component (dihydrolipoamide acetyltransferase) [EC: 2.3.1.12]
109	G18607.t1	K00382	DLD, lpd, pdhD	dihydrolipoamide dehydrogenase [EC: 1.8.1.4]
110	G23327.t1	K00161	aceE	pyruvate dehydrogenase E1 component [EC: 1.2.4.1]
111	G28266.t1	K00031	IDH1, IDH2, icd	isocitrate dehydrogenase [EC: 1.1.1.42]
112	G28544.t1	K00030	IDH3	isocitrate dehydrogenase (NAD+) [EC: 1.1.1.41]
113	G39479.t1	K01681	ACO, acnA	aconitate hydratase [EC: 4.2.1.3]

MVA pathway to yield IPP units. The geranyl diphosphate (GPP) mediated step produces GOL from IPP in lemongrass plastids [34] [Table 4 and Figure 2].

IPP and dimethylallyl diphosphate (DMAPP) units are condensed to form GPP. IPP is converted to GPP by GPP synthase or GPS (E.C. 2.5.1.1) through the MVA and MEP pathways. GOL is a precursor for essential oil biosynthesis in lemongrass and yields all the major components through multiple reversible and irreversible reactions [35].

The number of genes identified in terpene synthesis is 34, and Supplementary Table 5 presents the detailed table. The number of genes identified in MEP and mevalonic acid (MVA) is 37. Supplementary Table 6 shows the detailed table. The genes identified in the metabolic pathways of MEP and MVA, can further be validated in the wet laboratory study.

4. CONCLUSION

The biosynthesis of essential oil starts with glucose production through photosynthesis. Glucose undergoes glycolysis in the cytoplasm, yielding pyruvate. Pyruvate is a substrate for the biosynthesis of IPP through the MVA or MEP pathways. The IPP and DMAPP units are condensed, forming GPP by GPP synthase leading to GOL. GOL is the precursor for essential oil (GAL, NAL, and CAL) biosynthesis through multiple reversible and irreversible reactions. This study presents the draft *de-novo* assembly (scaffold-level assembly with gaps) and annotation of *C. citratus* as a valuable resource for the scientific community. This study also identified and mapped genes participating in pathways of photosynthesis, glycolysis, pyruvate, terpenoid backbone synthesis, and TCA cycle, which are associated with essential oil production in lemon grass. Future studies include validating the genes identified in terpene synthesis, MEP and MVA through wet laboratory studies. This study will help in understanding the biosynthesis of essential oil production.

5. ACKNOWLEDGMENT

NC and NNNR are grateful to the management of GITAM (Deemed to be University) for providing the necessary facilities to carry out the research work and extending constant support. The authors are grateful to Dr. Stacy Pirro, Iridian Genomes Inc, USA, for allowing us to use their public data sets for whole-genome or organelle assembly and/or annotation; and submit genome assemblies to NCBI GenBank as Third-Party Annotation (TPA).

6. AUTHORS' CONTRIBUTIONS

All authors made substantial contributions to the conception and design, acquisition of data, or analysis and interpretation of data; took part in drafting the article or revising it critically for important intellectual content; agreed to submit to the current journal; gave final approval of the version to be published; and agreed to be accountable for all aspects of the work. All the authors are eligible to be an author as per the International Committee of Medical Journal Editors (ICMJE) requirements/guidelines.

7. FUNDING

There is no funding to report.

8. CONFLICTS OF INTEREST

The authors report no financial or any other conflicts of interest in this work.

9. ETHICAL APPROVALS

This study does not involve experiments on animals or human subjects.

10. DATA AVAILABILITY

The assembled nuclear genome, mitochondrial genome, and chloroplast genome of lemon grass (C. citratus L.) were deposited to NCBI Genome as TPA (Third Party Annotation) submission with accession numbers DXKC00000000, BK059359, and BK059356 respectively. The supplementary files generated in this study and the nuclear and organelle genome annotations were deposited to Harvard dataverse (https://doi.org/10.7910/DVN/ZTM70X).

11. PUBLISHER'S NOTE

This journal remains neutral with regard to jurisdictional claims in published institutional affiliation.

REFERENCES

1. Meena S, Kumar SR, Venkata Rao DK, Dwivedi V, Shilpashree HB, Rastogi S, *et al*. *De novo* sequencing and analysis of lemongrass transcriptome provide first insights into the essential oil biosynthesis of aromatic grasses. Front Plant Sci 2016;7:1129.
2. Bertea CM, Maffei ME. The genus *Cymbopogon*-botany, including anatomy, physiology, biochemistry, and molecular biology. In: Akhila A, editor. Essential Oil-bearing Grasses, The Genus *Cymbopogon*. Boca Raton: CRC Press; 2010. p. 1-24.
3. Padalia RC, Verma RS, Chanotiya CS, Yadav A. Chemical fingerprinting of the fragrant volatiles of nineteen Indian cultivars of *Cymbopogon* spreng (*Poaceae*). Rec Nat Prod 2011;5:290-9.
4. Devi K, Dehury B, Phukon M, Modi MK, Sen P. Novel insights into structure-function mechanism and tissue-specific expression profiling of full-length dxr gene from Cymbopogon winterianus. FEBS Open Bio 2015;5:325-34.
5. Khanuja SP, Shasany AK, Pawar A, Lal RK, Darokar MP, Naqvi AA, *et al.* Essential oil constituents and RAPD markers to establish species relationship in *Cymbopogon* Spreng. (*Poaceae*). Biochem Syst Ecol 2005;33:171-86.
6. Moyler DA. Citral from lemongrass and other natural sources: Its toxicology and legislation. In: Akhila A, editor. Essential Oil-bearing Grasses. Boca Raton: CRC Press; 2010. p. 223-38.
7. Pimentel MR, Molina G, Bertucci TC, Pastore GM. Biotransformation of citronellol in rose oxide by *Pseudomonas* spp. Chem Eng Trans 2012;27:295-300.
8. Bayala B, Bassole IH, Scifo R, Gnoula C, Morel L, Lobaccaro JM, *et al.* Anticancer activity of essential oils and their chemical components-a review. Am J Cancer Res 2014;4:591-607.
9. *Cymbopogon*. National Center for Biotechnology Information; 2022. Available from: https://www.ncbi.nlm.nih.gov/search/all/?term=cymbopogo n%20 [Last accessed on 2022 Nov 17].
10. *Cymbopogon citratus*. National Center for Biotechnology Information; 2022. Available from: https://www.ncbi.nlm.nih.gov/search/all/?term=cymbopogon++citratus [Last accessed on 2022 Nov 17].
11. Neelapu NR, Surekha C. Next-generation sequencing and metagenomics. In: Wong KC, editor. Computational Biology and Bioinformatics: Gene Regulation. Boca Raton: CRC Press; 2016. p. 331-51.
12. Yadav V, Lekkala MM, Surekha C, Neelapu NR. Global scenario of advance fungal research in crop protection. In: Yadav AN, Mishra S, Kour D, Yadav N, Kumar A, editors. Agriculturally Important Fungi for Sustainable Agriculture. Cham: Springer; 2020. p. 313-46.
13. *Cymbopogon citratus*. National Center for Biotechnology Information; 2022. Available from: https://www.ncbi.nlm.nih.gov/bioproject [Last accessed on 2022 Nov 17].
14. Chakravartty N, Neelapu NR. The *de novo* genome assembly (nuclear, chloroplast and mitochondria) of ornamental plant pygmy date palm *Phoenix roebelenii*. J Appl Biol Biotech 2023;11:113-22.
15. Schubert M, Lindgreen S, Orlando L. AdapterRemoval v2: Rapid adapter trimming, identification, and read merging. BMC Res Notes 2016;9:88.
16. Marçais G, Kingford C. A fast, lock-free approach for efficient parallel counting of occurrences of k-mers. Bioinformatics 2011;27:764-70.
17. Vurture GW, Sedlazeck FJ, Nattestad M, Underwood CJ, Fang H, Gurtowski J, *et al*. GenomeScope: Fast reference-free genome profiling from short reads. Bioinformatics 2017;33:2202-4.
18. Zimin AV, Marçais G, Puiu D, Roberts M, Salzberg SL, Yorke JA.

The MaSuRCA genome assembler. Bioinformatics 2013;29: 2669-77.
19. Seppey M, Manni M, Zdobnov EM. BUSCO: Assessing genome assembly and annotation completeness. Methods Mol Biol 2019;1962:227-45.
20. Institute for Systems Biology. RepeatModeler. Seattle: Institute for Systems Biology; 2021. Available from: https://www.repeatmasker.org.repeatmodeler [Last accessed on 2022 Feb 04].
21. Tarailo-Graovac M, Chen N. Using RepeatMasker to identify repetitive elements in genomic sequences. Curr Protoc Bioinformatics 2009;Chapter 4:Unit 4.10. doi: 10.1002/0471250953.bi0410s25.
22. Stanke M, Diekhans M, Baertsch R, Haussler D. Using native and syntenically mapped cDNA alignments to improve *de novo* gene finding. Bioinformatics 2008;24:637-44.
23. Chan PP, Lin BY, Mak AJ, Lowe TM. tRNAscan-SE 2.0: Improved detection and functional classification of transfer RNA genes. Nucleic Acids Res 2021;49:9077-96.
24. Emms DM, Kelly S. OrthoFinder: Phylogenetic orthology inference for comparative genomics. Genome Biol 2019;20:238.
25. UniProt Consortium. UniProt: The universal protein knowledgebase in 2021. Nucleic Acids Res 2021;49:D480-9.
26. Beier S, Thiel T, Münch T, Scholz U, Mascher M. MISA-web: A web server for microsatellite prediction. Bioinformatics 2017;33:2583-5.
27. Untergasser A, Cutcutache I, Koressaar T, Ye J, Faircloth BC, Remm M, *et al.* Primer3--new capabilities and interfaces. Nucleic Acids Res 2012;40:e115.
28. Thimm O, Bläsing O, Gibon Y, Nagel A, Meyer S, Krüger P, *et al*. MAPMAN: A user-driven tool to display genomics data sets onto diagrams of metabolic pathways and other biological processes. Plant J 2004;37:914-39.
29. Kanehisa M, Furumichi M, Sato Y, Kawashima M, Ishiguro-Watanabe M. KEGG for taxonomy-based analysis of pathways and genomes. Nucleic Acids Res 2023;51:D587-92.
30. Jin JJ, Yu WB, Yang JB, Song Y, dePamphilis CW, Yi TS, *et al.* GetOrganelle: A fast and versatile toolkit for accurate *de novo* assembly of organelle genomes. Genome Biol 2020;21:241.
31. Shi L, Chen H, Jiang M, Wang L, Wu X, Huang L, *et al.* CPGAVAS2, an integrated plastome sequence annotator and analyzer. Nucleic Acids Res 2019;47:W65-73.
32. Jung J, Kim JI, Jeong YS, Yi G. AGORA: Organellar genome annotation from the amino acid and nucleotide references. Bioinformatics 2018;34:2661-3.
33. Challa S, Neelapu NR. Phylogenetic trees: Applications, construction, and assessment. In: Hakeem KR, Shaik N, Banaganapalli B, Elango R, editors. Essentials of Bioinformatics. Vol. 3. Cham: Springer; 2019. p. 167-92.
34. FigTree Version 1.4.4. Edinburgh: Produce High-quality Figures of Phylogenetic Trees; 2022. Available from: https://www.tree.bio.ed.ac.uk/software/figtree [Last accessed on 2022 Aug 27].
35. Mukarram M, Choudhary S, Khan MA, Poltronieri P, Khan MM, Ali J, *et al*. Lemongrass essential oil components with antimicrobial and anticancer activities. Antioxidants (Basel) 2021;11:20.
36. Mukarram M, Khan MM, Zehra A, Choudhary S, Naeem M. Biosynthesis of lemongrass essential oil and the underlying mechanism for its insecticidal activity. In: Aftab T, Hakeem KR, editors. Medicinal and Aromatic Plants. Cham: Springer; 2021. p. 429-43.

How to cite this article:
Chakravartty N, Neelapu NRR. The *de novo* genome assembly of lemon grass to identify the genes in essential oil production. J App Biol Biotech. 2024;12(2):100-149. DOI: 10.7324/JABB.2024.125317

SUPPLEMENTARY MATERIALS

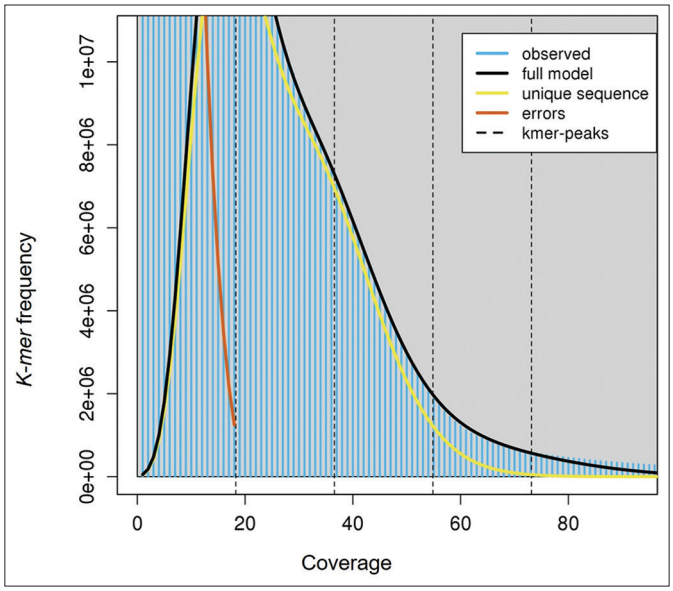

Supplementary Figure 1: The K-mer histogram for estimation of genome size in lemon grass. The figure shows K-mers frequency in lemon grass's genome, which is predicted using Jellyfish and visualized using GenomeScope. A graph was plotted with K-mer frequency on the X-axis and the coverage on the Y-axis. The predicted genome size of lemon grass is 454,049,232 bp.

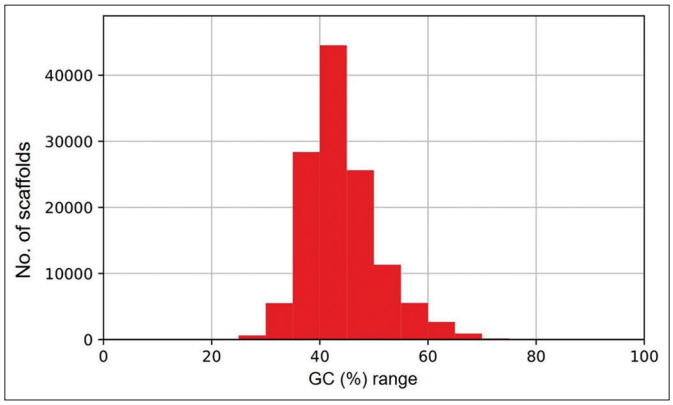

Supplementary Figure 2: The distribution of G.C. percentage in the assembled genome of lemon grass. The figure shows the distribution of G.C. percentage in the assembled genome of lemon grass. A graph was plotted with the G.C. percentage range (G.C. %) on the X-axis and the number of scaffolds (contigs) on the Y-axis. The G.C. percentage in the assembled genome of lemon grass is ~ 43.86%.

Supplementary Table 1: The summary of BUSCO score parameters to evaluate the completeness of lemon grass.

S. No	BUSCO Statistics	Count	Percentage
1	Complete BUSCOs (C)	259	60.90%
2	Complete and single-copy BUSCOs (S)	250	58.80%
3	Complete and duplicated BUSCOs (D)	9	2.10%
4	Fragmented BUSCOs (F)	91	21.40%
5	Missing BUSCOs (M)	75	17.7%
6	Total BUSCO groups searched	425	100.00%

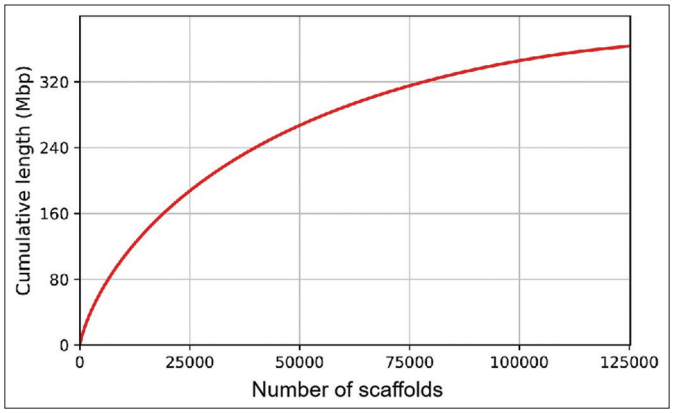

Supplementary Figure 3: The cumulative length distribution of the assembled genome in lemon grass. The figure shows the distribution of scaffold length distribution in the assembled genome of lemon grass. A graph was plotted with the scaffold length range on the X-axis and the number of scaffolds on the Y-axis.

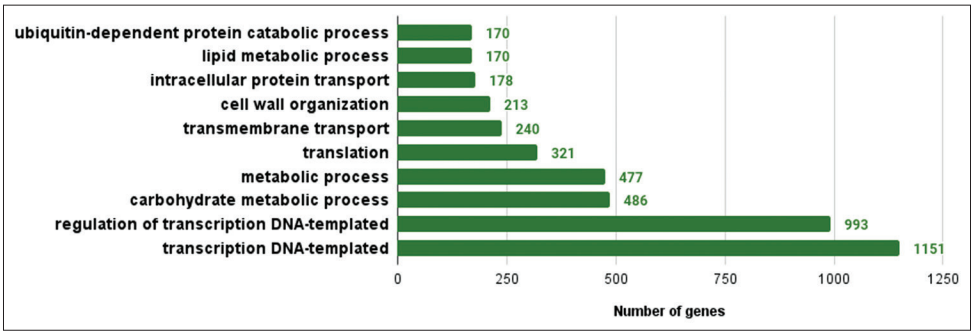

Supplementary Figure 4: The gene ontologies related to biological process observed in lemon grass. The figure shows gene ontologies related to biological processes observed in lemon grass. A graph with gene ontologies of biological processes on the X-axis and the number of genes on the Y-axis is plotted.

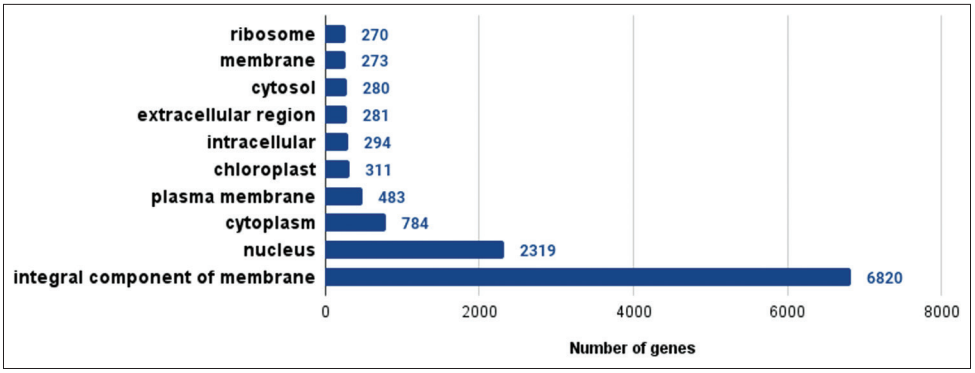

Supplementary Figure 5: The gene ontologies related to cellular components observed in lemon grass. The figure shows gene ontologies related to cellular components observed in lemon grass. A graph with gene ontologies of cellular components on the X-axis and the number of genes on the Y-axis is plotted.

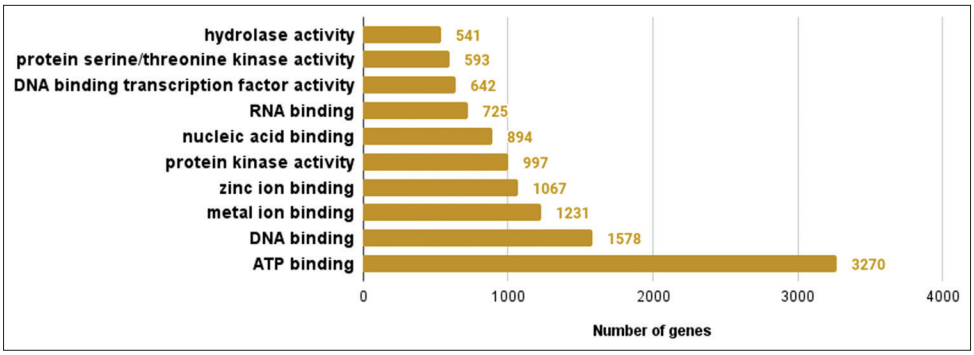

Supplementary Figure 6: The gene ontologies related to molecular function observed in lemon grass. The figure shows gene ontologies related to molecular functions observed in lemon grass. A graph with gene ontologies of molecular functions on the X-axis and a number of genes on the Y-axis is plotted.

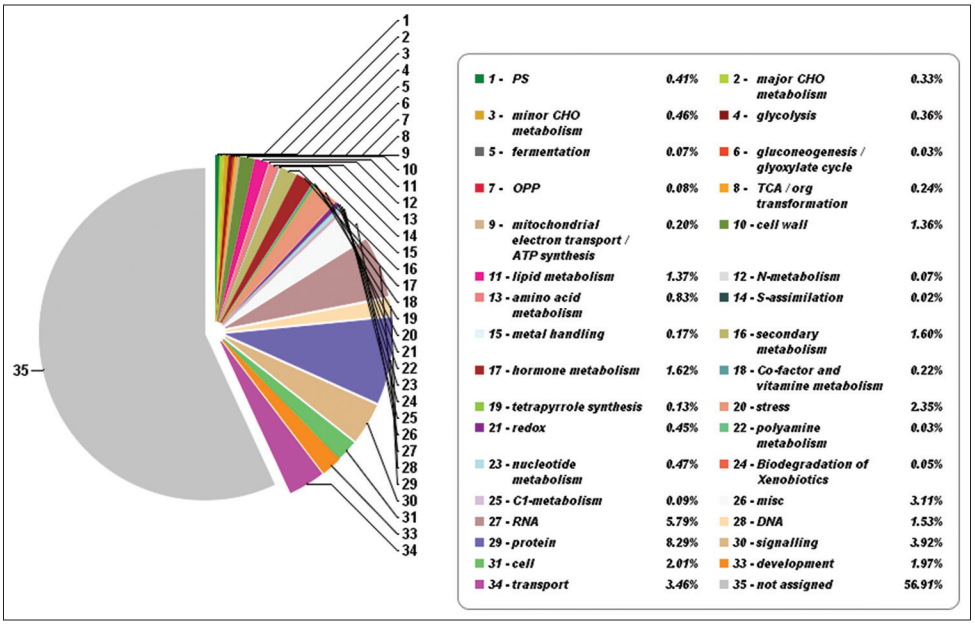

Supplementary Figure 7: The pathway summary predicted with Mapman. This figure shows thirty-four metabolic categories along with the participating percentage of genes having a significant role in the metabolic pathways of lemon grass. Mapman analysis identified 43.09% of genes having a significant role in metabolic pathways.

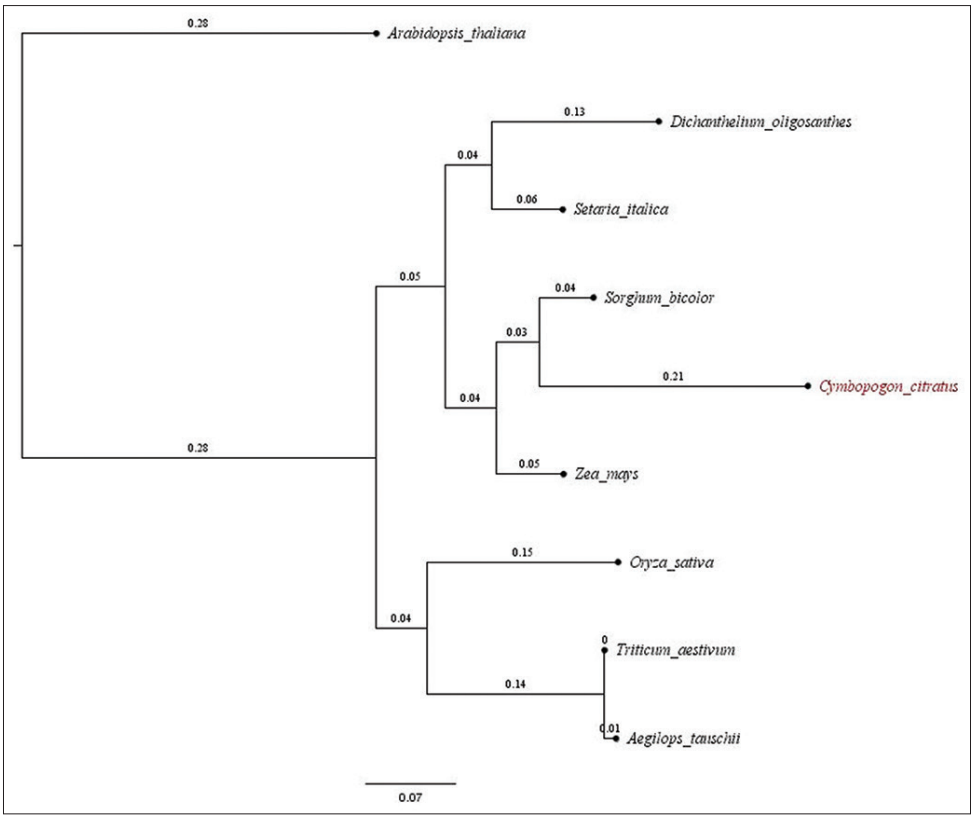

Supplementary Figure 8: The linear tree generated between model plants and *Cymbopogon citratus*. This figure shows the linear tree generated based on orthology between *Aegilops tauschii, Arabidopsis thaliana, Dichanthelium oligosanthes, Oryza sativa, Setaria italica, Sorghum bicolor, Triticum aestivu, Zea mays*. The orthology data was generated using OrthoFinder version 2.3.11 for the above species. The orthology data was used to construct a linear tree based on the maximum likelihood method, and the tree was viewed in FigTree version 1.4.4.

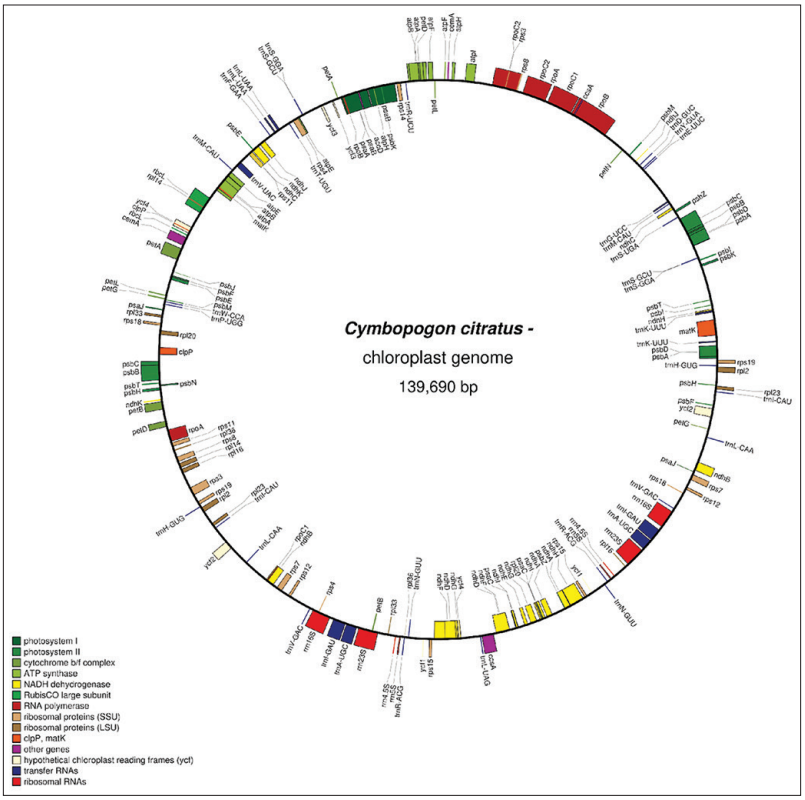

Supplementary Figure 9: The chloroplast genome and annotation of lemon grass. This figure shows a circular chloroplast genome of 139,690 bps generated without gaps using GetOrganelle version 1.6.4. This figure also shows chloroplast genome annotation predicted using CPGAVAS2 version 1.

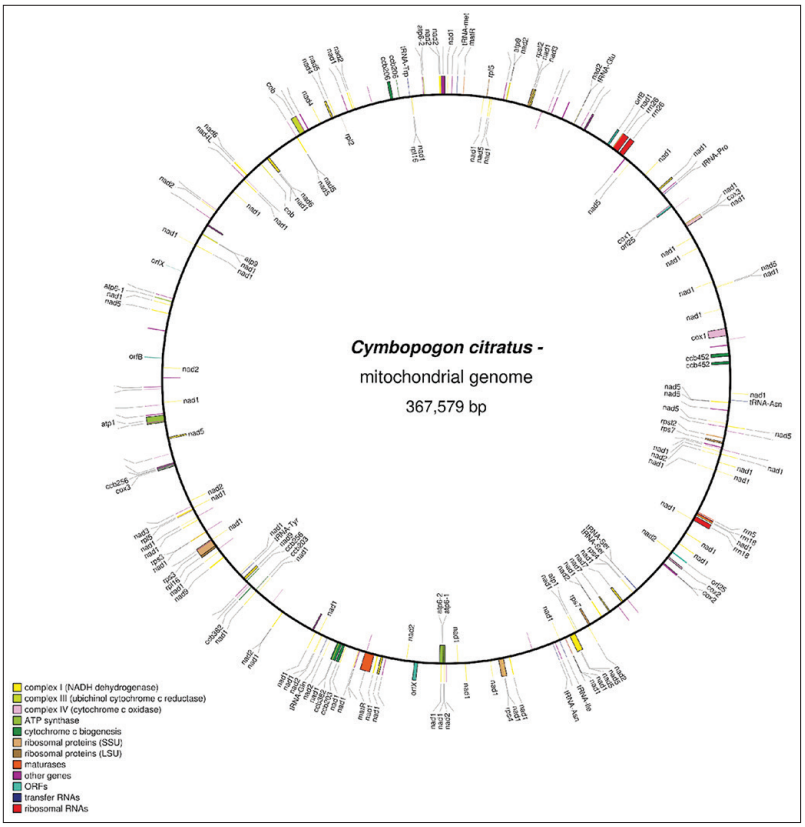

Supplementary Figure 10: The mitochondrial genome and annotation of lemon grass. This figure shows a circular mitochondrial genome of 367,579 bps generated without any gap using GetOrganelle version 1.6.4. This figure also shows mitochondrial genome annotation predicted using AGORA version 1.

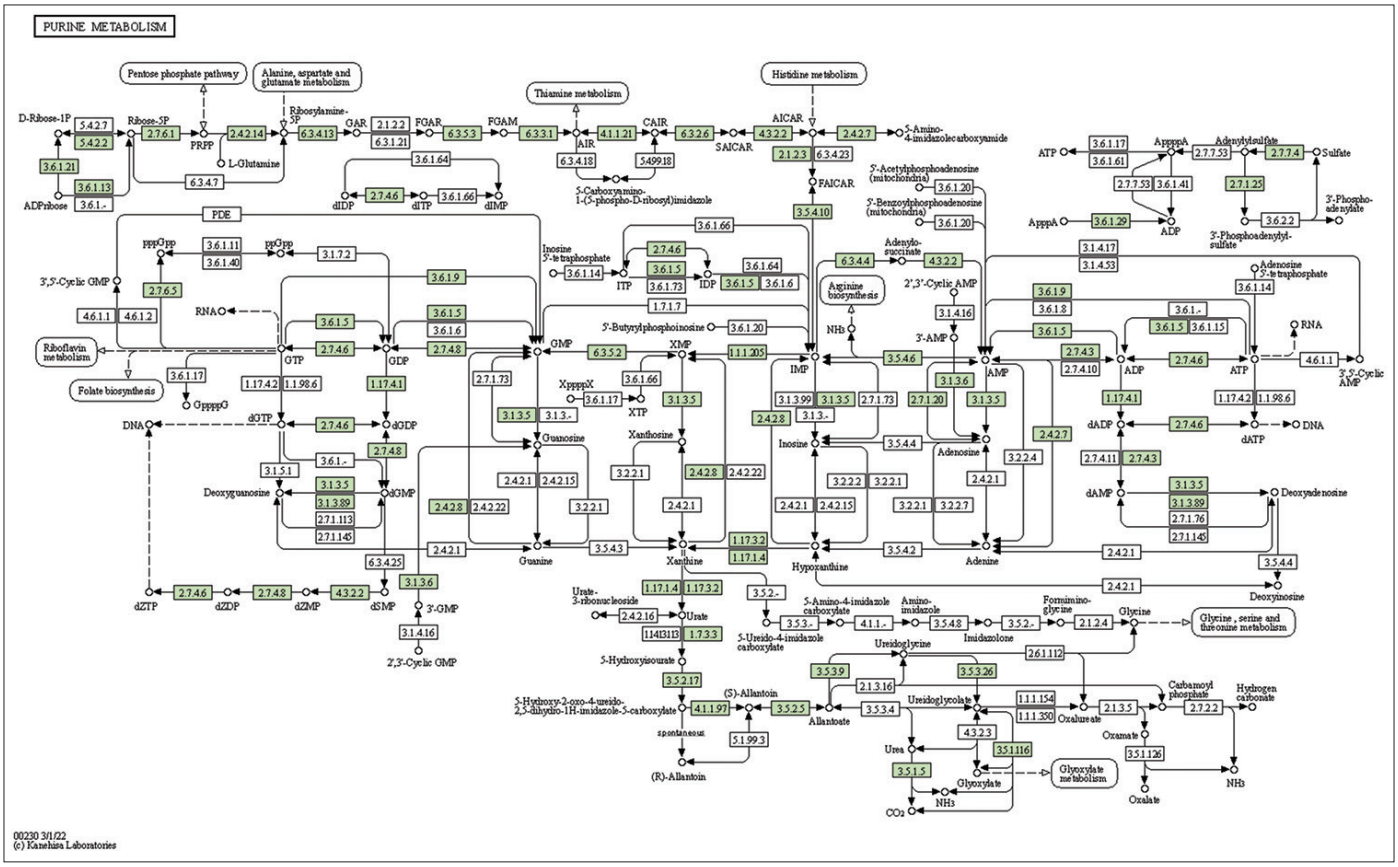

Supplementary Figure 11: The genes associated with metabolites of purine metabolism. This figure shows 43 genes associated with metabolites of purine metabolism, and the genes were highlighted in the pathway. These genes are mapped onto the pathway and were retrieved from KAAS.

Supplementary Table 2: The summary of repeats predicted in the genome of lemon grass.

S.No.	Type of repeats	Number of repeats	Length of repeats	Elements occupied(%)
1	SINEs	665	72070 bp	0.02%
2	LINEs	26231	13279888 bp	3.64%
3	LTR elements	51540	36376114 bp	9.98%
4	DNA elements	12288	5427562 bp	1.49%
5	Unclassified	366513	92614638 bp	25.41%
6	Total interspersed repeats		147770272 bp	40.55%
7	Small RNA	355	80194 bp	0.02%
8	Satellites	229	159256 bp	0.04%
9	Simple repeats	63921	2647666 bp	0.73%
10	Low complexity	7157	352141 bp	0.10%

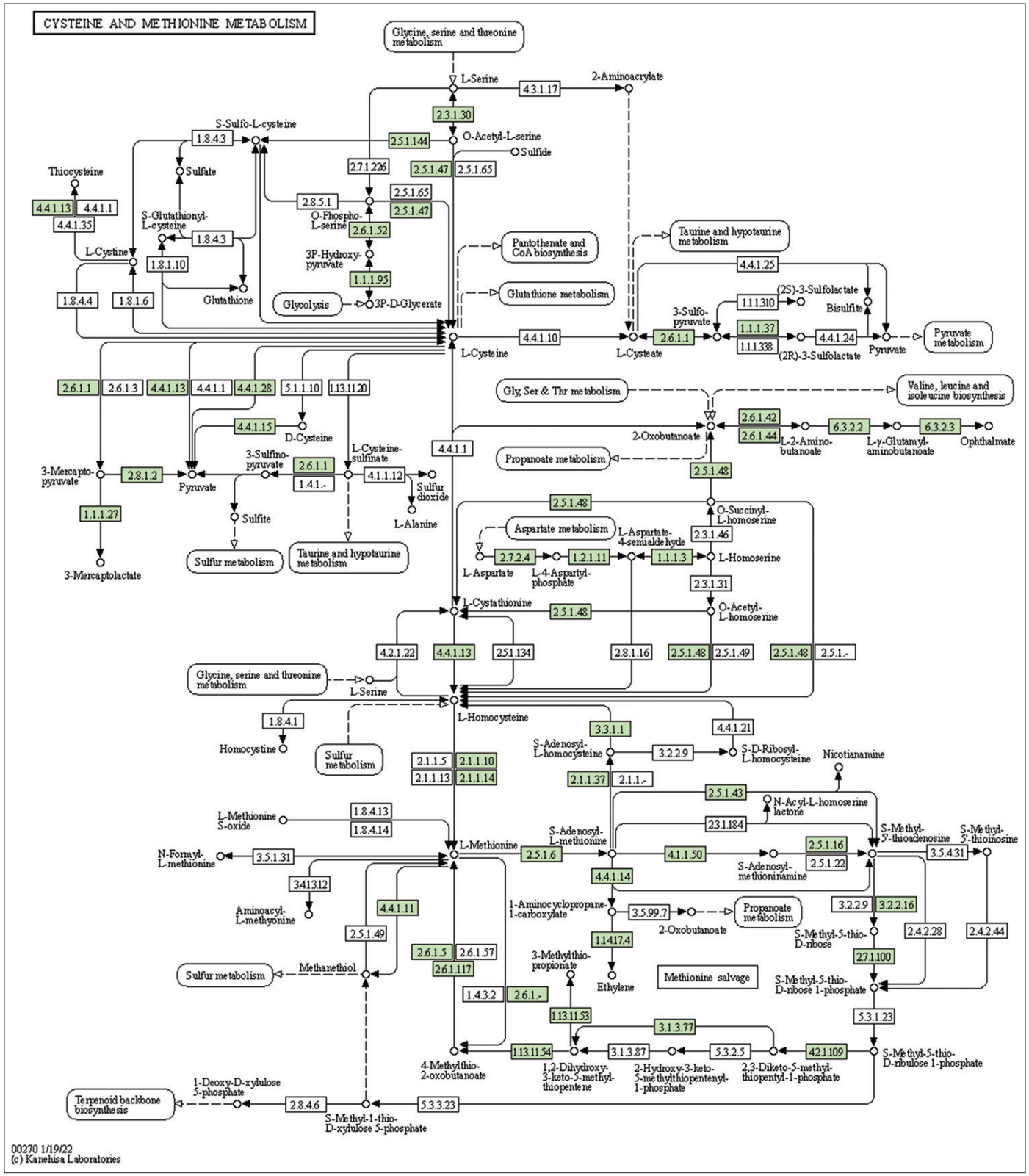

Supplementary Figure 12: The genes associated with metabolites of cysteine and methionine metabolism. This figure shows 43 genes associated with cysteine and methionine metabolism, and the genes were highlighted in the pathway. These genes are mapped onto the pathway and were retrieved from KAAS.

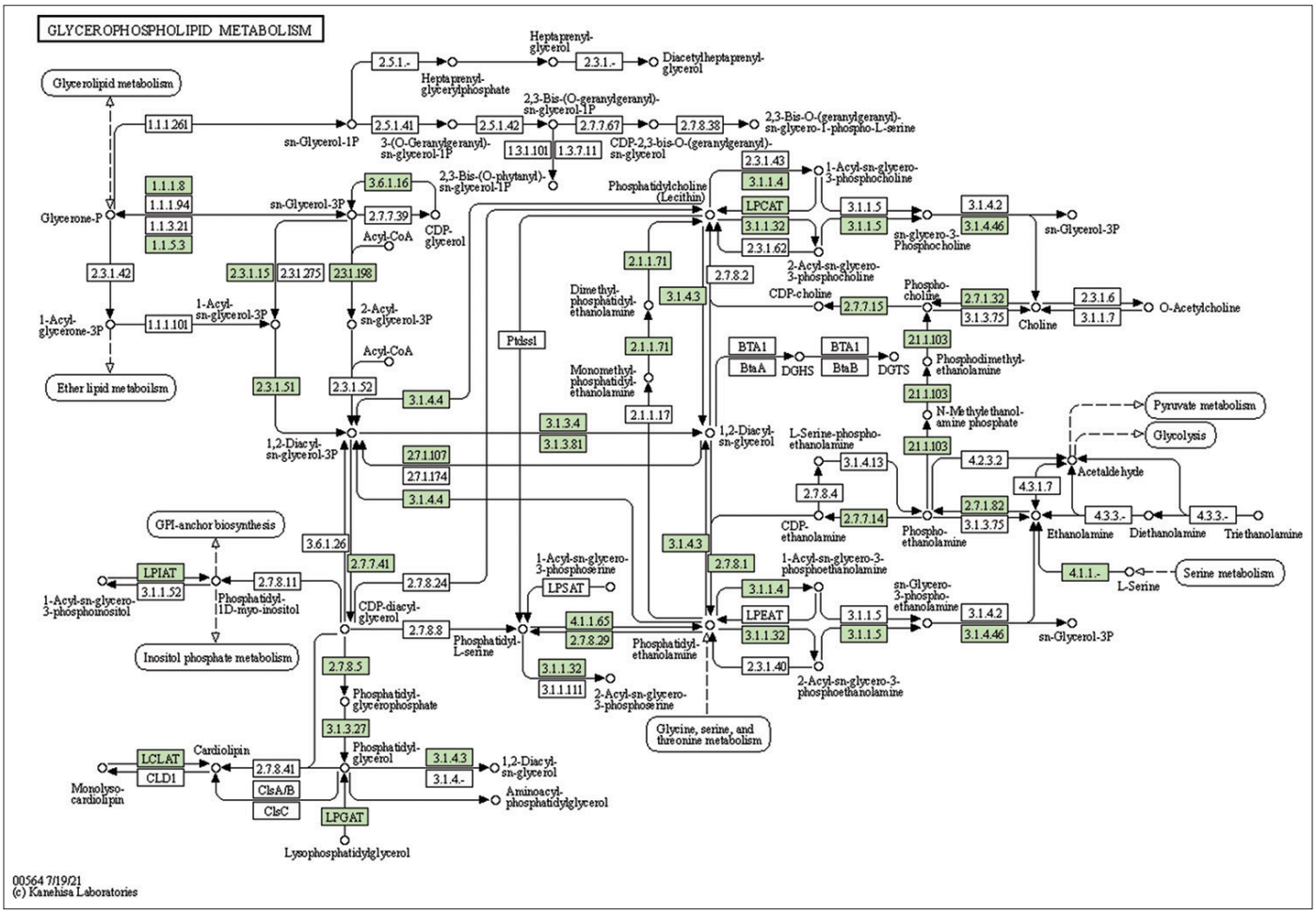

Supplementary Figure 13: The genes associated with metabolites of glycerophospholipid metabolism. This figure shows 35 genes associated with glycerophospholipid metabolism, and the genes were highlighted in the pathway. These genes are mapped onto the pathway and were retrieved from KAAS.

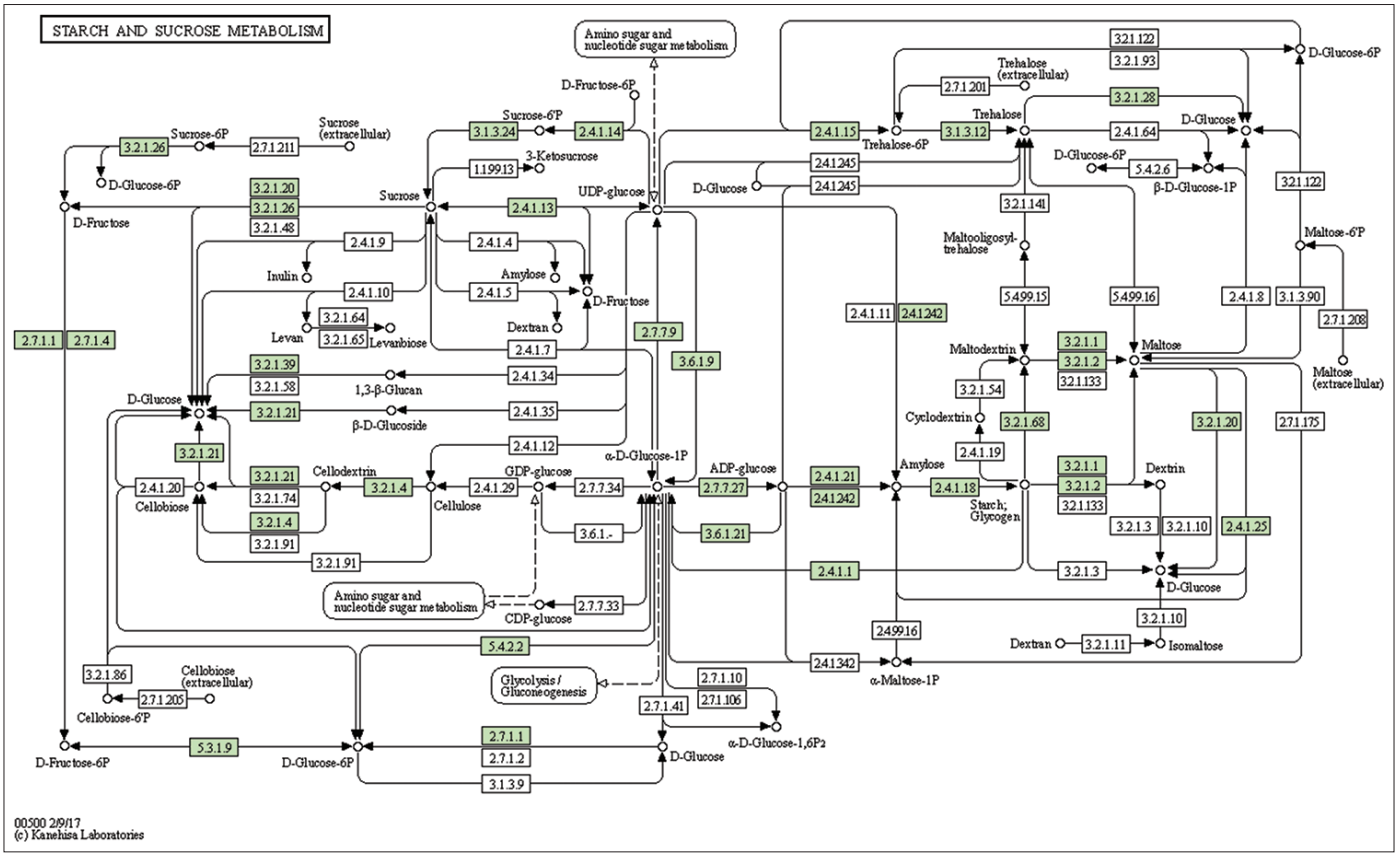

Supplementary Figure 14: The genes associated with metabolites of starch and sucrose metabolism. This figure shows 31 genes associated with starch and sucrose metabolism, and the genes were highlighted in the pathway. These genes are mapped onto the pathway and were retrieved from KAAS.

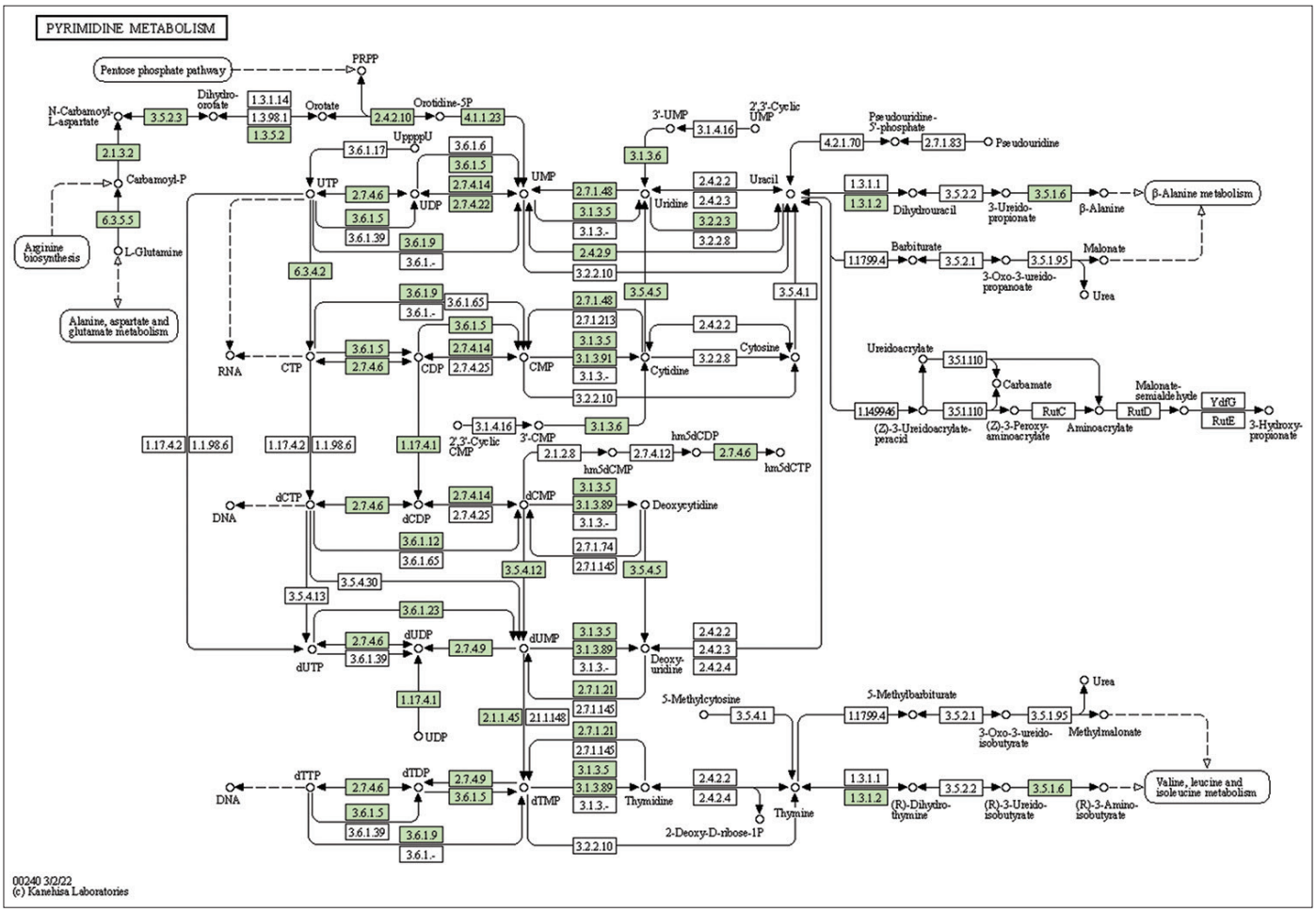

Supplementary Figure 15: The genes associated with metabolites of pyrimidine metabolism. This figure shows 30 genes associated with pyrimidine metabolism, and the genes were highlighted in the pathway. These genes are mapped onto the pathway and were retrieved from KAAS.

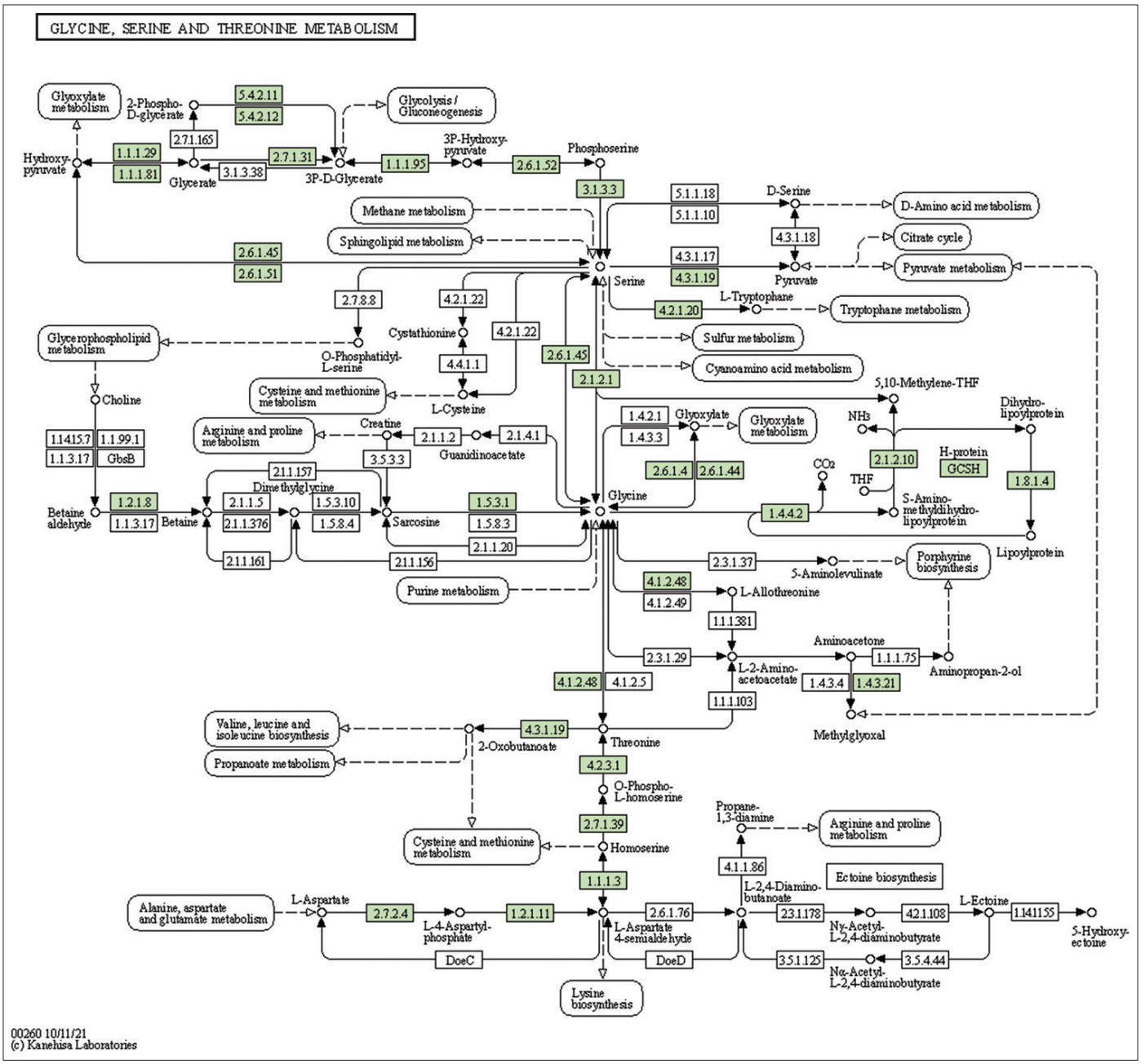

Supplementary Figure 16: The genes associated with metabolites of glycine, serine, and threonine metabolism. This figure shows 29 genes associated with glycine, serine, and threonine metabolism, and the genes were highlighted in the pathway. These genes are mapped onto the pathway and were retrieved from KAAS.

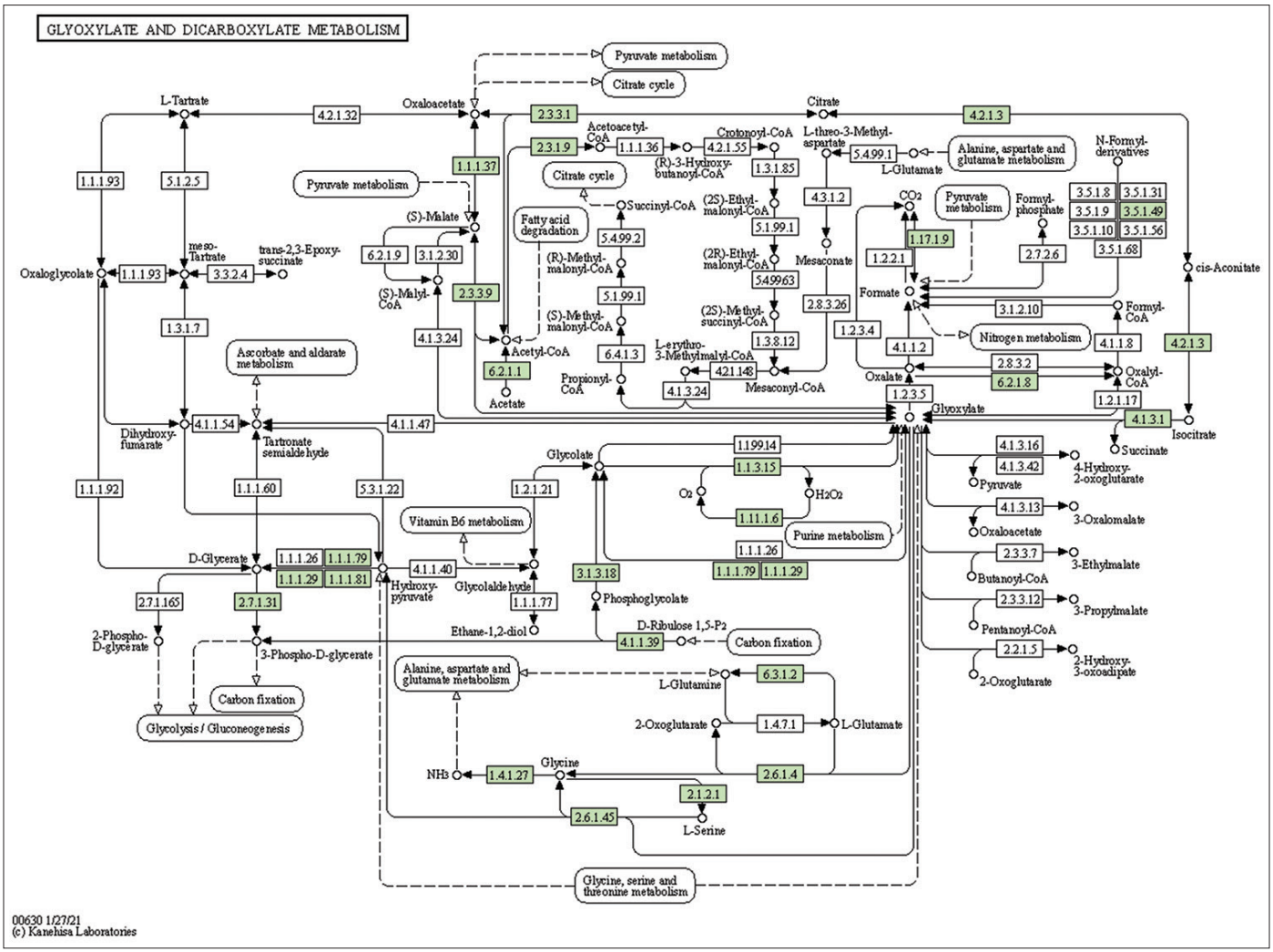

Supplementary Figure 17: The genes associated with metabolites of glyoxylate and dicarboxylate metabolism. This figure shows 28 genes associated with glyoxylate and dicarboxylate metabolism, and the genes were highlighted in the pathway. These genes are mapped onto the pathway and were retrieved from KAAS.

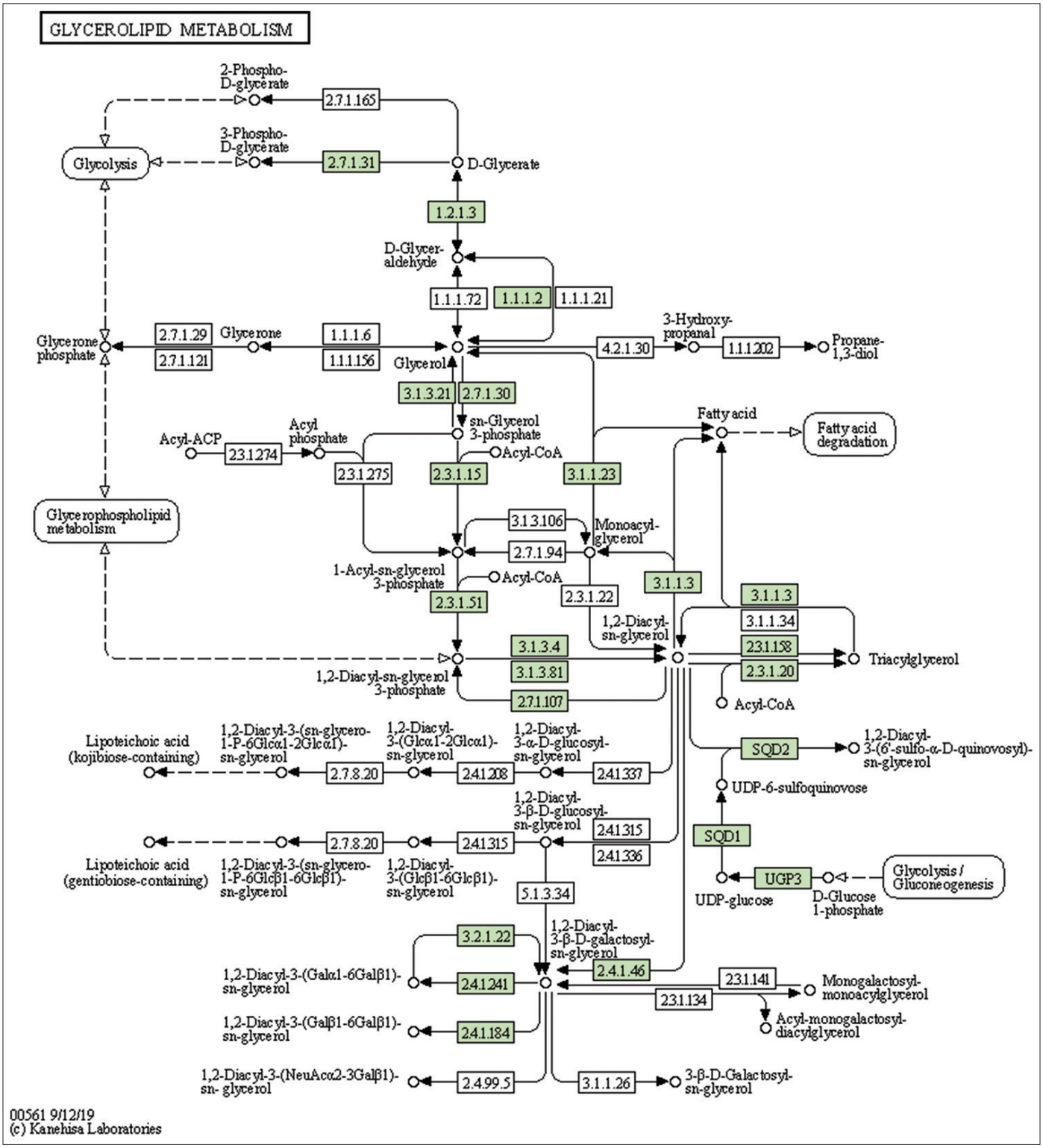

Supplementary Figure 18: The genes associated with metabolites of glycerolipid metabolism. This figure shows 29 genes associated with glycerolipid metabolism, and the genes were highlighted in the pathway. These genes are mapped onto the pathway and were retrieved from KAAS.

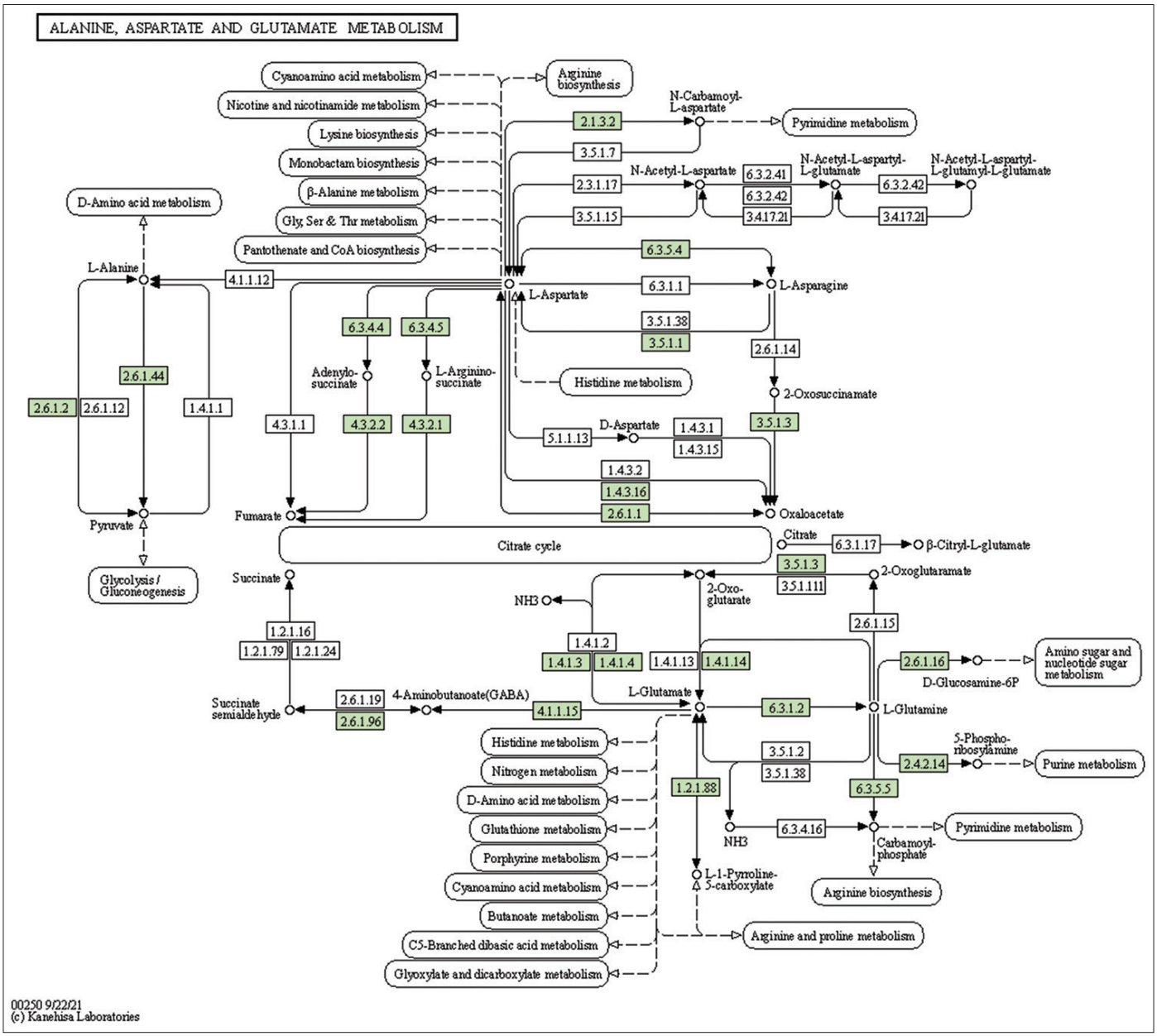

Supplementary Figure 19: The genes associated with metabolites of alanine, aspartate and glutamate metabolism. This figure shows 27 genes associated with alanine, aspartate, and glutamate metabolism, and the genes were highlighted in the pathway. These genes are mapped onto the pathway and were retrieved from KAAS.

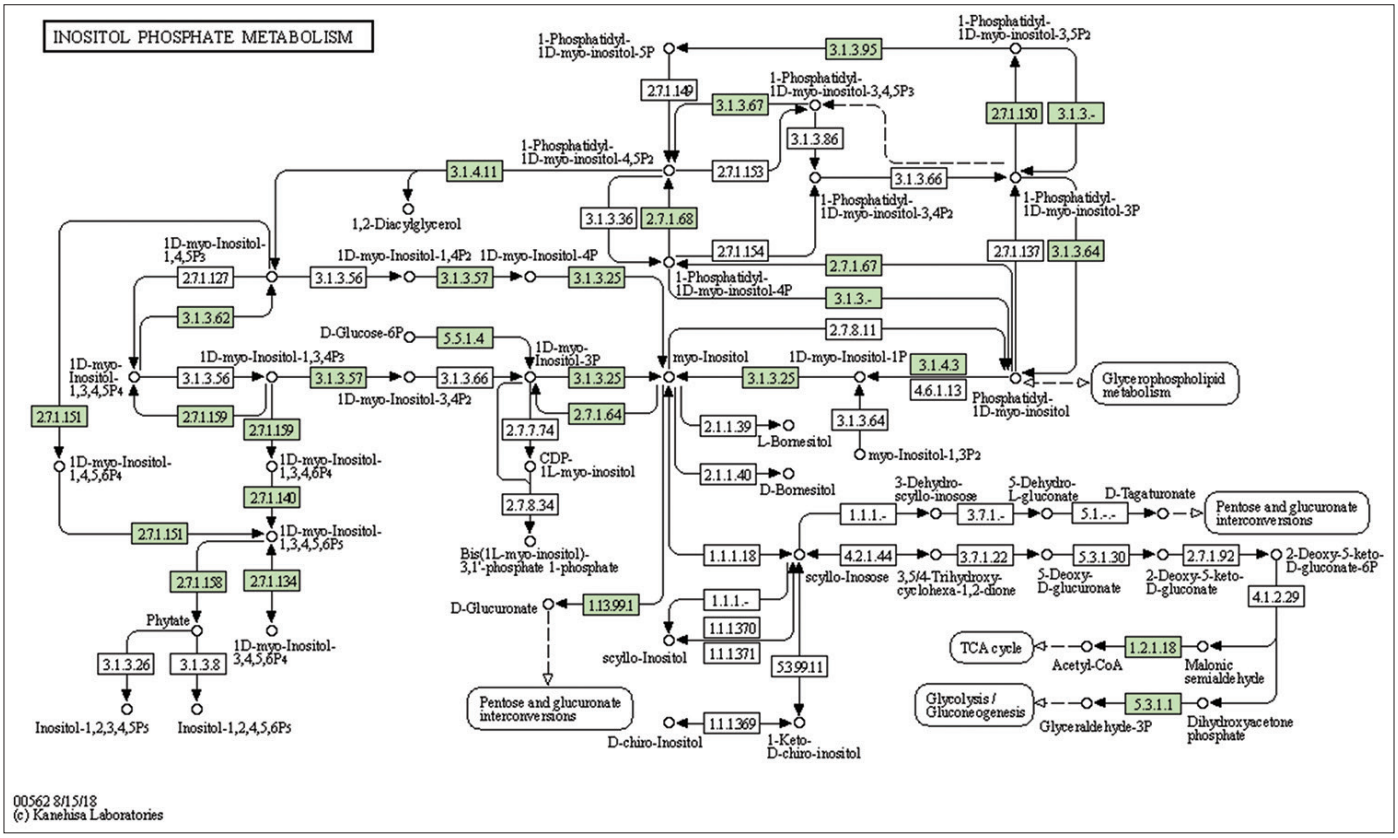

Supplementary Figure 20: The genes associated with metabolites of inositol phosphate metabolism. This figure shows 23 genes associated with inositol phosphate metabolism, and the genes were highlighted in the pathway. These genes are mapped onto the pathway and were retrieved from KAAS.

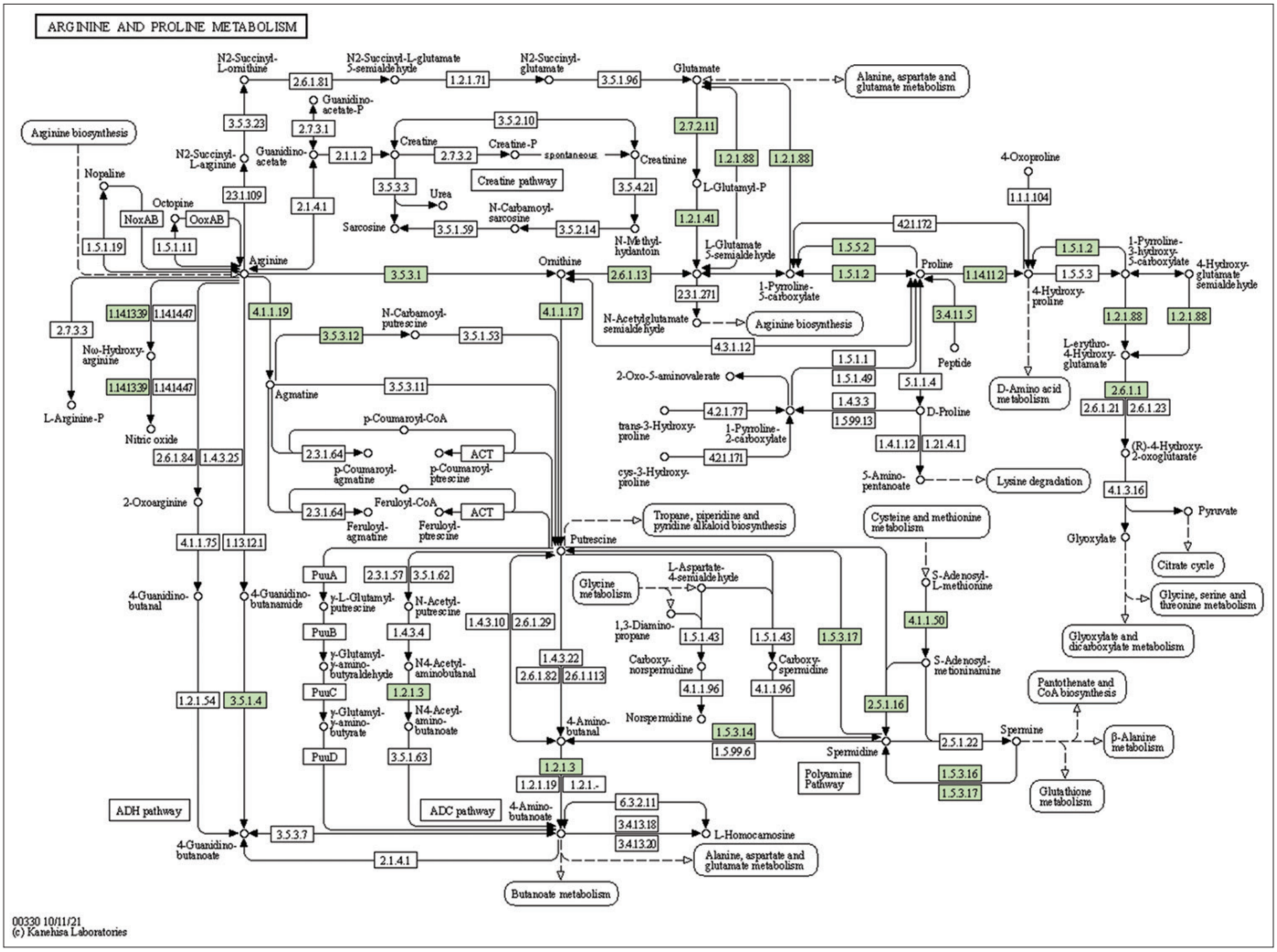

Supplementary Figure 21: The genes associated with metabolites of arginine and proline metabolism. This figure shows 22 genes associated with arginine and proline metabolism, and the genes were highlighted in the pathway. These genes are mapped onto the pathway and were retrieved from KAAS.

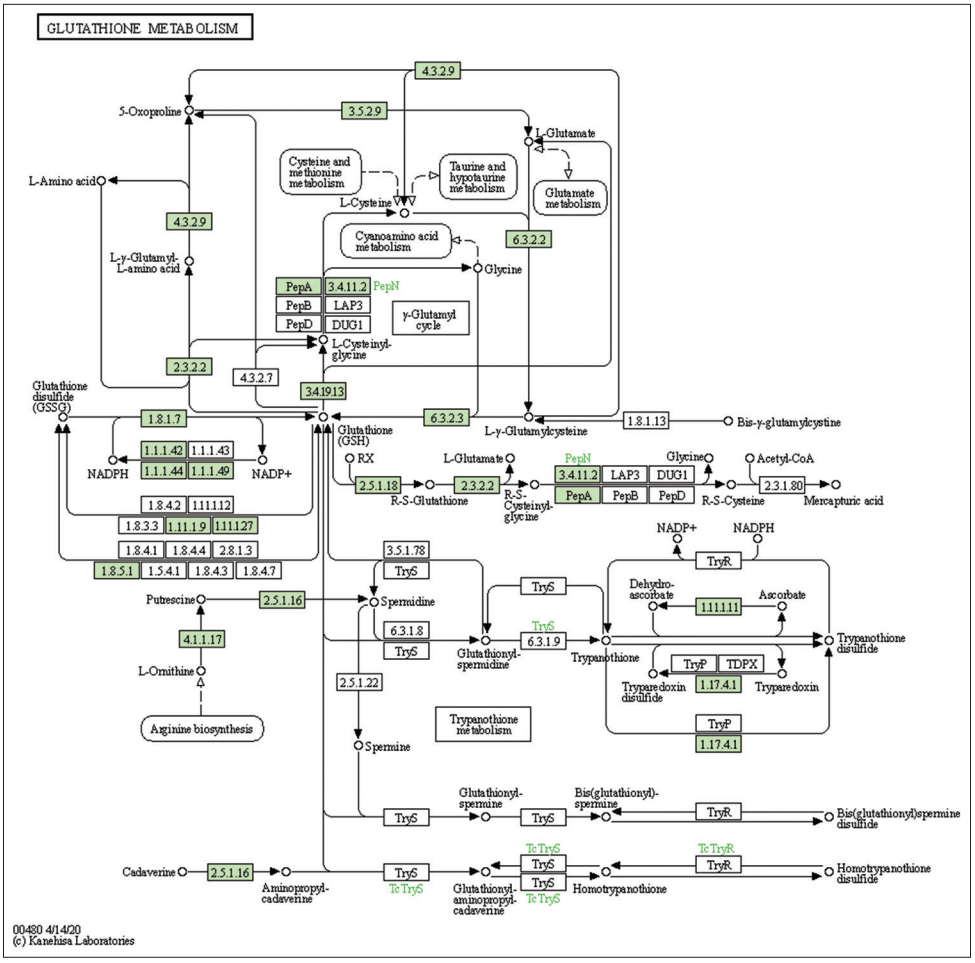

Supplementary Figure 22: The genes associated with metabolites of glutathione metabolism. This figure shows 20 genes associated with glutathione metabolism, and the genes were highlighted in the pathway. These genes are mapped onto the pathway and were retrieved from KAAS.

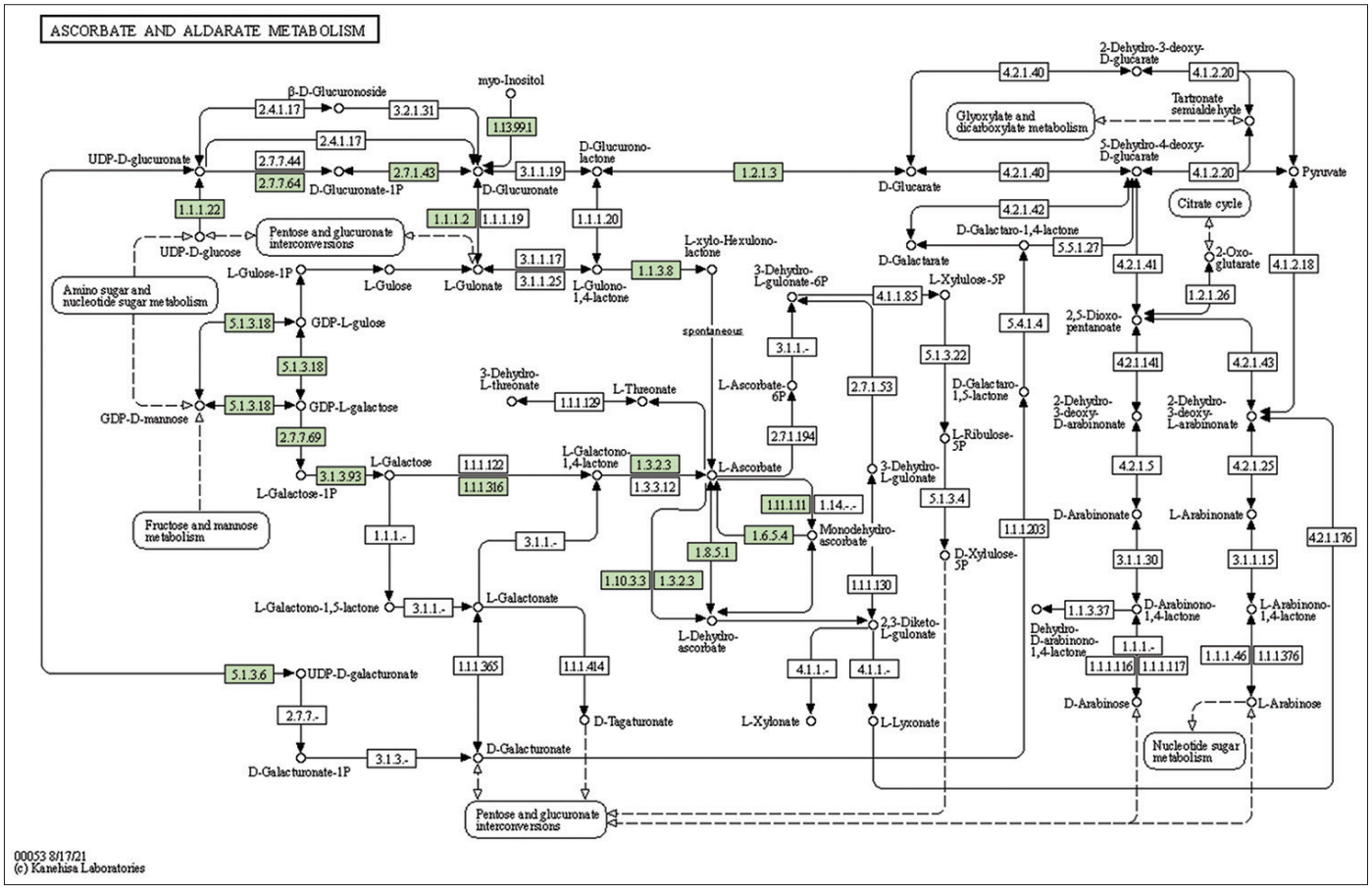

Supplementary Figure 23: The genes associated with metabolites of ascorbate and aldarate metabolism. This figure shows 19 genes associated with ascorbate and aldarate metabolism, and the genes were highlighted in the pathway. These genes are mapped onto the pathway and were retrieved from KAAS.

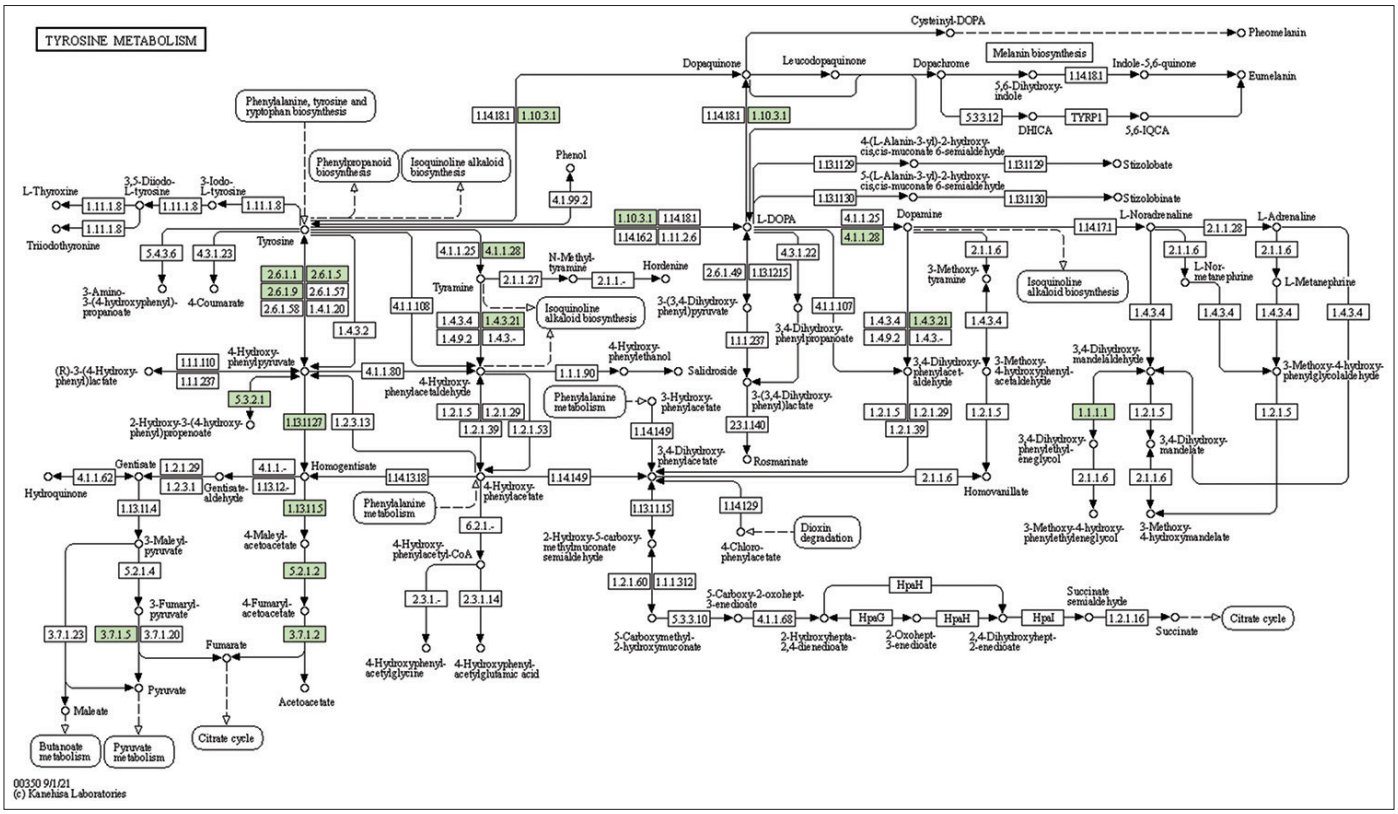

Supplementary Figure 24: The genes associated with metabolites of tyrosine metabolism. This figure shows 18 genes associated with tyrosine metabolism, and the genes were highlighted in the pathway. These genes are mapped onto the pathway and were retrieved from KAAS.

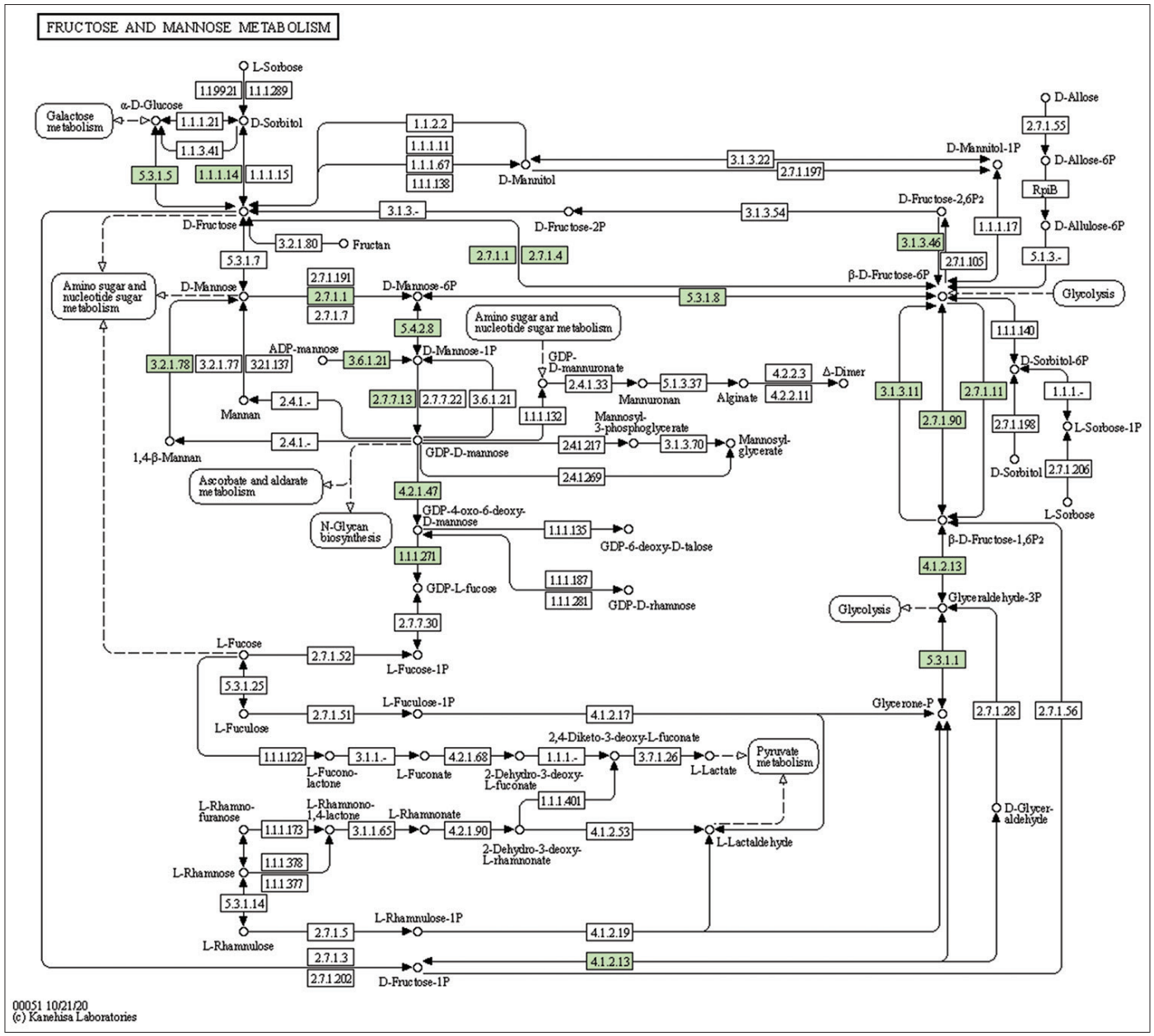

Supplementary Figure 25: The genes associated with metabolites of fructose and mannose metabolism. This figure shows 17 genes associated with fructose and mannose metabolism, and the genes were highlighted in the pathway. These genes are mapped onto the pathway and were retrieved from KAAS.

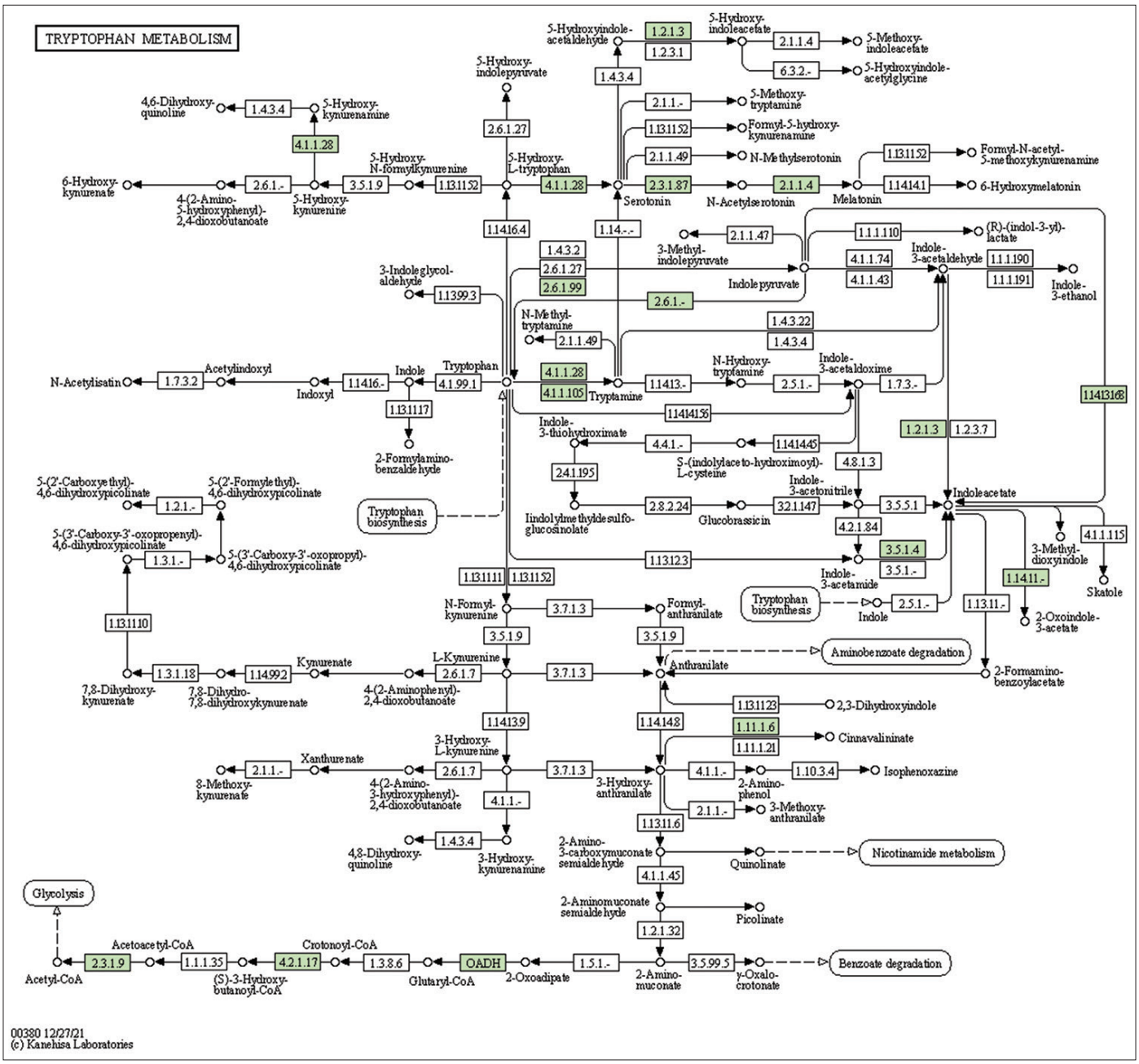

Supplementary Figure 26: The genes associated with metabolites of tryptophan metabolism. This figure shows 15 genes associated with tryptophan metabolism, and the genes were highlighted in the pathway. These genes are mapped onto the pathway and were retrieved from KAAS.

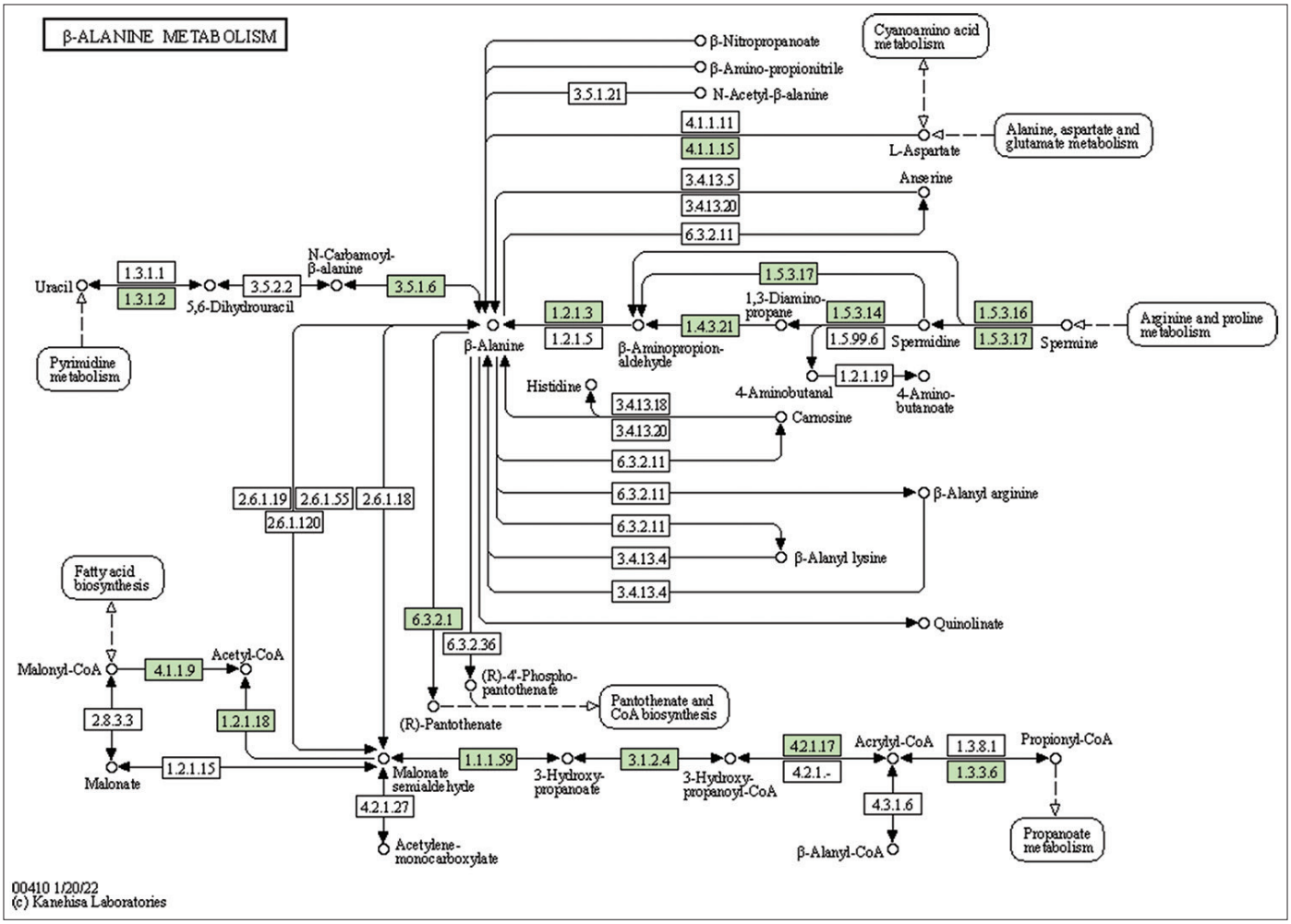

Supplementary Figure 27: The genes associated with metabolites of beta-alanine metabolism. This figure shows 15 genes associated with beta-alanine metabolism, and the genes were highlighted in the pathway. These genes are mapped onto the pathway and were retrieved from KAAS.

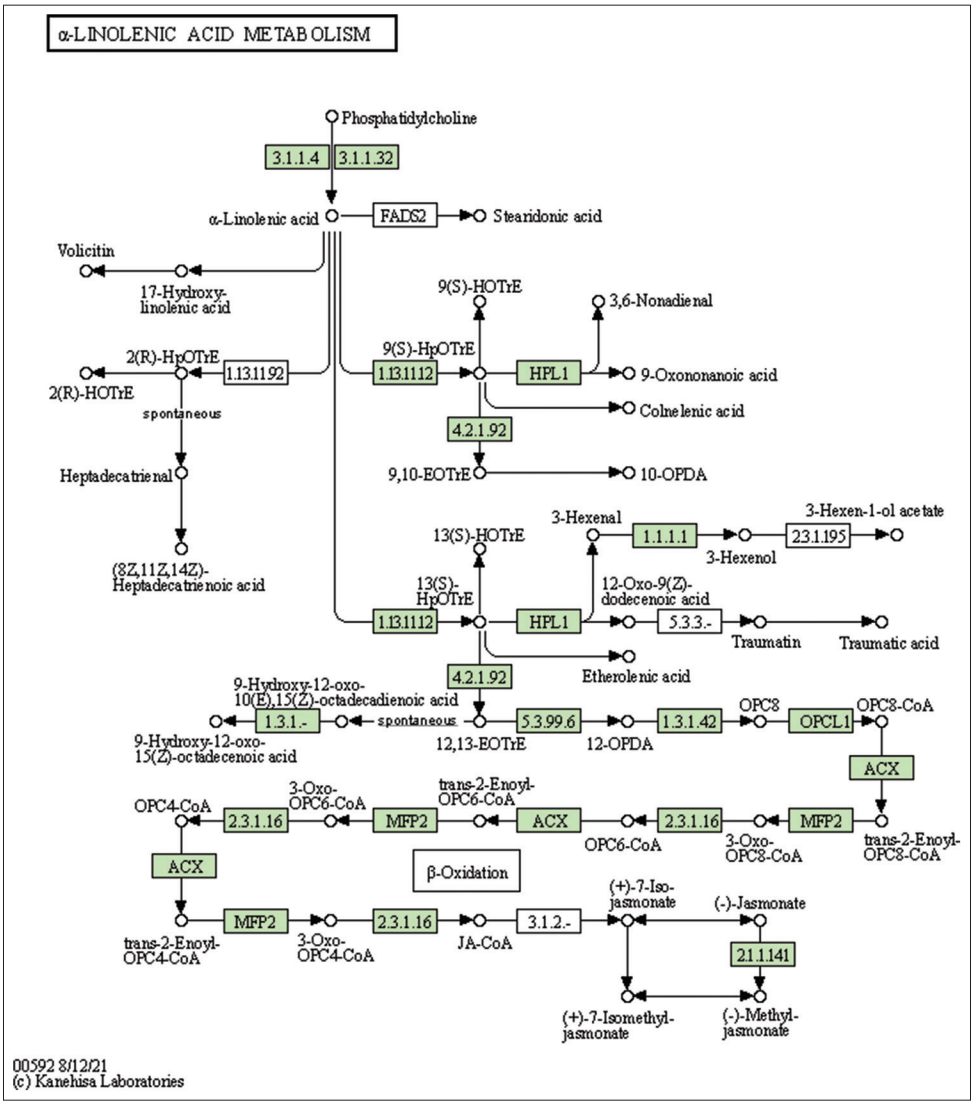

Supplementary Figure 28: The genes associated with alpha-linolenic acid metabolism metabolites. This figure shows 15 genes associated with alpha-linolenic acid metabolism, and the genes were highlighted in the pathway. These genes are mapped onto the pathway and were retrieved from KAAS.

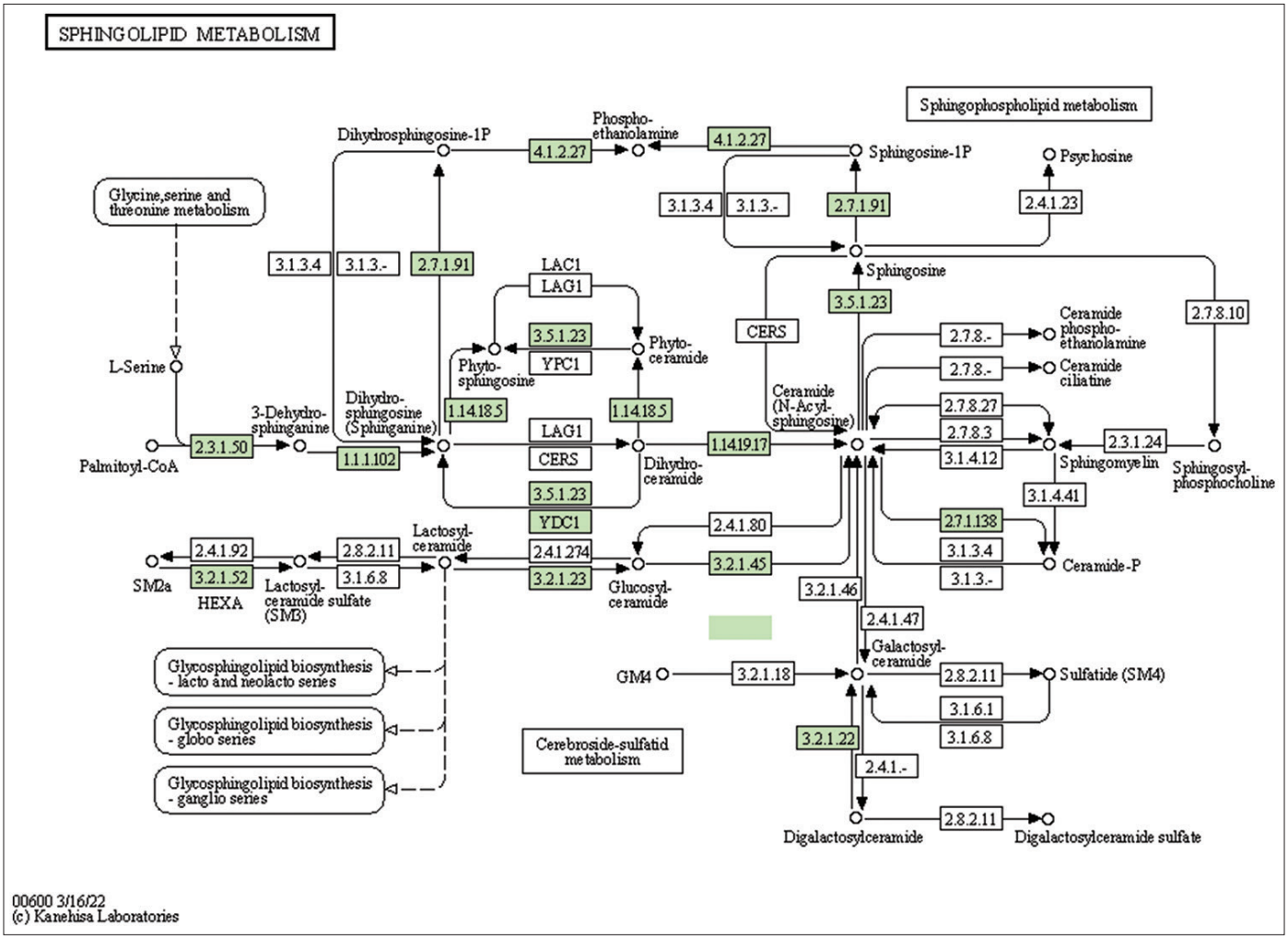

Supplementary Figure 29: The genes associated with metabolites of sphingolipid metabolism. This figure shows 15 genes associated with sphingolipid metabolism, and the genes were highlighted in the pathway. These genes are mapped onto the pathway and were retrieved from KAAS.

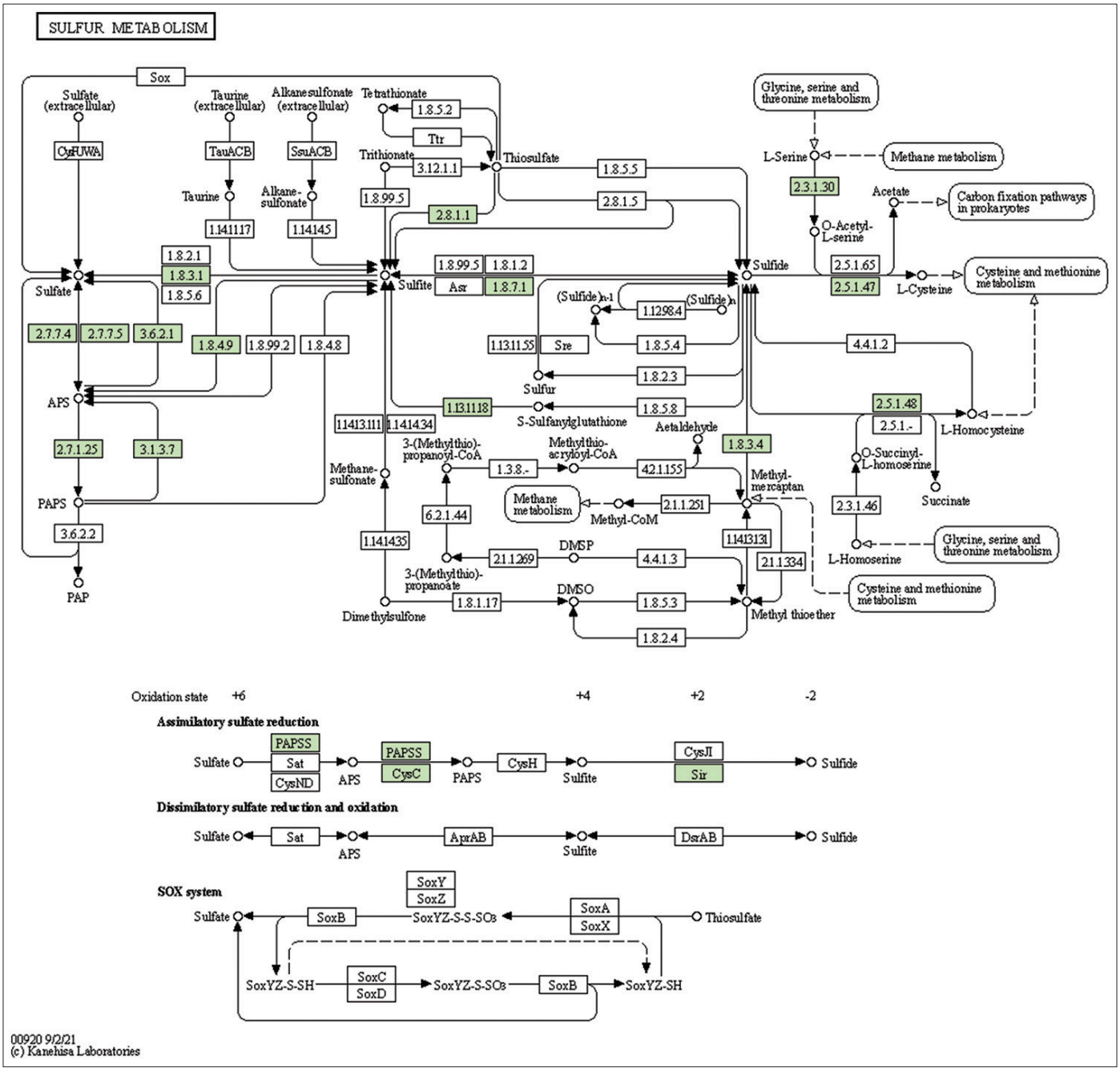

Supplementary Figure 30: The genes associated with metabolites of sulfur metabolism. This figure shows 15 genes associated with sulfur metabolism, and the genes were highlighted in the pathway. These genes are mapped onto the pathway and were retrieved from KAAS.

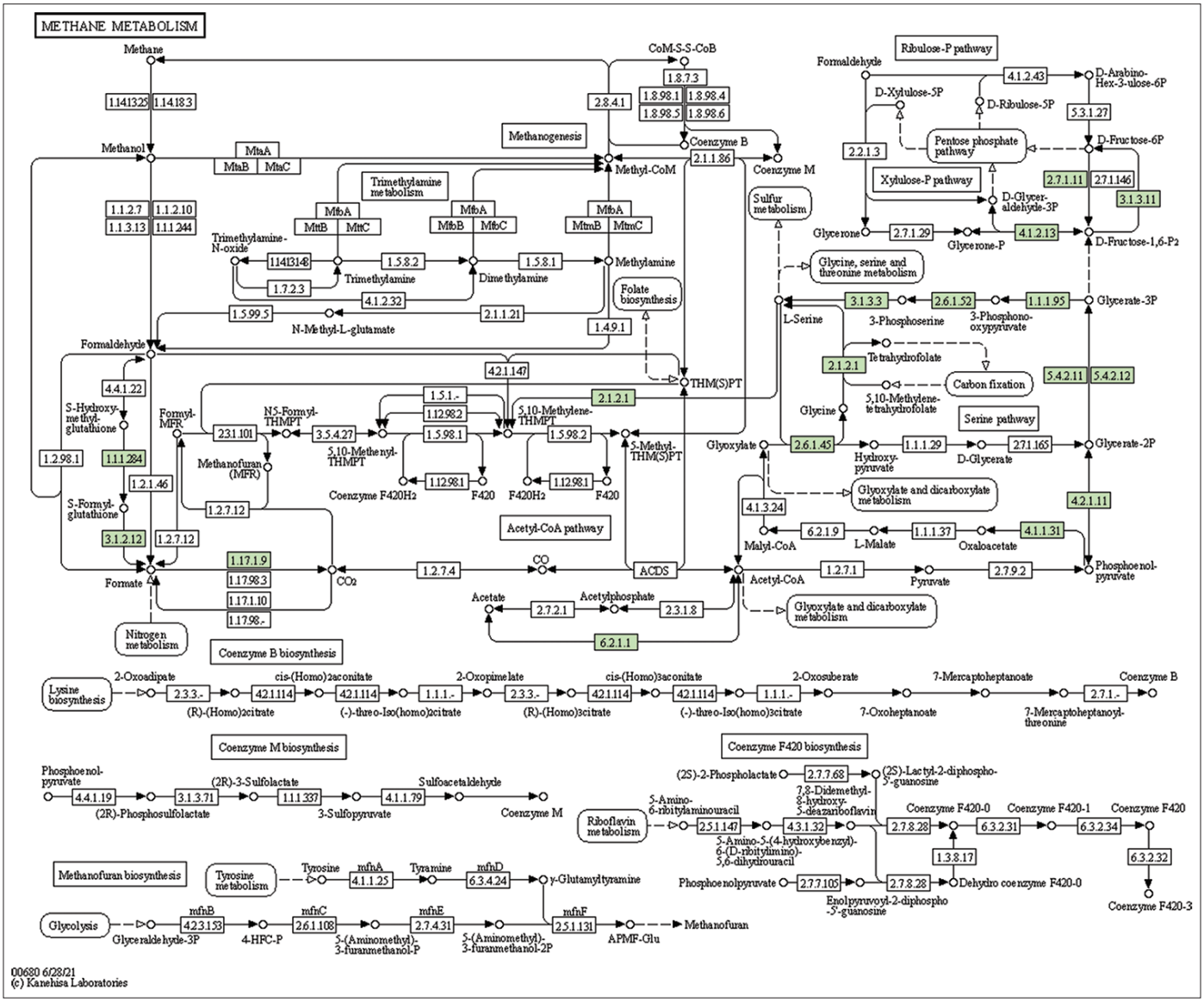

Supplementary Figure 31: The genes associated with metabolites of methane metabolism. This figure shows 16 genes associated with methane metabolism, and the genes were highlighted in the pathway. These genes are mapped onto the pathway and were retrieved from KAAS.

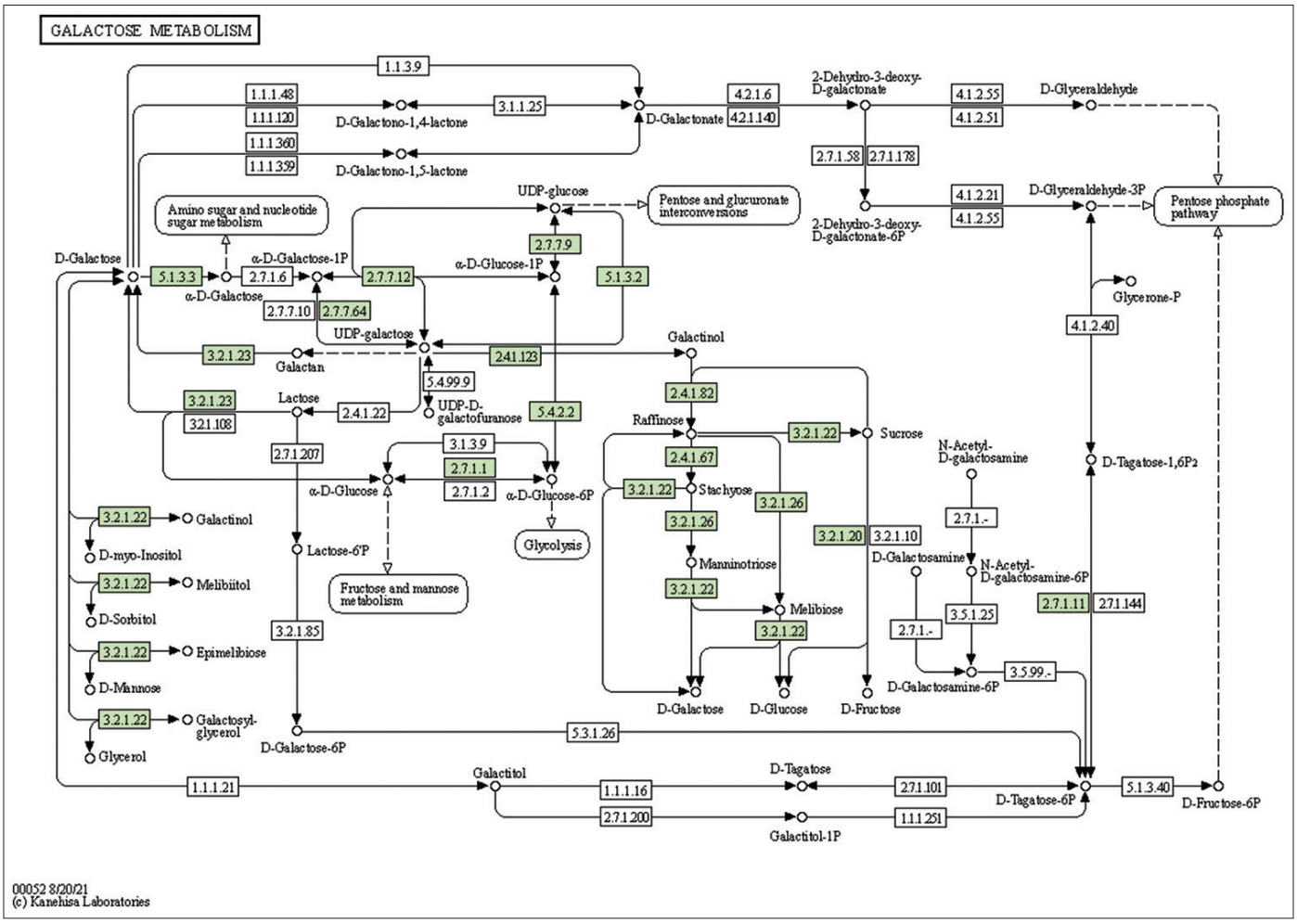

Supplementary Figure 32: The genes associated with metabolites of galactose metabolism. This figure shows 16 genes associated with galactose metabolism, and the genes were highlighted in the pathway. These genes are mapped onto the pathway and were retrieved from KAAS.

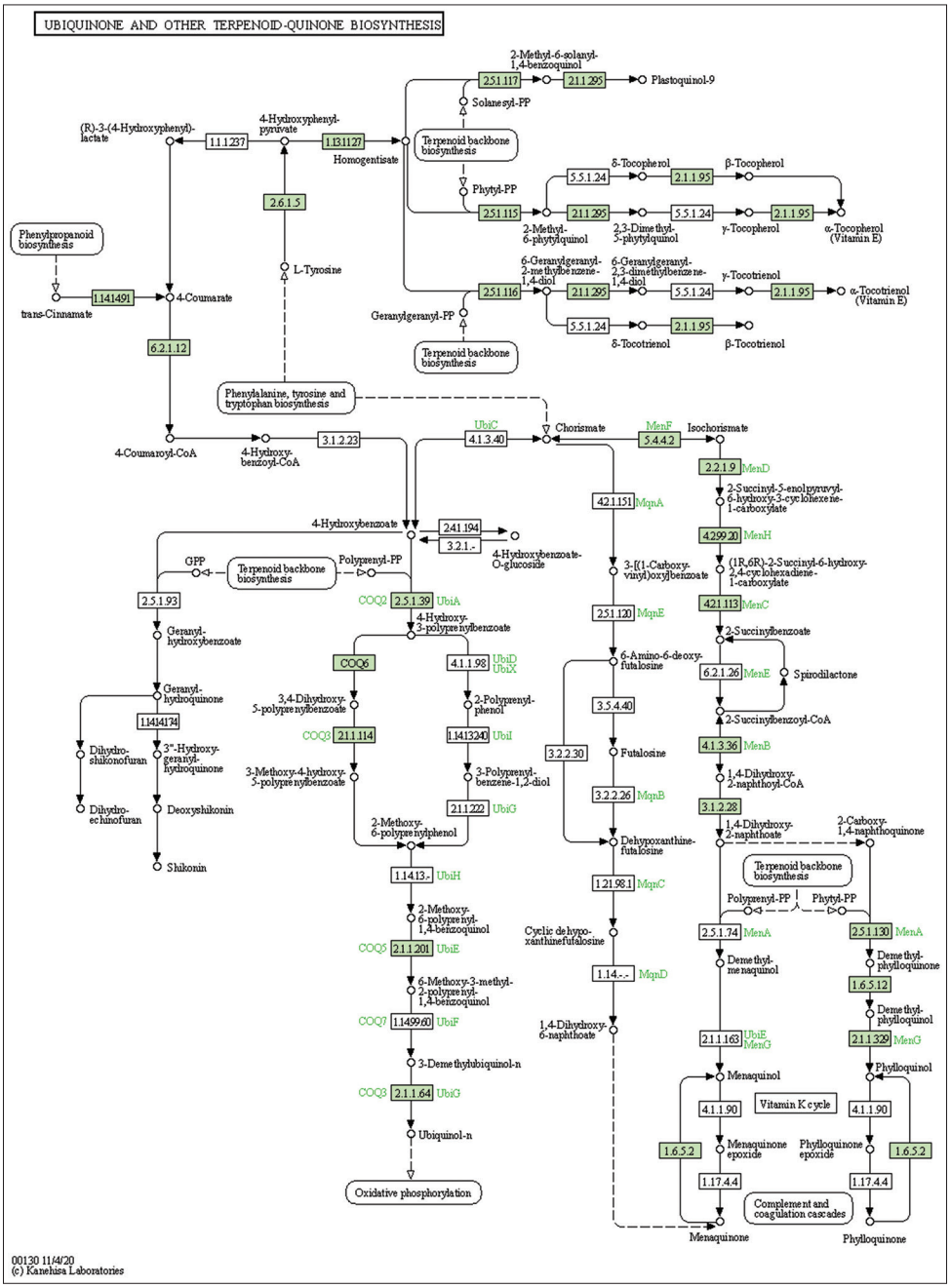

Supplementary Figure 33: The genes associated with metabolites of ubiquinone and other terpenoid-quinone biosynthesis metabolism. This figure shows 20 genes associated with ubiquinone and other terpenoid-quinone biosynthesis metabolism, and the genes were highlighted in the pathway. These genes are mapped onto the pathway and were retrieved from KAAS.

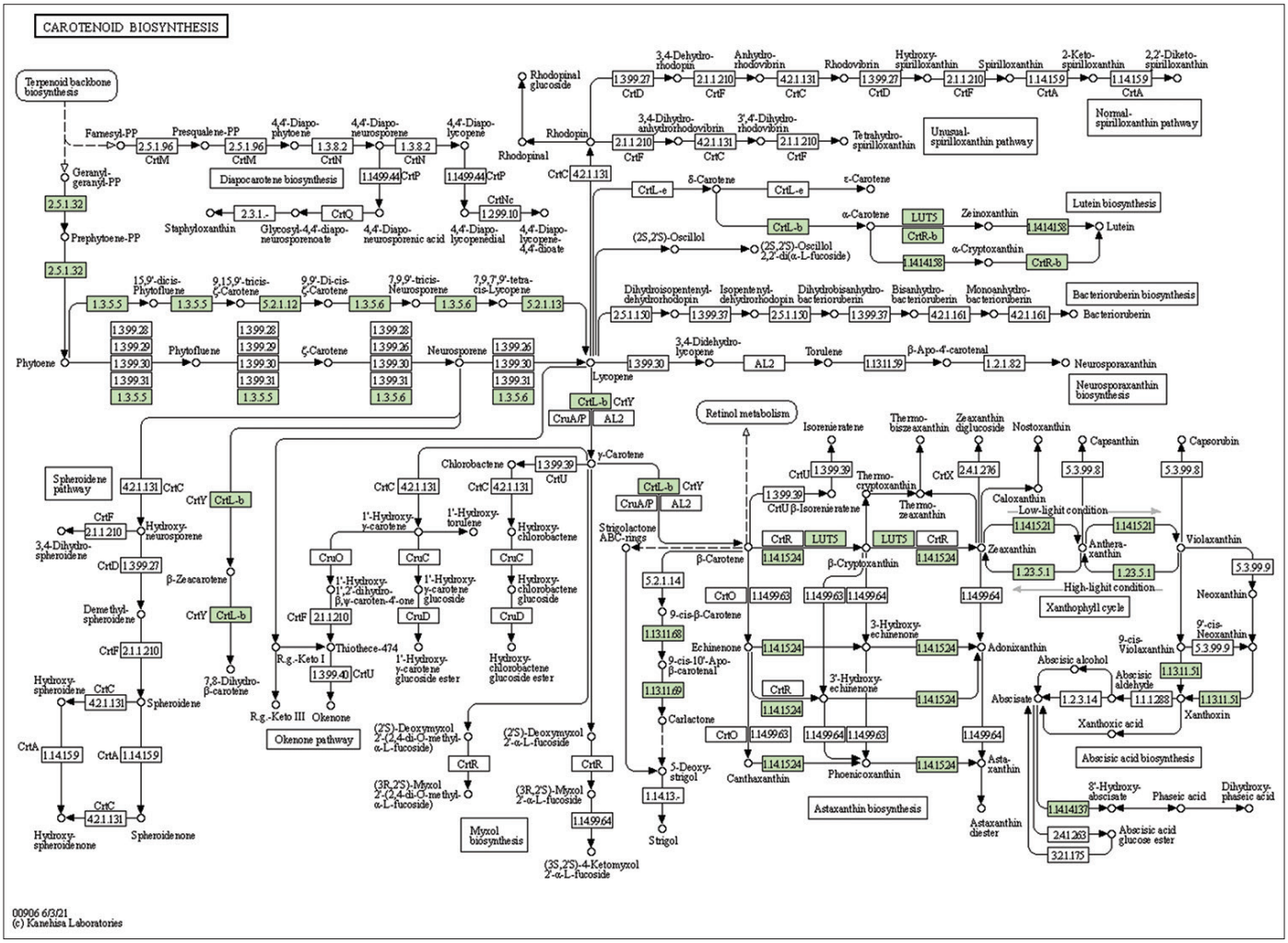

Supplementary Figure 34: The genes associated with metabolites of carotenoid biosynthesis metabolism. This figure shows 15 genes associated with carotenoid biosynthesis metabolism, and the genes were highlighted in the pathway. These genes are mapped onto the pathway and were retrieved from KAAS.

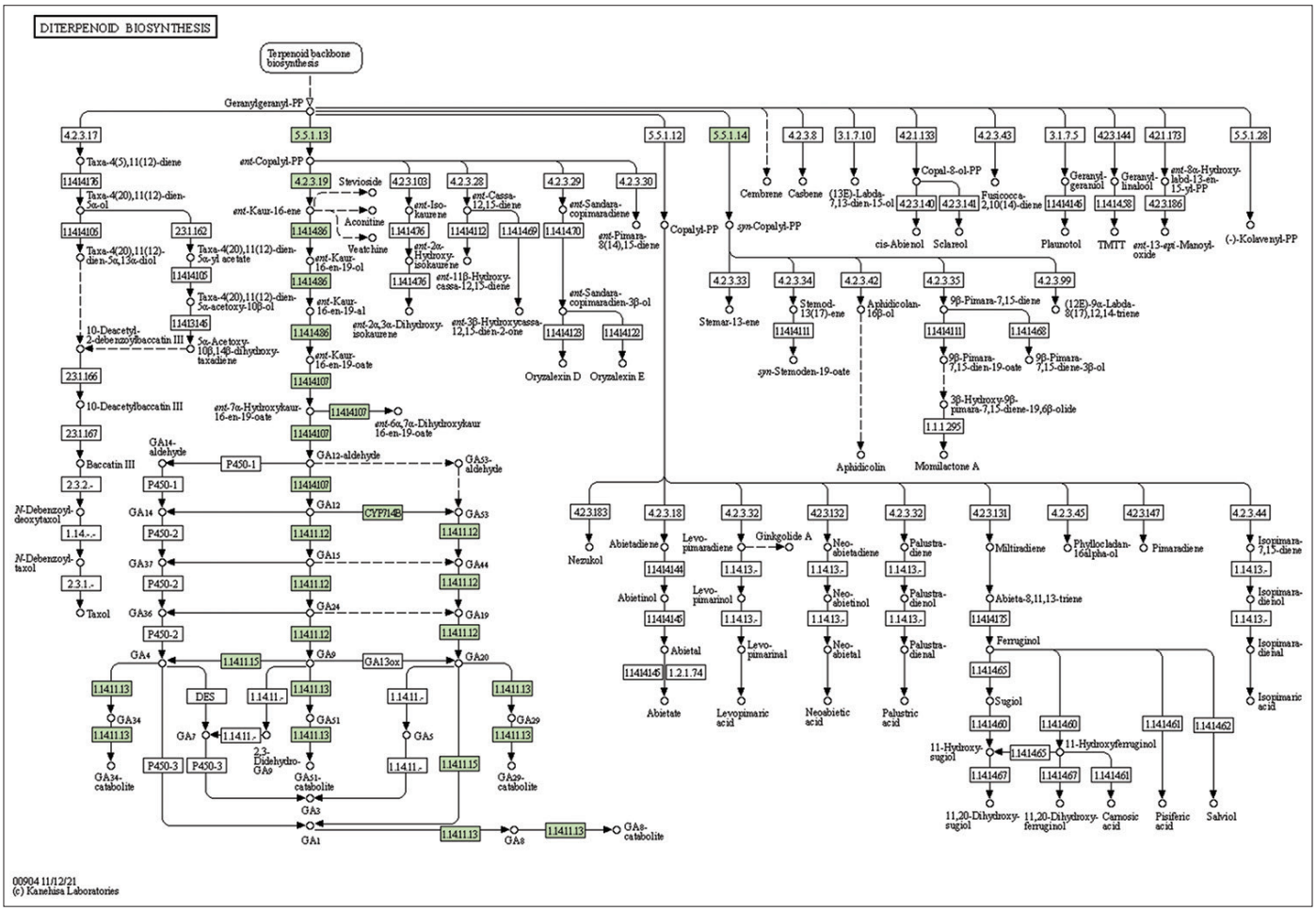

Supplementary Figure 35: The genes associated with metabolites of diterpenoid biosynthesis metabolism. This figure shows nine genes associated with diterpenoid biosynthesis metabolism, and the genes were highlighted in the pathway. These genes are mapped onto the pathway and were retrieved from KAAS.

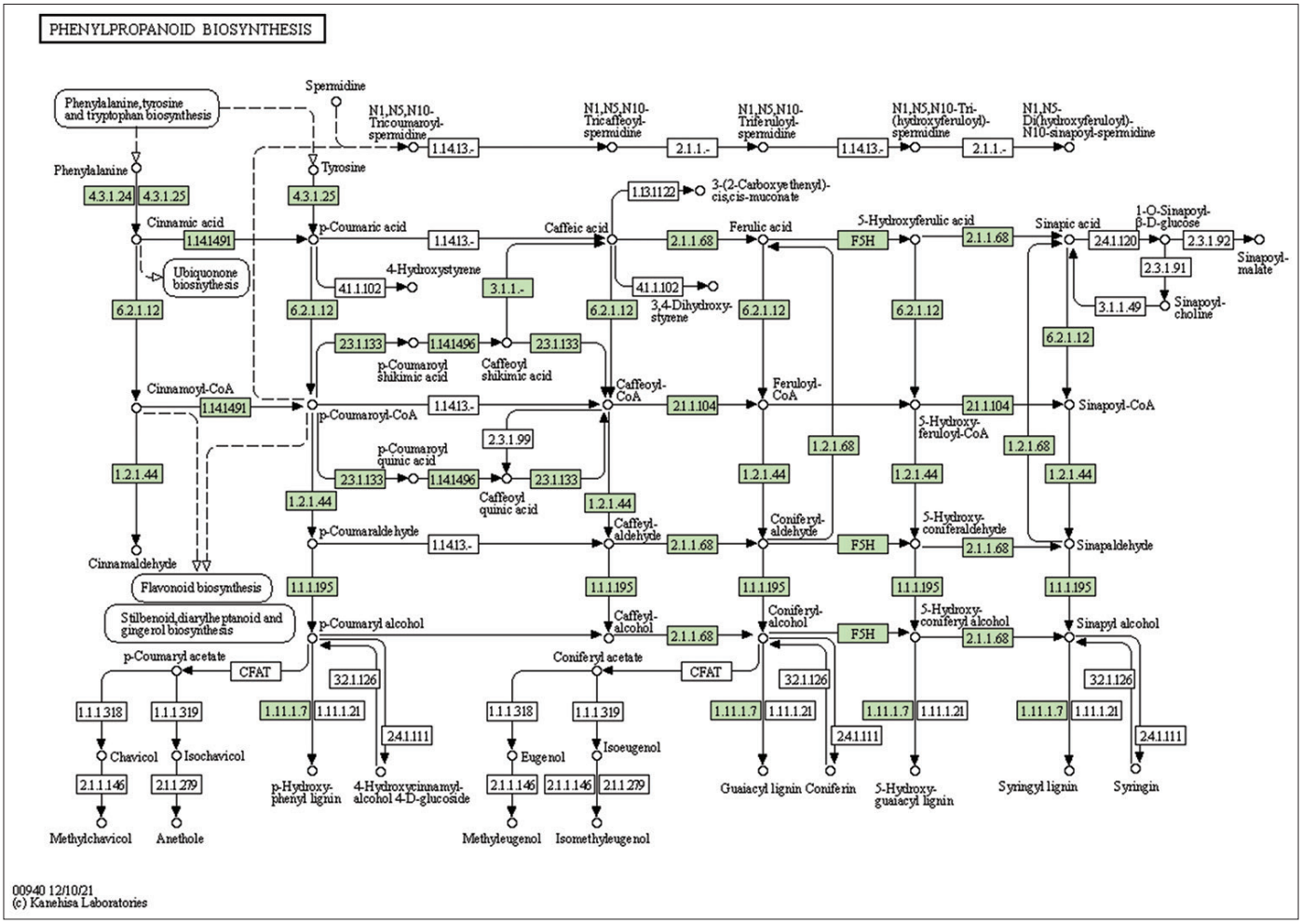

Supplementary Figure 36: The genes associated with metabolites of phenylpropanoid biosynthesis metabolism. This figure shows 15 genes associated with phenylpropanoid biosynthesis metabolism, and the genes were highlighted in the pathway. These genes are mapped onto the pathway and were retrieved from KAAS.

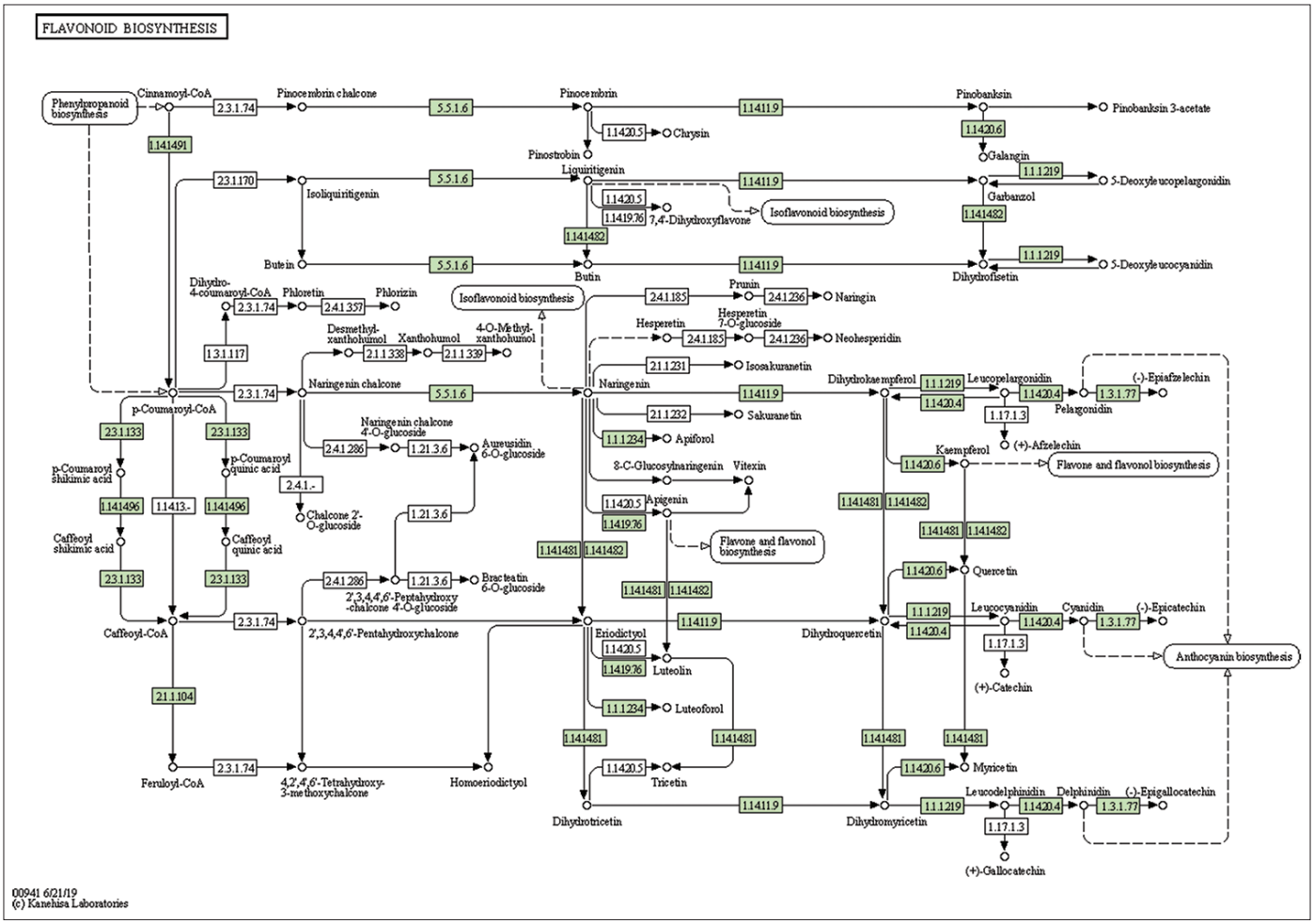

Supplementary Figure 37: The genes associated with metabolites of flavonoid biosynthesis metabolism. This figure shows 13 genes associated with flavonoid biosynthesis metabolism, and the genes were highlighted in the pathway. These genes are mapped onto the pathway and were retrieved from KAAS.

Supplementary Table 3: The summary of primers designed successfully for SSRs repeats in lemon grass

S. No.	Type of simple repeats	Count of simple repeat	Count of primers designed
1	Mononucleotides (p1)	50,779	47,048
2	Dinucleotides (p2)	10,874	9,321
3	trinucleotides (p3)	11,942	10,901
4	Tetranucleotides (p4)	1,515	1,378
5	Pentanucleotides (p5)	461	414
6	Hexanucleotides (p6)	451	385
7	Complex type of repeats (c)	4,784	4,241

Supplementary Table 4: The summary of orthogroups and genes in lemon grass as revealed by the orthologous analysis

S.No.	Summary of orthogroups and genes	Counts
1	Number of genes	562517
2	Number of genes in orthogroups	447596
3	Number of unassigned genes	114921
4	Percentage of genes in orthogroups	79.6
5	Percentage of unassigned genes	20.4
6	Number of orthogroups	26100
7	Number of species-specific orthogroups	714
8	Number of genes in species-specific orthogroups	4138
9	Percentage of genes in species-specific orthogroups	0.7
10	Mean orthogroup size	17.1
11	Median orthogroup size	13
12	G50 (assigned genes)	26
13	G50 (all genes)	20
14	O50 (assigned genes)	4770
15	O50 (all genes)	7256
16	Number of orthogroups with all species present	7898
17	Number of single-copy orthogroups	8

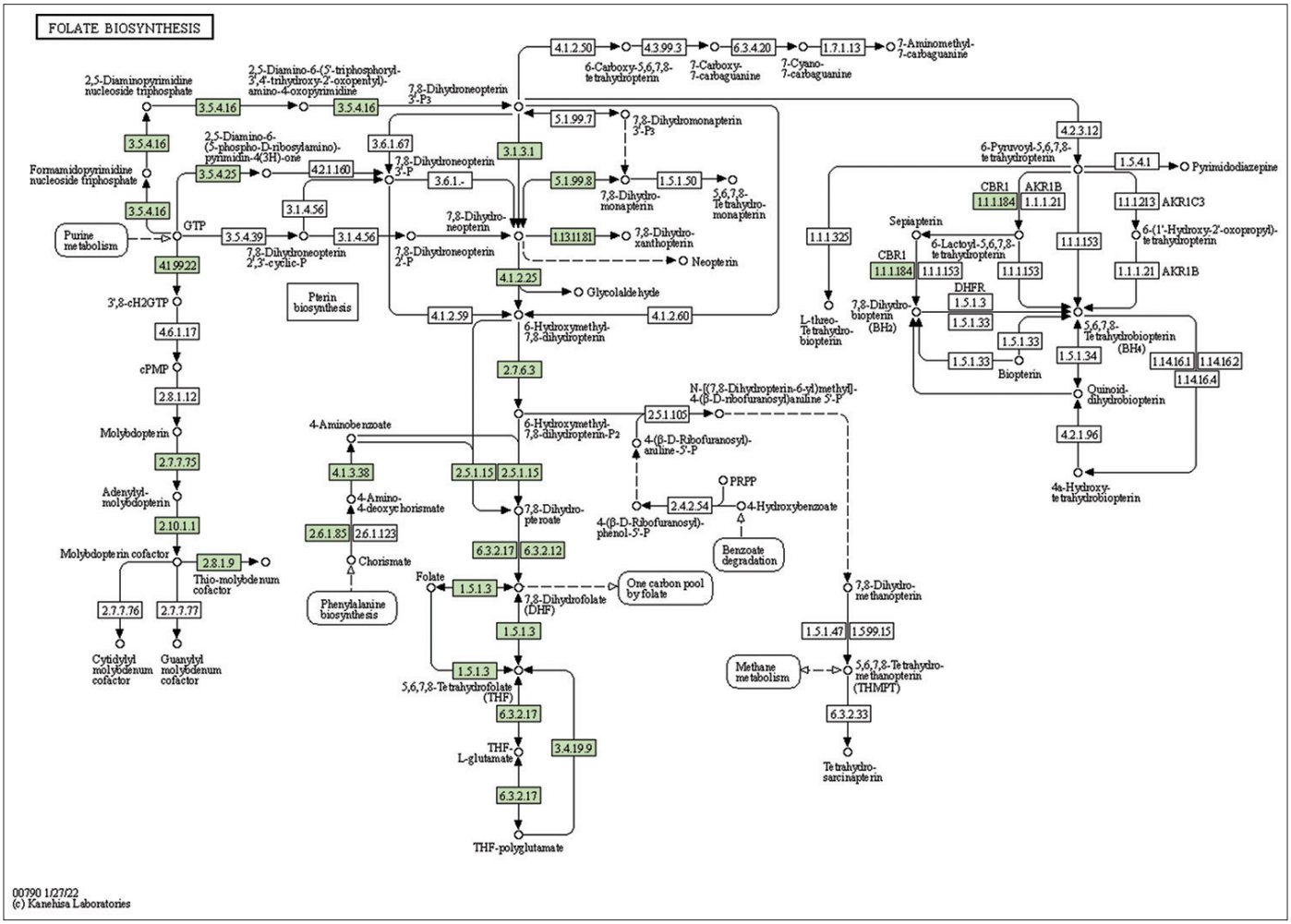

Supplementary Figure 38: The genes associated with metabolites of folate metabolism. This figure shows 15 genes associated with folate metabolism, and the genes were highlighted in the pathway. These genes are mapped onto the pathway and were retrieved from KAAS.

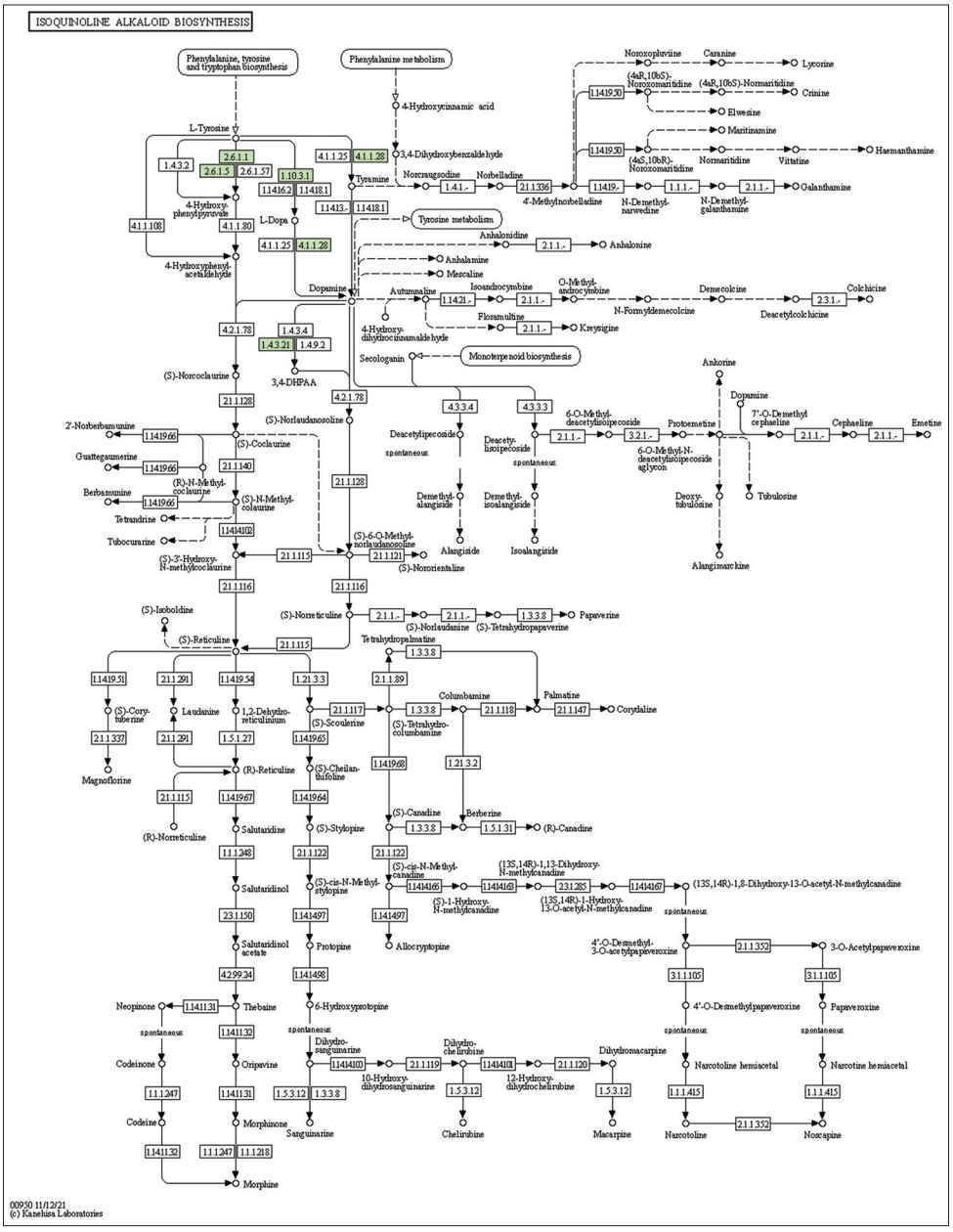

Supplementary Figure 39: The genes associated with metabolites of isoquinoline alkaloid biosynthesis metabolism. This figure shows eight genes associated with isoquinoline alkaloid biosynthesis metabolism. The genes were highlighted in the pathway. These genes are mapped onto the pathway and were retrieved from KAAS.

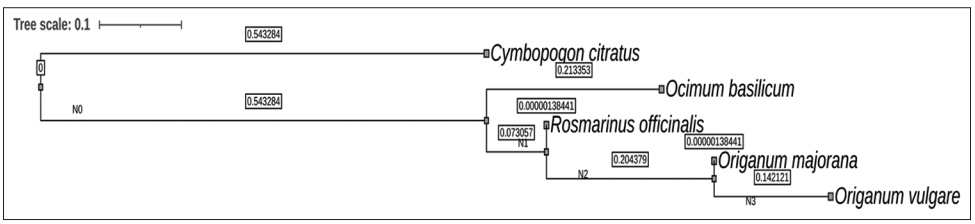

Supplementary Figure 40: The phylogenetic tree between five economically important culinary herbs. This figure shows a phylogenetic relationship between *Cymbopogon citratus* and four economically important culinary herbs, namely, sweet basil (*Ocimum basilicum* L.), sweet marjoram (*Origanum majorana* L.), oregano (*Origanum vulgare* L.), and rosemary (*Rosmarinus officinalis* L.). The orthology data was generated using OrthoFinder version 2.3.11 for the above species. The orthology data was used to construct a linear tree based on maximum likelihood method and the tree was viewed in FigTree version 1.4.4.

Supplementary Table 5: Identification of genes from lemon grass taking part in terpene synthases

S. No.	GeneID	Annotation	GeneID_short	Gene name	TPS family	Swiss Prot Entry	SwissProt gene names	Gene ID in lemongrass
1	AT2G24210.1	terpene synthase 10	AT2G24210	TPS10	TPSb	Q9ZUH4	TPS10 At2g24210 F27D4.12	g38217.t1
2	AT3G25810.1	Terpenoid cyclases/Protein prenyltransferases superfamily protein	AT3G25810	TPS24	TPSb	Q9LRZ6	TPS24 At3g25810 K13N2.7	g34393.t1
3	AT3G25820.1	terpene synthase-like sequence-1,8-cineole	AT3G25820	TPS27; TPS-CIN1	TPSb	P0DI76	TPS27 TPS-CIN1 At3g25820 K13N2.19	g34393.t1
4	AT3G25830.1	terpene synthase-like sequence-1,8-cineole	AT3G25830	TPS23; TPS-CIN2	TPSb	P0DI77	TPS23 TPS-CIN2 At3g25830 K9I22.3	g34393.t1
5	AT4G16730.1	terpene synthase 02	AT4G16730	TPS02	TPSb	P0CJ42	TPS02 At4g16730 dl4390w FCAALL.15	g32271.t1
6	AT4G16740.1	terpene synthase 03	AT4G16740	TPS03	TPSb	A4FVP2	TPS03 At4g16740 dl4395w FCAALL.18	g34393.t1
7	AT5G23960.1	terpene synthase 21	AT5G23960	TPS21; PUP8	TPSa	Q84UU4	TPS21 PUP8 At5g23960 MZF18.16	g3033.t1
8	AT4G02780.1	Terpenoid cyclases/Protein prenyltransferases superfamily protein	AT4G02780	TPS31; TPSGA1; GA1; CPS; CPS1	TPSc	Q38802	GA1 ABC33 CPS CPS1 TPSGA1 At4g02780 T5J8.9	g17067.t1
9	AT1G79460.1	Terpenoid cyclases/Protein prenyltransferases superfamily protein	AT1G79460	TPS32; TPSGA2; GA2; KS; KS1	TPSe/f	Q9SAK2	GA2 KS KS1 TPSGA2 At1g79460 T8K14.12	g12107.t1
10	AT1G61120.1	terpene synthase 04	AT1G61120	TPS04; GES; LIS	TPSe/f	Q93YV0	GES LIS TPS04 At1g61120 F11P17.15	g12107.t1
11	AT1G61680.1	terpene synthase 14	AT1G61680	TPS14	TPSg	Q84UV0	TPS14 At1g61680 T13M11.3	g9415.t1
12	AT1G66020.1	Terpenoid cyclases/Protein prenyltransferases superfamily protein	AT1G66020	TPS26	TPSa	Q9C8E3	TPS26 At1g66020 F15E12.3	g3033.t1
13	AT3G29190.1	Terpenoid cyclases/Protein prenyltransferases superfamily protein	AT3G29190	TPS15	TPSa	Q9LS76	TPS15 At3g29190 MXO21.3	g3033.t1
14	AT4G20200.1	Terpenoid cyclases/Protein prenyltransferases superfamily protein	AT4G20200	TPS07	TPSa	O65434	TPS07 At4g20200 F1C12.120	g3033.t1
15	AT4G20210.1	Terpenoid cyclases/Protein prenyltransferases superfamily protein	AT4G20210	TPS08	TPSa	O65435	TPS08 At4g20210 F1C12.130	g3033.t1
16	AT4G20230.2	terpenoid synthase superfamily protein	AT4G20230	TPS09	TPSa	Q8L7G4	TPS09 At4g20230 F1C12.150	g3033.t1

(*Contd...*)

Supplementary Table 5: (*Continued*).

S. No.	GeneID	Annotation	GeneID_short	Gene name	TPS family	Swiss Prot Entry	SwissProt gene names	Gene ID in lemongrass
17	AT1G31950.3	Terpenoid cyclases/Protein prenyltransferases superfamily protein	AT1G31950	TPS29	TPSa	Q9C6W6	TPS29 At1g31950 F5M6.5 T12O21.14	g3033.t1
18	AT3G14520.1	Terpenoid cyclases/Protein prenyltransferases superfamily protein	AT3G14520	TPS18	TPSa	Q9LUE2	TPS18 At3g14520 MIE1.2	g3033.t1
19	AT3G14540.1	Terpenoid cyclases/Protein prenyltransferases superfamily protein	AT3G14540	TPS19	TPSa	Q9LUE0	TPS19 At3g14540 MIE1.4	g3033.t1
20	AT4G13280.2	terpenoid synthase 12	AT4G13280	TPS12	TPSa	Q9T0J9	TPS12 At4g13280 T9E8.20	g3033.t1
21	AT4G13300.1	terpenoid synthase 13	AT4G13300	TPS13	TPSa	Q9T0K1	TPS13 At4g13300 T9E8.40	g3033.t1
22	AT5G44630.1	Terpenoid cyclases/Protein prenyltransferases superfamily protein	AT5G44630	TPS11; BS	TPSa	Q4KSH9	BS TPS11 At5g44630 K15C23.7	g3033.t1
23	AT1G48800.1	Terpenoid cyclases/Protein prenyltransferases superfamily protein	AT1G48800	TPS28	TPSa	Q9C748	TPS28 At1g48800 F11I4_3	g3033.t1
25	AT1G70080.1	Terpenoid cyclases/Protein prenyltransferases superfamily protein	AT1G70080	TPS06	TPSa	Q84UU9	TPS06 At1g70080 F20P5.19	g3033.t1
26	AT5G48110.1	Terpenoid cyclases/Protein prenyltransferases superfamily protein	AT5G48110	TPS20	TPSa	Q9FI27	TPS20 At5g48110 MDN11.20	g3033.t1
27	AT2G37140.1	Terpenoid synthases superfamily protein	AT2G37140	pseudo-C	(TPSa)	Q1PEW2	At2g37140	g26763.t1
28	AT4G15870.1	terpene synthase 1	AT4G15870	TPS01; TC1; TS1	TPSa	O23651	TPS01 TC1 TS1 At4g15870 dl3975c FCAALL.405	g3033.t1
29	AT1G33750.1	Terpenoid cyclases/Protein prenyltransferases superfamily protein	AT1G33750	TPS22	TPSa	Q9LQ27	TPS22 At1g33750 F14M2.13	g3033.t1
30	AT2G23230.2	Terpenoid cyclases/Protein prenyltransferases superfamily protein	AT2G23230	TPS05	TPSa	O22184	TPS05 At2g23230 T20D16.14	g3033.t1
31	AT3G14490.1	Terpenoid cyclases/Protein prenyltransferases superfamily protein	AT3G14490	TPS17	TPSa	Q9LRR2	TPS17 At3g14490 MOA2.12	g3033.t1
32	AT3G29110.1	Terpenoid cyclases/Protein prenyltransferases superfamily protein	AT3G29110	TPS16	TPSa	Q9LVP7	TPS16 At3g29110 MXE2.1	g3033.t1

(*Contd...*)

Supplementary Table 5: (*Continued*).

S. No.	GeneID	Annotation	GeneID_short	Gene name	TPS family	Swiss Prot Entry	SwissProt gene names	Gene ID in lemongrass
33	AT3G29410.1	Terpenoid cyclases/Protein prenyltransferases superfamily protein	AT3G29410	TPS25	TPSa	Q9LIA1	TPS25 At3g29410 MUO10.2	g3033.t1
34	AT3G32030.1	Terpenoid cyclases/Protein prenyltransferases superfamily protein	AT3G32030	TPS30	TPSa	Q9LH31	TPS30 At3g32030 T8O3.12	g3033.t1

Supplementary Table 6: Identification of methylerythritol phosphate (MEP) and mevalonic acid (MVA) genes in lemon grass

S. No.	Gene ID from Lemongrass	Uniprot ID	Uniprot Entry	Annotation
1	g38362.t1	F4JCU3	MVD2_ARATH	Diphosphomevalonate decarboxylase MVD2, peroxisomal OS=Arabidopsis thaliana OX=3702 GN=MVD2 PE=1 SV=1
2	g8212.t1	F4K0E8	ISPG_ARATH	4 hydroxy 3 methylbut 2 en 1 yl diphosphate synthase (ferredoxin), chloroplastic OS=Arabidopsis thaliana OX=3702 GN=ISPG PE=1 SV=1
3	g38362.t1	O23722	MVD1_ARATH	Diphosphomevalonate decarboxylase MVD1, peroxisomal OS=Arabidopsis thaliana OX=3702 GN=MVD1 PE=1 SV=1
4	g11679.t1	O81014	ISPE_ARATH	4 diphosphocytidyl 2 C methyl D erythritol kinase, chloroplastic OS=Arabidopsis thaliana OX=3702 GN=ISPE PE=2 SV=1
5	g33940.t1	P14891	HMDH1_ARATH	3 hydroxy 3 methylglutaryl coenzyme A reductase 1 OS=Arabidopsis thaliana OX=3702 GN=HMG1 PE=1 SV=1
6	g23454.t1	P34802	GGPP1_ARATH	Heterodimeric geranylgeranyl pyrophosphate synthase large subunit 1, chloroplastic OS=Arabidopsis thaliana OX=3702 GN=GGPPS1 PE=1 SV=2
7	g33940.t1	P43256	HMDH2_ARATH	3 hydroxy 3 methylglutaryl coenzyme A reductase 2 OS=Arabidopsis thaliana OX=3702 GN=HMG2 PE=2 SV=1
8	g4041.t1	P46086	KIME_ARATH	Mevalonate kinase OS=Arabidopsis thaliana OX=3702 GN=At5g27450 PE=2 SV=1
9	g10131.t1	P54873	HMCS_ARATH	Hydroxymethylglutaryl CoA synthase OS=Arabidopsis thaliana OX=3702 GN=HMGS PE=1 SV=2
10	g11653.t1	P69834	ISPD_ARATH	2 C methyl D erythritol 4 phosphate cytidylyltransferase, chloroplastic OS=Arabidopsis thaliana OX=3702 GN=ISPD PE=1 SV=1
11	g2230.t1	Q09152	FPPS1_ARATH	Farnesyl pyrophosphate synthase 1, mitochondrial OS=Arabidopsis thaliana OX=3702 GN=FPS1 PE=2 SV=2
12	g10476.t1	Q38854	DXS_ARATH	1 deoxy D xylulose 5 phosphate synthase, chloroplastic OS=Arabidopsis thaliana OX=3702 GN=DXS PE=1 SV=2
13	g8827.t1	Q38929	IDI1_ARATH	Isopentenyl diphosphate Delta isomerase I, chloroplastic OS=Arabidopsis thaliana OX=3702 GN=IPP1 PE=1 SV=3
14	g9222.t1	Q39108	GGR_ARATH	Heterodimeric geranylgeranyl pyrophosphate synthase small subunit, chloroplastic OS=Arabidopsis thaliana OX=3702 GN=GGR PE=1 SV=2
15	g8827.t1	Q42553	IDI2_ARATH	Isopentenyl diphosphate Delta isomerase II, chloroplastic OS=Arabidopsis thaliana OX=3702 GN=IPP2 PE=1 SV=1
16	g2230.t1	Q43315	FPPS2_ARATH	Farnesyl pyrophosphate synthase 2 OS=Arabidopsis thaliana OX=3702 GN=FPS2 PE=2 SV=1
17	g3152.t1	Q8S4Y1	THIC1_ARATH	Acetyl CoA acetyltransferase, cytosolic 1 OS=Arabidopsis thaliana OX=3702 GN=AAT1 PE=1 SV=1
18	g36791.t1	Q94B35	ISPH_ARATH	4 hydroxy 3 methylbut 2 enyl diphosphate reductase, chloroplastic OS=Arabidopsis thaliana OX=3702 GN=ISPH PE=1 SV=1
19	g13764.t1	Q9C6T1	PMK_ARATH	Phosphomevalonate kinase, peroxisomal OS=Arabidopsis thaliana OX=3702 GN=PMK PE=1 SV=1
20	g15260.t1	Q9CAK8	ISPF_ARATH	2 C methyl D erythritol 2,4 cyclodiphosphate synthase, chloroplastic OS=Arabidopsis thaliana OX=3702 GN=ISPF PE=1 SV=1
21	g3152.t1	Q9FIK7	THIC2_ARATH	Probable acetyl CoA acetyltransferase, cytosolic 2 OS=Arabidopsis thaliana OX=3702 GN=At5g47720 PE=2 SV=1
22	g9071.t1	Q9XFS9	DXR_ARATH	1 deoxy D xylulose 5 phosphate reductoisomerase, chloroplastic OS=Arabidopsis thaliana OX=3702 GN=DXR PE=2 SV=2

(*Contd...*)

Supplementary Table 6: (*Continued*).

S. No.	Gene ID from Lemongrass	Uniprot ID	Uniprot Entry	Annotation
23	g8827.t1	A0A178ULI3	A0A178ULI3_ ARATH	Isopentenyl diphosphate Delta isomerase OS=Arabidopsis thaliana OX=3702 GN=At5g16440 PE=3 SV=1
24	g3152.t1	A0A178UN67	A0A178UN67_ ARATH	AACT1 OS=Arabidopsis thaliana OX=3702 GN=At5g47720 PE=3 SV=1
25	g8827.t1	A0A1I9LM15	A0A1I9LM15_ ARATH	Isopentenyl diphosphate Delta isomerase OS=Arabidopsis thaliana OX=3702 GN=IPP2 PE=1 SV=1
26	g38362.t1	A0A1I9LME2	A0A1I9LME2_ ARATH	Diphosphomevalonate decarboxylase OS=Arabidopsis thaliana OX=3702 GN=At3g54250 PE=1 SV=1
27	g2230.t1	A0A1P8B4W4	A0A1P8B4W4_ ARATH	Farnesyl diphosphate synthase 2 OS=Arabidopsis thaliana OX=3702 GN=FPS2 PE=1 SV=1
28	g22151.t1	A0A2H1ZEF4	A0A2H1ZEF4_ ARATH	2 C methyl D erythritol 2,4 cyclodiphosphate synthase OS=Arabidopsis thaliana OX=3702 GN=ISPF PE=1 SV=1
29	g3152.t1	A0A5S9YC31	A0A5S9YC31_ ARATH	Uncharacterized protein OS=Arabidopsis thaliana OX=3702 GN=At5g48230 PE=3 SV=1
30	g33940.t1	A0A654ER34	A0A654ER34_ ARATH	3 hydroxy 3 methylglutaryl coenzyme A reductase OS=Arabidopsis thaliana OX=3702 GN=At1g76490 PE=3 SV=1
31	g8212.t1	B3H725	B3H725_ARATH	4 hydroxy 3 methylbut 2 enyl diphosphate synthase OS=Arabidopsis thaliana OX=3702 GN=HDS PE=1 SV=1
32	g27299.t1	C0Z3D4	C0Z3D4_ARATH	Hydroxymethylglutaryl CoA reductase (NADPH) OS=Arabidopsis thaliana OX=3702 GN=At1g76490 PE=2 SV=1
33	g2230.t1	F4JNF1	F4JNF1_ARATH	Farnesyl diphosphate synthase 2 OS=Arabidopsis thaliana OX=3702 GN=FPS2 PE=1 SV=1
34	g3152.t1	F4JYM8	F4JYM8_ARATH	Thiolase family protein OS=Arabidopsis thaliana OX=3702 GN=AACT1 PE=1 SV=1
35	g9071.t1	F4K7T6	F4K7T6_ARATH	1 deoxy D xylulose 5 phosphate reductoisomerase OS=Arabidopsis thaliana OX=3702 GN=DXR PE=1 SV=1
36	g19714.t1	Q67XB6	Q67XB6_ARATH	Uncharacterized protein At1g31910 OS=Arabidopsis thaliana OX=3702 GN=At1g31910 PE=2 SV=1
37	g23015.t1	Q944G7	Q944G7_ARATH	1 deoxy D xylulose 5 phosphate synthase OS=Arabidopsis thaliana OX=3702 GN=At4g15560 PE=2 SV=1